New Approaches for Studying Nutrient Kinetics in Humans: Folic Acid, Accelerator Mass Spectrometry and Mathematical Modeling

By

Ali Arjomand

B.S. (University of California, Davis) 1989

DISSERTATION

Submitted in partial satisfaction of the requirements for the degree of

DOCTOR OF PHILOSOPHY

in

NUTRITION

in the

GRADUATE DIVISION

of the

UNIVERSITY OF CALIFORNIA

DAVIS

Approved:

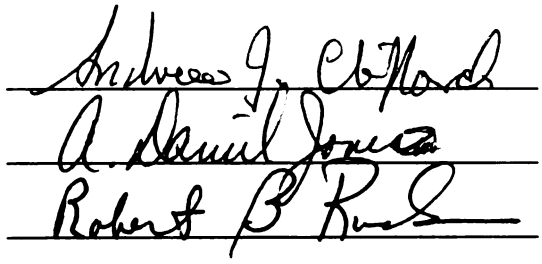

Committee in Charge

To my Parents, Sima and Aziz,

and my Sisters, Maryam and Leili,

ACKNOWLEDGEMENTS

The guidance, support and friendship of a number of people helped make this work possible. First, I thank Dr. Andrew Clifford for the opportunities he gave me, for his direction and for his many invaluable suggestions. I thank Dr. Robert Rucker for guiding me through graduate school. I also thank Dr. Steve Dueker for patiently teaching me the process of good analytical method development, Dr. Dan Jones of the Facility for Advanced Instrumentation for his insight, Dr. John Vogel and Dr. Bruce Buchholz of the Center for Accelerator Mass Spectrometry at Lawrence Livermore National Laboratory for their expert opinion, and Dr. Yumei Lin for making the laboratory environment a pleasant experience. I greatly appreciate the help of the staff of the Division of Agriculture and Natural Resources Analytical Laboratory and the Clinical Nutrition Assessment Laboratory. Finally, I want to thank my friends for their support and companionship especially Shadi, Babak, Ali, and Mehran.

TABLE OF CONTENTS

LIST OF FIGURES- Chapter 3

LIST OF FIGURES- Chapter 5

LIST OF TABLES

Chapter 3

Chapter 5

Ali Arjomand
June 1998
Nutrition

New Approaches for Studying Nutrient Kinetics in Humans: Folic Acid, Accelerator Mass Spectrometry and Mathematical Modeling

ABSTRACT

Folic acid is required in the diet for the prevention of a multitude of conditions ranging from anemia and heart disease to birth defects and cancer. Much of our current understanding of folic acid's role in these diseases is based on population studies that have shown associative relationships between folic acid intake and disease prevalence. Estimation of folic acid intake and requirement demands reliable methodologies to address these questions. The multiple forms of folic acid present in biological samples, as well as its instability and low concentration, has made estimation of actual folic acid intake and requirement difficult. In this study, improvements were made to current methodologies to permit more specific estimation of folic acid concentration in samples. The method centered on folate binding protein, which was highly purified and characterized at milligram quantities. Understanding the kinetics of folic acid in humans will help to determine requirements and identify differences in the absorption and disposition of the vitamin between groups. ^{14}C-Folic acid tracer was used to assess the bioavailability and kinetics of folic acid in a healthy human subject. Radiolabel concentration in plasma, red blood cells, urine and feces was measured by accelerator mass spectrometry (AMS). The extreme sensitivity of this instrument permitted the study to be conducted under physiological conditions with minimal exposure to radiation. Data from samples collected over a 200-day period was modeled by linear, non-linear and

compartmental modeling. Folic acid bioavailability and kinetics was quantified for the first time in a healthy human subject under physiologic conditions. These models will help to design future studies for better estimation of folic acid requirement. The study was the first application of AMS to human biomedical research of this kind.

Chapter One

Introduction: Folic acid, nutrition and metabolism

In its most basic form, the science of nutrition aims to define levels of nutrient intake required to prevent disease and to monitor populations and individuals to ensure this requirement is met. Difficulties in estimating nutrient requirement in a heterogeneous population necessitates safety factors to be incorporated into these requirements. Dietary habits that produce a discrepancy between required and actual intakes for prolonged periods can be expected to lead to clinical signs and symptoms.

Measuring the gap between nutrient requirement and nutrient intake helps health officials to develop public policies and dieticians to plan menus to close such gaps and minimize nutrient-related health risks. This presupposes that measures of nutrient requirement and intake can be made reliably. These measures include reliable methods of compiling food nutrient databases, measuring food consumption and estimating nutrient requirement (National Research Council, 1989; Hartman, 1996). Combined uncertainty in these measures can result in variable and inaccurate estimations of requirement and intake. More reliable estimates of these parameters must be made using newer and more vigorous analytical approaches (Santhosh-Kumar, 1995).

Estimating folate requirement and intake levels has posed a challenge to nutrition scientists. This has been due to the complicated biology of folate and the lack of sufficiently reliable analytical methods for measuring the folate content of foods, estimating intakes of folate and defining requirements (Gunter, 1996).

Folate compounds are a class of water-soluble vitamins required for health and normal growth. They are found in nature with different levels of oxidation, polyglutamate chain-length and have a transferable methyl moiety (Bailey, 1995). Folate functions as co-enzymes in a variety of single-carbon transfer reactions of nucleotide and amino acid synthesis (Ziegler, 1996). Inadequate folate intake or low blood folate concentrations are associated with a variety of clinical conditions such as anemia, neural tube defects, hyperhomocystenemia and some cancers.

Epidemiological studies have shown a relationship between folate nutrition and precancerous dysplastic changes in cervical and colorectal epithelia (Liu, 1995; Brock, 1988; Potischman, 1991). Folate deficiency in animals has been shown to increase the severity of carcinogen-induced colon cancer (Cravo, 1992). Recently, a large intervention study showed reduced incidence of colorectal adenomatous polyps with increased folate intake (Giovannucci, 1993).

Folate has also been implicated in the etiology of neural tube defects. In a randomized clinical trial a nutritional supplement containing folic acid reduced the incidence of spina bifida and anencephaly (Czeizel, 1992). In another study, folic acid supplemented to mothers of children with neural tube defects prevented the recurrence of another pregnancy complicated by neural tube defects (National Research Council, 1991).

Recently, high plasma homocysteine concentrations were shown to be associated with an increased risk of cardiovascular disease and stroke (Ueland, 1989; Graham, 1997). Plasma folic acid was found to be the strongest correlate of plasma homocysteine

(Selhub, 1993). Current intervention trials will help to address whether folic acid supplementation can reduce the risk for cardiovascular disease.

Further understanding of the role of folic acid in health and disease requires a better understanding of the dynamics and metabolism of this vitamin in healthy and diseased humans. The aims of this study were to develop a more specific approach for estimating folate concentration and to determine folate bioavailability and turnover in a healthy human subject. The first section describes the isolation of folate binding protein to high purity. The protein can be used to isolate and measure folate from biological samples such as plasma and tissues as well as folate in foods. The second section describes a kinetic study of the dynamics of folic acid in a human subject. The study was the first application of accelerator mass spectrometry to human nutrition research. Protocols were developed to take advantage of the phenomenal sensitivity of the instrument. Using a tracer-kinetic approach, the bioavailability and dynamics of a single oral dose of radiolabeled folic acid was determined in a healthy human subject. Models describing these dynamics were developed including a compartmental model. Folate requirement in humans, as well as genetic and environmental factors that influence these requirements can now be determined with greater confidence.

Literature cited

Bailey, L. B. (1995). *Folate in health and disease*. Dekker, New York.

Brock, K. E., Berry, G., Mock, P. A., MacLennan, R., Truswell, A. S. & Brinton, L. A. (1988). Nutrients in diet and plasma and risk of in situ cervical cancer. *Journal of the National Cancer Institute* **80,** 580-5.

Cravo, M. L., Mason, J. B., Dayal, Y., Hutchinson, M., Smith, D., Selhub, J. & Rosenberg, I. H. (1992). Folate deficiency enhances the development of colonic neoplasia in dimethylhydrazine-treated rats. *Cancer Research* **52,** 5002-6.

Czeizel, A. E. & Dudas, I. (1992). Prevention of the first occurrence of neural-tube defects by periconceptional vitamin supplementation. *New England Journal of Medicine* **327,** 1832-5.

Giovannucci, E., Stampfer, M. J., Colditz, G. A., Rimm, E. B., Trichopoulos, D., Rosner, B. A., Speizer, F. E. & Willett, W. C. (1993). Folate, methionine, and alcohol intake and risk of colorectal adenoma. *Journal of the National Cancer Institute* **85,** 875-84.

Graham, I. M., Daly, L. E., Refsum, H. M., Robinson, K., Brattstrom, L. E. & Ueland, P. M. (1997). Plasma homocysteine as a risk factor for vascular disease: The European Concerted Action Project. *JAMA* **277**.

Gunter, E. W., Bowman, B. A., Caudill, S. P., Twite, D. B., Adams, M. J. & Sampson, E. J. (1996). Results of an international round robin for serum and whole-blood folate. *Clin Chem* **42,** 1689-94.

Hartman, A. M., Block, G., Chan, W., Williams, J., McAdams, M., Banks, W. L., Jr. & Robbins, A. (1996). Reproducibility of a self-administered diet history questionnaire administered three times over three different seasons. *Nutr and Cancer* **25,** 305-15.

Liu, T., Soong, S. J., Alvarez, R. D. & Butterworth, C. E., Jr. (1995). A longitudinal analysis of human papillomavirus 16 infection, nutritional status, and cervical dysplasia progression. *Cancer Epidemiology, Biomarkers and Prevention* **4,** 373-80.

National Research Council. (1991). Prevention of neural tube defects: results of the Medical Research Council Vitamin Study. MRC Vitamin Study Research Group. *Lancet* **338,** 131-7.

National Research Council. (1989). *Recommended dietary allowances*. National Academy Press, Washington, D.C.Potischman, N., Brinton, L. A., Laiming, V. A., Reeves, W. C., Brenes, M. M., Herrero, R., Tenorio, F., de Britton, R. C. & Gaitan, E. (1991). A case-control study of serum folate levels and invasive cervical cancer. *Cancer Research* **51,** 4785-9.

Santhosh-Kumar, C. R., Deutsch, J. C., Hassell, K. L., Kolhouse, N. M. & Kolhouse, J. F. (1995). Quantitation of red blood cell folates by stable isotope dilution gas chromatography-mass spectrometry utilizing a folate internal standard. *Anal Biochem* **225,** 1-9.

Selhub, J., Jacques, P. F., Wilson, P. W., Rush, D. & Rosenberg, I. H. (1993). Vitamin status and intake as primary determinants of homocysteinemia in an elderly population. *Jama* **270,** 2693-8.

Ueland, P. M. & Refsum, H. (1989). Plasma homocysteine, a risk factor for vascular disease: plasma levels in health, disease, and drug therapy. *Journal of Laboratory and Clinical Medicine* **114,** 473-501.

Ziegler, E. E. & Filer, L. J. (1996). *Present knowledge in nutrition*. International Life Sciences Institute, Washington, D.C.

Chapter Two

Literature review: Folate Assays and Folate Binding Protein Purification

Folate Assays

Folate Binding Protein Purification

Folate Assays

Microbiological assay

The realization that some microbes require folate for growth spawned the development of the microbiological growth assay for folate. Several key advancements to the development of this assay were the formulation of growth media lacking folate, optimization of enzymatic procedures for hydrolyzing folate polyglutamates, adaptation of the procedure to microwell plates and establishment of *Lactobacillus casei* strains with antibiotic resistance.

The growth response of *Lactobacillus casei* is a measure of folate concentration in the media only if the media contains all the necessary factors for growth, except folate, which is introduced by the sample or standard. Any factor other than folate affecting the growth response reduces the specificity of the assay. This is a problem inherent to most biological assays of this type (Hunter, 1958; Snell, 1948). Indeed, thymidine and alanine were found to stimulate *L. casei* growth regardless of folic acid concentration (Broquist, 1949; Snell, 1945).

Originally, casein hydrolyzates (acid and enzymatic), dextrose and acetate formed the major components of the media with additional micronutrients to meet the organism's nutritional requirements. The composition of the media underwent several modifications as understanding of the nutritional requirements of the microorganism increased (Jukes, 1955; Landy, 1942; Stokes, 1949; Tamura, 1972; Teply, 1945). It was noted that casein contributed factors which influenced bacterial growth (Peeler, 1949). The casein hydrolyzate had to be treated with charcoal to remove some of these factors, yet, their

complete removal was never satisfactorily attained. Use of crystalline amino acids to formulate a defined growth media helped to minimize some of these external factors (Hutchings, 1943; Steele, 1949). These media, however, failed to meet growth rates as high as those attained by casein amino acids.

Another key component of the microbiological assay was the preparation of samples prior to analysis. The majority of serum folate, 5-methyltetrahydrofolic acid, was suitable for bacterial uptake. However, tissue and food folates existed as folate polyglutamates unsuitable for bacterial uptake and growth. The polyglutamate chain had to be enzymatically reduced to monoglutamate or diglutamate for bacterial uptake (Tamura, 1972). Polyglutamate chain length was reduced enzymatically to diglutamates by chicken pancreas extract (Kaferstein, 1972; Leichter, 1979) and monoglutamates by hog kidney extract (Bird, 1972).

Chicken pancreas folate hydrolase had a pH optimum of about 8.5 while the partially purified hog kidney folate hydrolase had optimum activity at about pH 4.7. Human and rat plasma folate hydrolases had pH optima of 4.5 (Lakshmaiah, 1975; Wolff, 1949). Whole blood folate was prepared by incubating lysed red blood cells with plasma (containing hydrolase) in a buffer at pH 4.5 containing ascorbic acid. Plasma folate concentration was measured separately and subtracted from total blood concentration to calculate folate concentration in red blood cells. Plasma folate contribution to total blood concentration was small, however, since the vast majority of blood folate was in the red blood cells.

In complex matrices such as food, additional enzymatic steps were included to ensure maximum folate extraction. Treatment with protease (EC 3.4.24.31) significantly

increased measured folate concentration by 61% in milk and 23 % in hog liver (Yamada, 1979). Foods rich in starch and glycogen produced 10 to 80 % higher folate values when treated with α-amylase (EC 3.2.1.1) (Cerna, 1983). These results were confirmed by DeSouza *et al.* who suggested the use of a triple-enzyme preparation of foods (DeSouza, 1990). A procedure using a triple-enzyme extraction protocol was soon developed and resulted in 51% higher folate values in tuna fish and 33% higher values in yogurt when compared to conjugase treatment alone (Martin, 1990). The authors concluded that unless such an extraction protocol is adopted food folate values may be underestimated. Recently, the triple-enzyme extraction protocol was compared to the conjugase method for the analysis of folate in four different food composites designed to be low in folate. Again, higher folate values were obtained by the triple-enzyme procedure, leading the authors to recommend revision of food folate tables using the triple-enzyme approach (Tamura, 1997).

One of the major drawbacks of the microbiological assay was long assay times involving many steps. Several milliliters of media were required for each sample which increased the time and effort required for preparation and sterilization of media and reagents. Another time-consuming step was assessment of the organism's growth response, usually measured spectrophotometrically.

These drawbacks were reduced when the assay procedure was adapted for use in 96-well microtiter plates (Newman, 1986). The modification reduced reagent cost and preparation time and made possible the analysis of hundreds of samples per day. The growth response was measured with computer-interfaced automated plate readers which simplified data collection and handling.

This protocol was further improved by use of glycerol-cryopreserved *L. casei* (Wilson, 1982) and sample handling modifications which reduced incubation time to 18 hours (Horne, 1988). Use of mylar plate sealers allowed mixing of the microorganisms prior to spectrophotometric reading without well-to-well contamination and eliminated the need for mixing by manual pipetting (O'Broin, 1992).

To further reduce cost and time associated with sterile techniques, a new *L. casei* strain was developed by transforming the ATCC 7469 strain with a plasmid containing a gene which conferred resistance to chloramphenicol antibiotic. This chloramphenicol resistant strain (NCIB 10463) was successfully used for determination of folate in serum and red blood cells in non-sterile environments (O'Broin, 1992).

The microbiological assay had great utility for the clinical diagnosis of folate deficiency in humans. Subjects with plasma folate <2 ng/mL and red blood cell folate <250 ng/mL were typically considered to have a low folate status (Gibson, 1990). The microbiological assay was capable of identifying these individuals since a large difference existed in their plasma or red blood cell folate concentrations compared to individuals with normal folate status. It was, however, unrealistic to use the assay to identify small differences in folate concentration because of limited assay precision.

Competitive binding assays

Although the microbiological assay was a useful tool for assessment of folate deficiency in individuals, in some clinical situations it was necessary to identify the folate status of an individual in a fastidious manner. The competitive binding assay has gained increasing popularity for rapid determination of folate concentration in plasma and red

blood cells. The assay is relatively cheap and hundreds of samples can be measured in a day.

The early 1970s saw the first development of competitive binding assays for the quantitative determination of folate concentration in serum and red blood cells (Archibald, 1972; Rothenberg, 1972; Waxman, 1971). Folate concentration was determined by adding a known, excess amount of folate binding protein (FBP) to an unknown sample, incubating for a short time and adding radiolabeled folic acid with known specific activity. The radiolabeled folic acid bound to the remaining sites to saturate FBP. Unbound radiolabeled folic acid was then removed by activated charcoal and the total radioactivity in the protein fraction measured by scintillation counting. The radioactivity was inversely proportional to the concentration of unlabeled folate in the unknown sample because folate from the sample competed with radiolabeled folic acid for a limited number of binding sites on FBP. A standard set of samples with known folate concentration was assayed in parallel to standardize the procedure for the quantification of folate in serum and red blood cells.

Waxman *et al.* first described a procedure to determine folate concentration by competitive-protein binding assay (Waxman, 1971). The principal requirement for this and other similar assays was the availability of a cheap source of folate binder. Milk folate binders met this requirement and were purified minimally to give a solution with high folate binding capacity. Instant powdered milk was resuspended in water (10 g/100 mL) and dialyzed against an isotonic solution for 60 hours at 4°C. The folate binding capacity of this solution was determined by its ability to bind to known amounts of ^{3}H-5-methyl-tetrahydrofolate (methyl-THFA).

Serum folate was assayed by incubating 0.4 mL serum with 0.6 mL saline buffer, 0.1 mL ^{3}H-5-methyl-THFA and 0.1 mL milk for 30 minutes at room temperature. Unbound ^{3}H-5-methyl THFA was removed by adsorption to hemoglobin-coated charcoal and centrifuged. The amount of radioactivity remaining in the supernatant was used to calculate the folate concentration in the serum sample by comparison to standard curves. Serum samples from 80 subjects ranged from 1 to 22 ng folate per milliliter serum. These values were sufficiently similar to values obtained by *Lactobacillus casei* microbiological assay to permit identification of subjects with low serum folate.

At lower serum folate concentrations the competitive-binding assay consistently yielded higher values. On the other hand, lower values were obtained by the competition assay at the higher end of folate concentrations. The authors attributed this to previous observations which showed a lower affinity of the *d*-form of the *dl*-5-methyl-THFA used to construct the standard curve (Ford, 1969). True folate values in serum could have been twice as high as values determined by the competition assay assuming only the *l*-form of 5-methyl-THFA bound to milk. Duplicate measurement of four serum samples resulted in less than 10 % variation. Methotrexate and folinic acid did not compete for the milk binder.

An advantage of the competitive binding assay was that folate concentration in the serum of individuals taking antibiotic medication could now be measured. Importantly, however, was that this procedure used a crude milk solution to bind folate. Since the specificity of the interactions between multiple milk binders and folate were not known, it could not be ruled out that factors other than folate could compete for binding sites and interfere with the competition assay to produce aberrant results.

To overcome this limitation Rothenberg *et al.* used milk binders that had been isolated from milk (Rothenberg, 1972). Pasteurized milk was processed by acidification to pH 4.8 with 5 percent glacial acetic acid and removal of the curd by filtration. Folate in the resulting whey was removed by reducing the pH to 2.5 with concentrated hydrochloric acid followed by addition of activated charcoal. After two hours of stirring at 4°C the charcoal-folate complex was removed by centrifugation. Proteins in the supernatant were precipitated by addition of ammonium sulfate to 45% saturation. Pelleted proteins were then resuspended in a small volume of 0.01 M borate buffer, pH 8.0, dialyzed against the same buffer for 18 hours at 4°C and assessed for binding capacity.

Observed increases in the specific-binding activity of this extract were partially due to co-isolation of β-lactoglobulin and other proteins in milk with a capacity to bind folate (Ford, 1967). The competitive assay procedure was essentially the same as the method discussed earlier (Waxman, 1971), with the exception that serum folate was incubated with the binder for at least two hours at room temperature before addition of the radiolabeled folate at 4°C. This modification minimized any dissociation of serum folate from the binder during the incubation period. It was, therefore, a sequential rather than a true competition assay.

The affinity of isolated folate binding proteins for methotrexate and formyl-tetrahydrofolic acid was substantially less than the affinity for folic acid and 5-methyl-THFA. The mean variation in the estimated value of duplicate serum samples was 6.8 % with a range of 1.1 to 23 %. Serum values determined by the competition assay were again approximately half the microbiological assay values.

This discrepancy had previously been attributed to possible differences in the binding affinity of the *d*- and *l*- forms of ^{3}H-5-methyl-THFA to the binding proteins (Waxman, 1971). However, this possibility was eliminated when it was observed that excess folate binder could bind 90 % of the *dl*-^{3}H-5-methyl-THFA, approximately equal to the purity of the radiolabeled compound. The authors concluded that there may exist other forms of serum folate with biological, but not binding, activity.

Using a powdered milk preparation described earlier (Waxman, 1971), serum milk folate concentration was compared to values obtained by the microbiological growth assay (Archibald, 1972). Although there was little difference between the mean of 30 samples, 6.2 ± 2.6 and 7.5 ± 4.2 ng/mL for *L. casei* and binding assays, respectively, the correlation coefficient between the two assays was only 0.61. The authors concluded, however, that the competitive binding assay was useful for diagnosis of folate deficiency since both assays identified the same low folate subjects (<3 ng/mL).

Some of the competitive binding assay discrepancy was explained by the observation that some serum proteins can bind to the ^{3}H-5-methyl-THFA. Subject-to-subject variability in the serum folate binding protein concentration added variation to the assay in an unpredictable manner. Some of this variability was reduced by first precipitating the proteins by heating in boiling water for 15 minutes.

Commercial kits utilizing milk FBP and intrinsic factor are now available and can simultaneously measure folate and vitamin B_{12} concentrations. This dual assay is important for identification of deficiencies associated with certain anemias. Although the kits have sufficient sensitivity for measuring folate in plasma (~0.5 ng/mL), the specificity and precision of the measurement were not ideal.

The issue of specificity was a problem with this and the microbiological assay because a folate response was being measured rather folate itself. In the case of the microbiological assay, the growth response was an indicator of folate concentration. However, factors other than folate have been shown to affect growth response (Broquist, 1949; Snell, 1945). Folate in the sample must be extracted from the matrix, dissociated from its binding proteins and reduced in glutamate chain-length before uptake by the organism. Sample-to-sample variability in these factors reduced the specificity of the assay so that the measured response did not directly correlate with folate concentration.

The competitive binding assay also measured a folate response rather than measuring folate directly. In this case, competition between folate and the radiolabeled tracer produced a response measured by scintillation counting. Folate in the sample was not measured directly (chemically). Any non-folate compounds capable of competing for the binder reduce the specificity of the assay. Bilirubin and plasma lipids and proteins at physiological concentrations have been shown to interfere with the determination of folate (Quantaphase II, BioRad Technical Bulletin). Methotrexate had sufficient cross-reactivity with FBP to interfere significantly with the assay.

The precision of the competitive binding assay was determined by duplicate measurement of control and serum samples. Intra-assay and inter-assay coefficients of variation for various commercial kits ranged from 4.0-11.1% and 6.0-12.4%, respectively (Staples, 1992). Others found intra-assay and inter-assay coefficients of variation ranging from 5.89-9.76% and 5.9-11.3%, respectively (Ciment, 1993; Bruzek, 1994). The accuracy of these assays was determined by comparison of results to results obtained by other commercial kits. Typical coefficients of correlation were 0.93 and higher.

Since there was no reference method to quantify folate concentration directly, the accuracy of these assays was relative and not absolute.

There was increasing effort to move away from the use of radiolabeled folate as a tracer in these competitive binding assays. Enzymes covalently linked to folate have been used as enzymatic tracers of folate whose activity can be measured by precursor-product relationships. Folate was traced by conjugating it to *o*-nitrophenol-β-D-galactopyranosidase and monitoring the hydrolysis of the enzyme's substrate, chlorophenol-red-β-D-galactopyranoside, at 405 nm. This assay (Microgenics, Concord, CA) was compared with a radioimmunoassay (Quantaphase, BioRad) and found to correlate well in serum samples ranging in folate concentration between 3 and 18 ng/mL. The intra-assay coefficient of variation was 2.5% and the inter-assay coefficient of variation ranged from 2.4 to 12.1% depending on folate concentration. (Ishiwata, 1994).

Folate covalently coupled to glucose-6-phosphate dehydrogenase (G6PDH) was used as a non-radioactive competitor of folate in competitive binding assays (Bachas, 1986). After removal of unbound tracer, the G6PDH–FBP complex was incubated under conditions that reduced NAD to NADH. The progress of this reaction was detected spectrophotometrically.

Recently, chemiluminescent compounds have become a popular choice for compound labeling because of the great sensitivity for their detection. A competitive bioluminescence assay that coupled bacterial luciferase to G6PDH was recently described (Huang, 1996). Folate from a sample competed with folate conjugated to G6PDH for folate binding protein. After removal of unbound tracer, NADH produced by G6PDH activity served as a substrate for luciferase to produce a luminescent signal. The

detection limit was in the 25 nanomolar range. Intra-assay coefficient of variation was 6.6%. Folate concentration in vitamin pills and culture media was within 10% of the claimed values.

HPLC of intact folate

Chemical approaches for determining folate concentration and identity involved more rigorous chromatographic techniques. Since samples of biological origin are a complex assortment of compounds, a more stringent sample preparation was required prior to analysis by high performance liquid chromatography.

In most cases, proteins were eliminated from the sample by precipitation with acid, heat or an organic solvent, while the oxidation state of folate was maintained by an antioxidant, typically ascorbic acid at a concentration of 1 mg/mL (Gregory, 1989; Newman, 1989). Folate was concentrated on ion-exchange resins and eluted with strong buffers (Duch, 1983; Gregory, 1984). A lyophilization step was required to concentrate the large volume of the eluent. The recoveries, however, were too low to make the procedure routine and reproducible.

Increased availability of solid phase extraction cartridges packed with a variety of reverse-phase, quaternary amine and phenyl sorbents permitted rapid and quantitative recovery of folate from biological samples (Rebello, 1987). Selhub *et al.* described a procedure for affinity isolation of folate from biological samples using immobilized folate binding protein covalently linked to a Sepharose matrix (Selhub, 1988). Affinity-isolated folate was then separated by reverse phase HPLC using tetrabutylammonium

dihydrogen phosphate (TBAP) as the ion pairing agent with detection by UV absorption at 280 nm (Selhub, 1989).

Tissue folates with polyglutamate chain lengths from 1 to 7 were resolved in a 40 minute chromatographic separation using a gradient solvent system consisting of water and acetonitrile containing 5 mM TBAP, 25 mM NaCl and 0.5 mM dithioerythritol, pH 6.8. This method was used for the determination of folate distribution in tissue extracts (Varela-Moreiras, 1991).

Chromatographically separated folate has been detected by UV absorbance, amperometric (Birmingham, 1983), fluorometric (Giulidori, 1981; Gounelle, 1989; Gregory, 1984) and electrochemical (Kohashi, 1986; Lankelma, 1980; Shimoda, 1992) detection methods in an attempt to increase specificity and sensitivity.

The most sensitive fluorometric detection of folate, with excitation at 290 nm and emission at 365 nm, had a detection limit of 0.16, 0.03 and 0.31 pmol for tetrahydrofolate, 5-methyltetrahydrofolate and 5-formyltetrahydrofolate, respectively (Gregory, 1984). Electrochemical detection was found to be useful only when the applied voltage was relatively low (Shimoda, 1992). Less selective detection of folate was observed when the applied voltage was above 300 mV.

Highly sensitive electrochemical detection was reported with detection limits of 6.8, 2.2 and 181 fmol for tetrahydrofolate, 5-methyltetrahydrofolate and folic acid, respectively (Kohashi, 1986). This method was used successfully for the detection of 5-methyltetrahydrofolate in plasma (Lucock, 1989) and tetrahydrofolate, 10-formyltetrahydrofolate and 5-mehtyltetrahydrofolate in rat bile (Shimoda, 1994). However, difficulties with background interference, mostly from the presence of ascorbic

acid, limited the applicability of this method for detection of folate in more complex biological matrices.

GC/MS of folate catabolites

Separation of folate by HPLC allowed the identification of individual folate molecules. This was in contrast with the microbiological assay that gave total folate concentration of the sample without regard to the chemical structure. There was, in fact, great interest in determining the total folate concentration rather than identifying individual folate compounds. Determining the total folate concentration in foods was important to the food industry where folate-supplemented foods were monitored for total folate concentration. Red blood cell total folate was used as a marker of folate status without regard to the folate form.

There was great need for an assay that measured total folate without identifying the folate form. These assays measured a common unique catabolite of folate, *para*-aminobenzoyl derivatives, by various mass spectrometric systems. Intact folate had to be first derivatized before mass spectrometric analysis because of their polar properties. Procedures for measuring nanogram quantities of intact folate by SIMS (Eicke, 1983a; Eicke, 1983b), FAB and MS/MS (Clifford, 1986) have been reported. Fluorinated derivatives of *para*-aminobenzoylglutamic acid standards were detected by single ion monitoring GC/MS with picogram sensitivity (Toth, 1988).

The difficulties in isolating folate catabolites from complex biological matrices were resolved by affinity-purification of folate from red blood cells (Santhosh-Kumar, 1995). In this procedure, red blood cells were heated to 102°C for 30 minutes in a 0.4%

ascorbic acid and 1% Triton X-100 buffer to extract the folate and remove proteins. The extract was mixed with a strong anion-exchange resin and poured into an empty column. The resin was washed and then incubated at 37°C with folate binding protein for 30 minutes in a solution of 0.1 M 2-mercaptoethanol, 2 M NaCl, 0.1 M ammonium bicarbonate, pH 9.6. The incubation condition favored the dissociation of folate from the anion-exchange resin for binding with folate binding protein. Bound folate was eluted from the binding protein with 0.2 M trifluoroacetic acid and heated to 110°C for 1 hour in 6 N HCl to chemically cleave all folates to *para*-aminobenzoic acid (PABA) and various pteridine and glutamic acid moieties. PABA was isolated over a strong cation-exchange resin, eluted with 5 M NH_4OH and derivatized with *N*-methyl-*N*-t-butyldimethylsilyl trifluoroacetamide and acetonitrile at 60°C for 30 minutes.

The PABA derivative was analyzed by GC/MS using selected ion monitoring of the $[M-57]^+$ ion (*m/z* 364). Bacterially synthesized folate from $[^2H_2]$PABA or $[^{13}C_6]$PABA precursors was isolated by folate binding protein affinity-chromatography and were added to the initial red blood cell extraction step as an internal standard. Intra-assay and inter-assay coefficients of variation were 4.7% and 4.5%, respectively. The limit of detection was 27 pmol folate, equivalent to the amount of folate in about 18 μL of whole blood.

Immunoassays

A completely different approach to estimate folate concentration was to use highly specific antibody-antiserum interactions. Antibodies that recognized and bound to folic acid were generated by coupling folic acid to a macromolecule, immunizing animals with

this antigen and isolating antiserum from blood (Jaton, 1967; Ricker, 1967; Rothenberg, 1969; Rubenstein, 1970). These antibodies, however, had low titer and specificity and were unsuitable for estimation of folate concentration. It was later recognized that the carrier conjugates influenced the type and avidity of the generated immunoglobulins (Butler, 1973; Siskind, 1966).

Folic acid conjugated to methylated bovine serum albumin was used to immunize rabbits (Hendel, 1981). Concentrations of folic acid, and dihydrofolic acid oxidized to folic acid, were determined in plasma, erythrocytes and urine using the antibodies obtained. The coefficient of variation varied between 4.01 and 14.6%.

To further enhance the specificity and immunogenecity, folic acid was esterified to ε-aminocaproic acid modified bovine serum albumin (Das Sarma, 1995a). The antibodies were used for direct measurement of serum folate in 96-well microtiter plates. Serum was heated to 50°C to disrupt interaction with folate binding protein, and folate measured by ELISA (Das Sarma, 1995b). The antibodies had >80% cross-reactivity with dihydrofolate and tetrahydrofolate but had no binding affinity for any 5-methyl derivatives of folate. Intra-assay coefficient of variation was 8.2%, while inter-assay coefficient of variation of duplicate samples measured on 6 different days was 13.3%. The method compared well with the microbiological assay and had a correlation coefficient of 0.99. The detection limit of the assay was 0.05 ng/mL.

Future directions

The issue of variability between assay types remains a problem. The microbiological growth assay is considered as the standard assay. Acceptance of new assay protocols is

contingent upon their close comparison with the microbiological assay. In this regard, the microbiological assay has become the standard assay. There is general agreement, however, that the lack of a true reference standard has stifled further advancements in our understanding of folate in fields as diverse as food science, clinical chemistry and pharmacokinetics.

A recent round robin assessment of inter- and intra-laboratory variability found large differences in the measured folate concentration of serum and red blood cell samples (Gunter, 1996). Six serum and six blood samples were prepared, ranging in folate concentration from about 4 to 60 nmol/L and 113 to 549 nmol/L, respectively. Aliquots were sent to 20 laboratories representing manufacturing, government, academic and clinical laboratories. Eight laboratories used the *L. casei* microbiological assay with either a culture tube or microtiter plate procedure. Another eight laboratories employed radioisotope competitive assay kits from three different manufacturers. Two laboratories used a chemiluminescent competitive assay kit. One laboratory used an ion capture procedure and another used an HPLC procedure with fluorescence detection.

Coefficient of variation for serum folate concentration measured by all the laboratories ranged from 17.9 to 48.0%. Within laboratory coefficient of variation ranged from 2.3 to 83.3%. The two low folate serum samples resulted in the largest variability. Measured serum folate concentration between the laboratories differed 2 to 9-fold, depending on the folate concentration. These values ranged from 0.90-8.36 nmol/L for the low folate samples and 24.12-81.20 nmol/L for the high folate samples.

Red blood cell coefficient of variation between all the laboratories ranged from 33.1 to 41.3%. Again, there was as much as a 9-fold difference between measured folate

concentration. The authors concluded that folate concentration measured by one laboratory could not be compared with values obtained by another laboratory without evaluating inter-laboratory differences. Further, method-specific ranges for normal and deficient folate status had to be clinically confirmed by independent hematological parameters such as hematocrit and red blood cell volume. The study underscored the need for development of a reference method for measuring folate concentration.

A reference method, such as a direct chemical assay, in conjunction with the availability of well-characterized reference standards, will help to establish uniformity in folate assessment protocols. Only then can multicenter studies with large sample numbers be conducted with confidence. Food folate databases should be updated for better estimation of folate intake by individuals and populations. These advances will lead to a more rational and confident reevaluation of folate requirement for humans.

Folate Binding Protein Purification

First identification

The existence of a folate binding protein was first proposed when it was found that factors in serum and milk can bind to folate (Ghitis, 1966; Ghitis, 1967; Metz, 1968). Ghitis *et al.* assessed the heat lability of folate in milk using *Lactobacillus casei* growth assay before and after boiling milk in the presence of ascorbic acid. They observed that milk folate existed in three fractions, each with a different degree of heat lability. Moreover, activated charcoal could bind milk folate only after the milk had been boiled. They concluded that folate in milk did not exist in a free form, rather, it was bound to a large molecule of unknown identity (Ghitis, 1966). Boiling disrupted this interaction generating free folate that could bind to activated charcoal.

To further characterize this folate binding factor in milk, boiled or autoclaved milk was assessed for its capacity to bind various folate molecules (Ghitis, 1967). Milk exhibited two binding properties for folate, a highly specific interaction that resisted ligand dissociation by autoclaving and a second less specific interaction that lost its association with folate upon boiling or autoclaving. The authors explained this by the existence of one or more binding proteins.

To facilitate further identification of these binders in milk and serum, Metz *et al.* developed a method that used ^{3}H-folic acid to trace the activity of the folate binders (Metz, 1968). Milk was analyzed whole or divided into four fractions by centrifugation at 30,000 rpm. Samples (0.5 mL) were incubated with 20 to 50 ng ^{3}H-folic acid for 15 minutes at room temperature and unbound ^{3}H-folic acid was removed by adding dextran-

coated charcoal followed by centrifugation. ^{3}H-Folic acid binding capacity was determined by measuring the amount of radioactivity remaining in the supernatant. Milk binding capacity was found to be in the range of 46-62 ng ^{3}H-folate/mL milk. The top three fractions of centrifuged milk had similar binding capacities.

Serum was autoclaved in an equal volume of 0.05 M phosphate buffer, pH 6.1, containing 1% ascorbate. The serum was then incubated with 20 ng ^{3}H-folic acid and processed as before. This resulted in a negligible amount of ^{3}H-folic acid remaining in the supernatant, indicating poor ^{3}H-folic acid binding in autoclaved serum.

This supported previous observations in humans where intravenously injected folic acid was cleared out of plasma within 3 minutes, as determined by microbiological assay (Chanarin, 1958; Metz, 1961). Poor folic acid binding by serum in conjunction with high affinity tissue receptors for folate could explain the rapid plasma clearance of injected folic acid (Metz, 1968). However, it was not known at the time that the folate binders in serum were in fact proteins. Autoclaving had denatured the serum proteins resulting in the negligible binding capacity for ^{3}H-folic acid.

Folate binding protein purification

The availability of radioisotopically labeled folic acid allowed further advancements in fractionation of the binders in milk. Milk was mixed with ^{3}H-folic acid, fractionated by DEAE cellulose chromatography and measured for radioactivity. Reitief *et al.* used this procedure to collect six consecutive fractions of milk proteins incubated with ^{3}H-folic acid by eluting with 0.06 M phosphate buffer, pH 6.3. These fractions contained gamma globulin, β_{2A} β_{1}, and albumin (Reitief, 1967). Five more fractions were collected by

eluting with 1.0 M NaCl and found to contain alpha globulin and macroglobulin. Radioactivity was measured by scintillation counting and indicated the majority of ^{3}H-folic acid eluted mainly in the phosphate fractions. This was supported by earlier reports that found the majority of folate binding activity in milk fractionated by DEAE cellulose chromatography was associated with the β-lactoglobulin fraction of milk (Ford, 1967).

Further attempts were made to isolate the folate binding factor in milk by a combination of chromatographic and gel filtration techniques. The most common source of folate binder was fresh bovine or goat milk because of their relatively high binding capacity. Whey was commonly produced by acid precipitation of caseins and the clarified whey further processed to enrich the folate binding protein (FBP).

Ammonium sulfate precipitation was commonly employed as a secondary purification step. This two-step procedure first produced a precipitate upon addition of ammonium sulfate to the whey at a concentration of about 45% saturation. This precipitate was removed by centrifugation and the concentration of ammonium sulfate increased to about 60% saturation to precipitate the majority of the remaining proteins, including FBP. The precipitates were centrifuged and resuspended in a smaller volume of a suitable buffer at a pH ~7. This procedure produced an extract of milk that retained the majority of the folate binding capacity of milk and was suitable for further purification of FBP.

Folate binding protein was further purified using DEAE-cellulose chromatography and Sephadex G-150 gel filtration yielding a mixture of several proteins as identified by gel electrophoresis. Only one minor component of this mixture had a strong and specific capacity to bind folate (Ford, 1969a; Ford, 1969b).

To further isolate and enrich FBP, affinity chromatography was employed to specifically isolate proteins that bind to folic acid. Following the procedure of Cuatrecasas (Cuatrecasas, 1968), agarose was activated with cyanogen bromide and folic acid coupled to the *o*-aminohexyl derivatives of the agarose by carbodiimide condensation (Salter, 1972).

Whey proteins purified by DEAE-cellulose chromatography were added to the folic acid affinity agarose and mixed as a slurry. The pH was dropped to 3.6 with HCl to dissociate bound native folate that would interfere with FBP-affinity matrix interaction. Upon adjustment of the pH back to 7.0, a majority of the FBP bound to the folic acid of the affinity matrix. The slurry was then packed into a column and washed successively with buffers of increasing ionic strength. FBP eluted from the affinity matrix by addition of 8 M urea at pH 5. The authors reported a 32-fold enrichment in folate binding capacity of the DEAE-cellulose fraction compared to whey and a 601-fold enrichment after affinity purification.

Modifications to this procedure have been developed for folic acid-affinity chromatographic purification of human milk FBP (Waxman, 1975b), goat milk (Rubinoff, 1977) and umbilical cord serum (Kamen, 1975b). Methotrexate, an analog of folic acid (Goldman, 1968), was also used as an affinity ligand for the purification of dihydrofolate reductases (Mell, 1968; Whiteley, 1972), FBP from goat milk (Selhub, 1973), human umbilical cord serum (Kamen, 1975b) and dihydropteridine reductase from rat and sheep liver (Webber, 1978). Methotrexate agarose is now commercially available and commonly used for affinity purification of a variety of folate binding proteins.

Determination of binding capacity

Purification of proteins by any method required assessment of the degree of enrichment of the target protein as well as its purity. Enrichment was calculated as the ratio of the target protein to total protein in the sample. This term is known as the specific activity of the protein. The activity can be assayed depending on the function of the protein. In the case of FBP, the total folate binding capacity was a measure of the amount of FBP in the sample.

Total binding capacity assays were developed for a variety of binding proteins and were based on the same basic principle. Typically, the sample to be assayed was mixed with an excess amount of radiolabeled ligand under conditions that favor binding. Unbound ligand was removed and total amount of radioactivity remaining in the sample was measured by scintillation counting. If the specific activity of the radiolabeled ligand was known, the concentration of the binding protein could be determined assuming the stochiometry of the interaction is known. In the case of FBP, one molecule of folate could bind to one molecule of FBP since there was one folate binding site on the protein.

The folate binding capacity measurement of a protein preparation was an indicator of the degree of its enrichment. Salter *et al.* measured the specific folate-binding capacity of samples along their purification scheme (Salter, 1972). Whey extract had a specific folate-binding activity of 0.006 μg folic acid/absorbance unit of protein. This value increased to 0.195 after DEAE-cellulose isolation and 3.64 after affinity chromatographic isolation of FBP corresponding to a 32-fold and 601-fold increase in FBP enrichment, respectively.

FBP was enriched 150-fold by a one-step DEAE-cellulose isolation of commercially available bovine ß-lactoglobulin (Waxman, 1975a). FBP from clarified human milk was purified using an affinity column followed by DEAE-cellulose chromatography resulting in a 1,000 and 10,000-fold enrichment, respectively (Waxman, 1975b). Rubinoff *et al.* isolated FBP from clarified goat milk using a similar purification scheme resulting in a 260 and 1,200-fold increase in FBP specific activity (Rubinoff, 1977). Folate binders in human umbilical cord serum (Kamen, 1975b) and hog kidney (Kamen, 1975a) have been enriched by similar methods 10,000 and 50,000-fold, respectively.

Determination of purity

Although the specific activity was an important measure of target protein enrichment along the purification process it was a poor indicator of purity. It was misleading to assume purity without checking for it, even in purification steps such as affinity chromatography where target protein function was used to aid the purification. The most common way to determine protein purity was by electrophoretic methods. Separated proteins were visualized by staining with dyes such as Coomassie.

Early attempts to purify FBP by DEAE-cellulose and gel filtration resulted in a preparation that was 'still grossly impure' (Ford, 1969a). Addition of an affinity chromatography step to this procedure resulted in a product with one main component and traces of impurities after separation by thin-layer starch gel electrophoresis (Salter, 1972). DEAE-cellulose isolated FBP from commercially purified bovine β-lactoglobulin produced three double bands after sodium dodecyl sulfate polyacrylamide gel

electrophoresis (SDS-PAGE) and three peaks after isoelectric focusing (pI values of 6.8, 7.5, 8.2) (Waxman, 1975a). Goat milk enriched 1,200-fold produced a single and distinct band by SDS-PAGE and 3 peaks by isoelectric focusing (pI values of 6.6, 7.3, 8.4) (Rubinoff, 1977).

These early studies showed that affinity chromatography increased the specific activity of FBP by three orders of magnitude resulting in a highly purified product. However, SDS-PAGE and isoelectric focusing of the purified FBP did not always indicate a homogeneous protein population. Rather, multiple peaks were observed after isoelectric focusing and represented isoproteins of FBP with varying carbohydrate content (Waxman, 1975b).

Determination of molecular weight

There was considerable discrepancy in determinations of the molecular weight of milk FBP. Gel filtration in Sephadex was used to separate proteins according to size. This technique was superceded by SDS-PAGE since the migration of a protein in an electrophoretic field was dependent on its charge-to-mass ratio. Addition of sodium dodecyl sulfate fulfilled two requirements. Firstly, the detergent eliminated differences in migration as a result of protein shape by disrupting the tertiary structure of the protein. Secondly, the detergent imparted a large negative charge to the protein so that it could migrate towards the anode. Any differences in the overall charge of the protein at the buffer pH were also eliminated. Since differences in the shape or charge of the protein were eliminated, migration became dependent on mass alone. The molecular weight of

milk FBP could then be estimated using proteins of known molecular weight as standards.

The molecular weight of FBP was reported in the literature to be about 35 kDa. Using gel filtration, Ford *et al.* reported the molecular weight of two bovine milk proteins with folate binding activity to be about 38 and 76 kDa, suggesting the latter was composed of a dimer of the smaller protein (Ford, 1969a). Other gel filtration estimates of the molecular weight of FBP were 35 kDa (Salter, 1972) and 36 kDa (Waxman, 1975a).

Waxman *et al.* described a high molecular weight FBP in human milk with a molecular weight >200 kDa as estimated by gel filtration (Waxman, 1975b). They also reported three double-bands of FBP with molecular weights of 87/80, 36.5/30 and 19/11.5 kDa as estimated by SDS-PAGE. Goat milk FBP had a molecular weight of 37 kDa by gel filtration and 38 kDa by SDS-PAGE (Rubinoff, 1977). Sedimentation equilibrium ultracentrifugation determined bovine milk FBP to have a molecular weight of 30 ±2 kDa (Svendson, 1979). Salter *et al.* reported the molecular weight of bovine FBP to be 35 ±1.5 kDa by SDS-PAGE (Salter, 1981).

The discrepancies in the molecular weight of milk FBP could be explained by the low resolution in the estimation technique. The FBP bands produced by SDS-PAGE were diffuse rather than distinct and sometimes showed up as double-bands (Waxman, 1975b). This made estimation of the molecular weight difficult since there was a heterogeneous population of proteins with varying molecular weights. This was likely due to glycosylation with varying amounts of carbohydrate.

Amino acid sequence

Identification of the amino acid sequence made it possible to calculate the molecular weight of the peptide moiety. The amino acid compositions of goat and bovine milk FBP were first identified by acid hydrolysis and amino acid analysis (Rubinoff, 1977; Svendson, 1979). Goat FBP was estimated to contain 22% carbohydrate and bovine FBP 3% carbohydrate. The carbohydrate content was calculated as the difference between the FBP molecular weight determined by SDS-PAGE and the predicted molecular weight of the non-glycosylated protein. It was, therefore, an average of a heterogeneous population of the FBP.

Partial amino acid sequences of bovine FBP were first identified by Edman degradation (Salter, 1981; Svendson, 1979). Sequence homology between bovine and human milk FBP was demonstrated when the partial human sequence became available (Antony, 1982; Svendson, 1982). Finally, the complete amino acid sequence of bovine FBP was identified and contained a single 222 amino acid polypeptide with eight disulfide bonds (Svendson, 1984). The peptides had a molecular weight of 25.7 kDa and carbohydrates comprised the remaining portion to give a total of ~30 kDa.

Folate binding protein function

While FBP had been sequenced and identified as a glycoprotein, its function remained a mystery. It was known that FBP concentration was higher in the colustrum of goat milk immediately postpartum than later in lactation (Ford, 1972). FBP in milk could prevent bacterial uptake of folate (Ford, 1974). It was speculated that FBP might help to

maximize folate bioavailability in the suckling animal by preventing bacterial uptake of the vitamin as well as aiding folate absorption from the intestinal lumen.

Sources other than milk have been found to contain folate binding proteins. Human patients with chronic granulocytic leukemia had serum and leukocyte lysates with a capacity to bind to added radiolabeled folic acid (Rothenberg, 1970). This binder had a molecular weight greater than 50 kDa and was the first evidence for the existence of a separate folate binding protein localized to cells distinguishable from cellular dihydrofolate reductase. Soon after, the properties of folate binding factors in the serum of subjects with folate deficiency were characterized (Waxman, 1973). Unsaturated serum folate binder had also been identified in patients with uremia, chronic alcohol liver disease, ulcerative colitis and carcinomas (Bentsen, 1990; Hines, 1973; Mantzos, 1975).

Cellular folate binders have been identified in a number of tissues. Isolated small intestinal cells were shown to have a capacity to bind to folate (Leslie, 1972). The presence of a liver folate binder was first described after isolation of a radiolabeled protein fraction from the liver of rats injected with radiolabeled folic acid (Corrocher, 1974; Zamierowski, 1974). Kidney brush-border folate binder was purified, characterized and postulated to aid in the reabsorption of folate from urine (Kamen, 1986; Selhub, 1984). Hog and rabbit choroid plexus were shown to have a saturable and specific transport mechanism for folate (Chen, 1975; Spector, 1975). This led to isolation of a folate binder from human cerebrospinal fluid with a molecular weight of about 26 kDa (Hansen, 1985). Human placenta folate binder was later isolated and localized to the plasma membrane fraction of the cell (Antony, 1981; Zwiener, 1992).

The findings of McHugh and Chen that cellular high-affinity folate binders were primarily localized to the plasma membrane significantly advanced understanding of the function of these binders (McHugh, 1979). Recent evidence suggested that these binders were localized to the plasma membrane because the protein underwent post-translational modifications that added a phosphatidyl-inositol moiety, making the molecule more hydrophobic. These membrane-soluble folate binders were considered to function as receptors aiding in the accumulation and possibly regulation of intracellular folate. The biochemistry and molecular biology of these receptors have been reviewed (Weitman, 1994; Antony, 1992).

Literature Cited

Antony, A. C. (1992). The biological chemistry of folate receptors. *Blood* **79,** 2807-20.

Antony, A. C., Utley, C. S., Marcell, P. D. & Kolhouse, J. F. (1982). Isolation, characterization, and comparison of the solubilized particulate and soluble folate binding proteins from human milk. *J Biol Chem* **257,** 10081-9.

Antony, A. C., Utley, C., Van Horne, K. C. & Kolhouse, J. F. (1981). Isolation and characterization of a folate receptor from human placenta. *J Biol Chem* **256,** 9684-92.

Archibald, E. L., Mincey, E. K. & Morrison, R. T. (1972). Estimation of serum folate levels by competitive protein binding assay. *Clin Biochem* **5,** 232-41.

Archibald, E. L., Mincey, E. K. & Morrison, R. T. (1972). Estimation of serum folate levels by competitive protein binding assay. *Clin Biochem* **5,** 232-41.

Bachas, L. G. & Meyerhoff, M. E. (1986). Homogeneous enzyme-linked competitive binding assay for the rapid determination of folate in vitamin tablets. *Anal Chem* **58,** 956-961.

Bentsen, K. D., Hansen, S. I., Holm, J. & Lyngbye, J. (1990). Abnormalities in folate binding pattern of serum from a pateint with megaloblastic anemia and folate deficiency. *Clin Chim Acta* **109,** 225-8.

Bird, O. D. & McGlohon, V. M. (1972). *Analytical Microbiology*. Academic Press, London.

Birmingham, B. K. & Greene, D. S. (1983). Analysis of folinic acid in human serum using high-performance liquid chromatography with amperometric detection. *J Pharm Sci* **72,** 1306-9.

Broquist, H. P., Stockstad, E. L. R., Hoffman, E. E., Belt, M. & Jukes, T. H. (1949). Some observations on growth factors required by *Leuconstoc citrovorum*. *Proc Soc Exp Biol Med* **71,** 549-552.

Bruzek, D., Harding, S. & Chan, D. W. (1994). Evaluation of a serum folate assay on the ACCESS Chemiluminescent Immunoassay System. *Clinical Chemistry* **40,** 1024.

Butler, V. P., Jr. & Beiser, S. M. (1973). Antibodies to small molecules: biological and clinical applications. *Adv Immunol* **17,** 255-310.

Cerna, L. & Kas, J. (1983). New conception of folacin assay in starch or glycogen containing food samples. *Nahrung* **10,** 957-64.

Chanarin, I., Mollin, D. L. & Anderson, B. B. (1958). The clearance from plasma of folic acid injected intravenously in normal subjects and patients with megaloblastic anemia. *Brit J Haematol* **4,** 435.

Chen, C. P. & Wagner, C. (1975). Folate transport in the choroid plexus. *Life Sci* **16,** 1571-81.

Ciment, P. R., O'Neil, M. T., Ingram, K., Jr. & Stewart, A. P. (1993). Performance of the Ciba-Corning Acs 180 Folate Assay and Comparison To Becton Dickinson Simultrac-S Folate. *Clinical Chemistry* **39,** 1254.

Clifford, A. J., Jones, A. D. & Missler, S. R. (1986). . In *34th Annual Conf. on Mass Spectrometry and Allied Topics*.

Corrocher, R., De Sandre, G., Pacor, M. L. & Hoffbrand, A. V. (1974). Hepatic protein binding of folate. *Clin Sci Mol Med* **46,** 551-4.

Cuatrecasas, P., Wilchek, M. & Anfinsen, C. (1968). Selective enzyme purification by affinity chromatography. *Proceedings of the National Academy of Sciences of the United States of America* **61,** 636-43.

Das Sarma, J., Duttagupta, C., Ali, E. & Dhar, T. K. (1995a). Antibody to folic acid: increased specificity and sensitivity in ELISA by using epsilon-aminocaproic acid modified BSA as the carrier protein. *J Immunol Methods* **184,** 1-6.

Das Sarma, J., Duttagupta, C., Ali, E. & Dhar, T. K. (1995b). Direct microtitre plate enzyme immunoassay of folic acid without heat denaturation of serum. *J Immunol Methods* **184,** 7-14.

DeSouza, S. & Eitenmiller, R. (1990). Effects of different enzyme treatments on extraction of total folate from various foods prior to microbiological assay and radioassay. *J Micronutr Anal* **7,** 37-57.

Duch, D. S., Bowers, S. W. & Nichol, C. A. (1983). Analysis of folate cofactor levels in tissues using high-performance liquid chromatography. *Anal Biochem* **130,** 385-92.

Eicke, A., Anders, V., Junack, M., Sichtermann, W. & Beninghoven, A. (1983a). *Anal Chem* **55,** 178.

Eicke, A., Anders, V., Junack, M., Sichtermann, W. & Beninghoven, A. (1983b). *Int J Mass Spectrom Ion Phys* **46,** 479.

Ford, J. E. & Salter, D. N. (1967). *Rep. Natn. Inst. Res. Dairy* , 134.

Ford, J. E. (1974). Some observations on the possible nutritional significance of vitamin B12-and folate-binding proteins in milk. *Br J Nutr* **31,** 243-57.

Ford, J. E., Knaggs, G. S., Salter, D. N. & Scott, K. J. (1972). Folate nutrition in the kid. *Br J Nutr* **27,** 571-83.

Ford, J. E., Salter, D. N. & Scott, K. J. (1969a). The folate-binding protein in milk. *Journal of Dairy Research* **36,** 435-446.

Ford, J. E., Salter, D. N. & Scott, K. J. (1969b). A folate-protein complex in cow's milk. *Proc Nutr Soc* **28,** 39A-40A.

Ghitis, J. (1966). The labile folate of milk. *Am J Clin Nutr* **18,** 452.

Ghitis, J. (1967). The folate binding in milk. *Am J Clin Nutr* **20,** 1-4.

Gibson, R. S. (1990). *Principles of Nutritional Assessment*. Oxford University Press, New York.

Giulidori, P., Galli-Kienle, M. & Stramentinoli, G. (1981). Liquid-chromatographic monitoring of 5-methyltetrahydrofolate in plasma. *Clin Chem* **27,** 2041-3.

Goldman, I. D. & Mehterly, L. H. Membrane transport of antineoplastic agents. In *International Encyclopedia of Pharmacology and Therapeutics*, pp. 283-302. Pergamon Press, Oxford.

Goldman, I. D., Lichtenstein, N. S. & Oliverio, V. T. (1968). Carrier-mediated transport of the folic acid analogue, methotrexate, in the L1210 leukemia cell. *J Biol Chem* **243,** 5007-17.

Gounelle, J. C., Ladjimi, H. & Prognon, P. (1989). A rapid and specific extraction procedure for folates determination in rat liver and analysis by high-performance liquid chromatography with fluorometric detection. *Anal Biochem* **176,** 406-11.

Gregory, J. F. (1989). Chemical and nutritional aspects of folate research: analytical procedures, methods of folate synthesis, stability, and bioavailability of dietary folates. *Adv Food Nutr Res* **33,** 1-101.

Gregory, J. F., Sartain, D. B. & Day, B. P. (1984). Fluorometric determination of folacin in biological materials using high performance liquid chromatography. *J Nutr* **114,** 341-53.

Gunter, E. W., Bowman, B. A., Caudill, S. P., Twite, D. B., Adams, M. J. & Sampson, E. J. (1996). Results of an international round robin for serum and whole-blood folate. *Clin Chem* **42,** 1689-94.

Hansen, S. I., Holm, J. & Lyngbye, J. (1985). A high-affinity folate binding protein in human cerebrospinal fluid. *Acta Neurol Scand* **71,** 133-5.

Hendel, J. (1981). Radioimmunoassay for pteroylglutamic acid. *Clin Chem* **27,** 701-703.

Hines, J. D., Kamen, B. A. & Caston, J. D. (1973). Abnormal folate binding proteins in azotemic pateints. *Blood* **42,** 997.

Horne, D. W. & Patterson, D. (1988). Lactobacillus casei microbiological assay of folic acid derivatives in 96-well microtiter plates. *Clin Chem* **34,** 2357-9.

Huang, W., Feltus, A., Witkowski, A. & Daunert, S. (1996). Homogeneous bioluminescence competitive binding assay for folate based on a coupled glucose-6-phosphate dehydrogenase-bacterial luciferase enzyme system. *Anal Chem* **68,** 1646-1650.

Hunter, S. H., Cury, A. & Baker, H. (1958). Microbiological Assays. *Anal Chem* **30,** 849-866.

Hutchings, B. L. & Peterson, W. H. (1943). Amino acid requirements of *Lactobacillus casei*. *Proc Soc Exp Biol Med* **52,** 36-8.

Ishiwata, Y., Yasuda, K., Ikeda, R. & Endo, N. (1994). Comparison between chemiluminescence receptor assay (CLIA) and cloned enzyme donor immunoassay (CEDIA) on serum vitamin B12 and folate. *Clinical Chemistry* **40,** 1039.

Jaton, J. C. & Ungar-Waron, H. (1967). Antibodies to folic acid and methotrexate obtained with conjugates of synthetic polypeptides. *Arch Biochem Biophys* **122,** 157-163.

Jukes, T. H. (1955). Assay of compounds with folic acid activity. *Methods Biochem Anal* **2,** 121-151.

Kaferstein, H. & Jaenicke, L. (1972). Gamma glutamyl carboxypeptidase from chicken pancreas. *Hoppe Seylers Z Physiol Chem* **353,** 1153-8.

Kamen, B. A. & Caston, J. D. (1975a). Identification of a folate binder in hog kidney. *J Biol Chem* **250,** 2203-5.

Kamen, B. A. & Caston, J. D. (1975b). Purification of folate binding factor in normal umbilical cord serum. *Proc Natl Acad Sci U S A* **72,** 4261-4.

Kamen, B. A. & Caston, J. D. (1986). Properties of a folate binding protein (FBP) isolated from porcine kidney. *Biochem Pharmacol* **35,** 2323-9.

Kohashi, M., Inoue, K., Sotobayashi, H. & Iwai, K. (1986). Microdetermination of folate monoglutamates in serum by liquid chromatography with electrochemical detection. *J Chromatogr* **382,** 303-7.

Lakshmaiah, N. & Ramasastri, B. V. (1975). Folic acid conjugase from Plasma. I. Partial purification and properties. *International Journal for Vitamin and Nutrition Research* **45,** 183-193.

Landy, M. & Dicken, D. M. (1942). A microbiological assay method for six B vitamins using *Lactobacillus casei* and a medium of essentially known composition. *J Lab Clin Med* **17,** 1086-1092.

Lankelma, J., van der Kleijn, E. & Jansen, M. J. (1980). Determination of 5-methyltetrahydrofolic acid in plasma and spinal fluid by high-performance liquid chromatography, using on-column concentration and electrochemical detection. *J Chromatogr* **182,** 35-45.

Leichter, J., Landymore, A. F. & Krumdieck, C. L. (1979). Folate conjugase activity in fresh vegetables and its effect on the determination of free folate content. *Am J Clin Nutr* **32,** 92-5.

Leslie, G. I. & Rowe, P. B. (1972). Folate binding by the brush border membrane proteins of small intestinal epithelial cells. *Biochemistry* **11,** 1696-703.

Lucock, M. D., Hartley, R. & Smithells, R. W. (1989). A rapid and specific HPLC-electrochemical method for the determination of endogenous 5-methyltetrahydrofolic acid in plasma using solid phase sample preparation with internal standardization. *Biomed Chromatogr* **3,** 58-63.

Mantzos, J. (1975). Radioassay of serum folate with use of pig plasma folate binders. *Acta Haematol* **54,** 289-96.

Martin, J. I., Landen, W. O., Jr., Soliman, A. G. & Eitenmiller, R. R. (1990). Application of a tri-enzyme extraction for total folate determination in foods. *J Assoc Off Anal Chem* **73,** 805-8.

McHugh, M. & Cheng, Y. C. (1979). Demonstration of a high affinity folate binder in human cell membranes and its characterization in cultured human KB cells. *J Biol Chem* **254,** 11312-8.

Mell, G. P., Whiteley, J. M. & Huennekens, F. M. (1968). Purification of dihydrofolate reductase via amethopterin-aminoethyl starch. *J Biol Chem* **243,** 6074-5.

Metz, J., Stevens, K., Krawtiz, S. & Brandt, V. (1961). The plasma clearance of injected doses of folic acid as an index of folic acid deficiency. *J Clin Pathol* **14,** 622.

Metz, J., Zalusky, R. & Herbert, V. (1968). Folic acid binding by serum and milk. *American Journal of Clinical Nutrition* **21,** 289-97.

Newman, E. M. & Tsai, J. F. (1986). Microbiological analysis of 5-formyltetrahydrofolic acid and other folates using an automatic 96-well plate reader. *Anal Biochem* **154,** 509-15.

Newman, E. M., Straw, J. A. & Doroshow, J. H. (1989). Pharmacokinetics of diastereoisomers of (6R,S)-folinic acid (leucovorin) in humans during constant high-dose intravenous infusion. *Cancer Res* **49,** 5755-60.

O'Broin, S. D. & Kelleher, B. (1992). Microbiological assay on microtitre plates of folate in serum and red cells. *J Clin Pathol* **45,** 344-7.

Peeler, H. T., Daniel, L. J., Norris, L. C. & Heuse, G. F. (1949). Unidentified factors requires by *Lactobacillus casei*. *J Biol Chem* **177,** 905-916.

Rebello, T. (1987). Trace enrichment of biological folates on solid-phase adsorption cartridges and analysis by high-pressure liquid chromatography. *Anal Biochem* **166,** 55-64.

Reitief, F. P., Gottlieb, C. W., Kochwa, S., Pratt, P. W. & Herbert, V. (1967). Separation of vitamin B 12-binding proteins of serum, gastric juice and saliva by rapid DEAE cellulose chromatography. *Blood* **29,** 501-16.

Ricker, R. & Stollar, B. D. (1967). Antibodies reactive with specific folic acid determinants. *Biochemistry* **6,** 2001-2005.

Rothenberg, S. P. (1970). A macromolecular factor in some leukemic cells which binds folic acid. *Proc Soc Exp Biol Med* **133,** 428-32.

Rothenberg, S. P., DaCosta, M. & Rosenberg, Z. (1972). A radioassay for serum folate: use of a two-phase sequential-incubation, ligand-binding system. *N Engl J Med* **286,** 1335-9.

Rothenberg, S. P., Gizis, F. & Kamen, B. (1969). Antibodies against folic acid. I. In vitro biophysical effect. *J Lab Clin Med* **74,** 662-671.

Rubenstein, W. A. & Little, J. R. (1970). Properties of the active sites of antibodies specific for folic acid. *Biochemistry* **9,** 2106-2114.

Rubinoff, M., Schreiber, C. & Waxman, S. (1977). The isolation and characterization of the folate binding protein from goat milk. *FEBS Lett* **75,** 244-8.

Salter, D. N., Ford, J. E., Scott, K. J. & Andrews, P. (1972). Isolation of the Folate-Binding Protein from cow's milk by the use of Affinity Chromatography. *FEBS Letters* **20,** 302-6.

Salter, D. N., Scott, K. J., Slade, H. & Andrews, P. (1981). The preparation and properties of folate-binding protein from cow's milk. *Biochem J* **193,** 469-76.

Santhosh-Kumar, C. R., Deutsch, J. C., Hassell, K. L., Kolhouse, N. M. & Kolhouse, J. F. (1995). Quantitation of red blood cell folates by stable isotope dilution gas

chromatography-mass spectrometry utilizing a folate internal standard. *Anal Biochem* **225,** 1-9.

Selhub, J. & Franklin, W. A. (1984). The folate-binding protein of rat kidney. Purification, properties, and cellular distribution. *J Biol Chem* **259,** 6601-6.

Selhub, J. & Grossowicz, N. (1973). Chemical fixation of folate binding protein to activated sepharose. *FEBS Lett* **35,** 76-8.

Selhub, J. (1989). Determination of tissue folate composition by affinity chromatography followed by high-pressure ion pair liquid chromatography. *Anal Biochem* **182,** 84-93.

Selhub, J., Darcy-Vrillon, B. & Fell, D. (1988). Affinity chromatography of naturally occurring folate derivatives. *Anal Biochem* **168,** 247-51.

Shimoda, M. (1992). Simultaneous determination of tetrahydrofolate and N5-methyltetrahydrofolate in pig plasma by high-performance liquid chromatography with electrochemical detection. *J Vet Med Sci* **54,** 249-53.

Shimoda, M., Shin, H. C. & Kokue, E. (1994). Simultaneous determination of tetrahydrofolate, 10-formyltetrahydrofolate and 5-methyltetrahydrofolate in rat bile by high-performance liquid chromatography with electrochemical detection. *J Vet Med Sci* **56,** 701-5.

Siskind, G. W., Paul, W. E. & Benacerraf, B. (1966). Studies on the effect of the carrier molecule on antihapten antibody synthesis. I. Effect of carrier on the nature of the antibody synthesized. *J Exp Med* **123,** 673-688.

Snell, E. E. (1945). Effect of alanine on response of *Lactobacillus casei* to pyridoxine and folic acid. *J Bact* **31,** 36-9.

Snell, E. E. (1948). Use of microorganisms for assay of vitamins. *Physiol Rev* **28,** 255-282.

Spector, R. & Lorenzo, A. V. (1975). Folate transport by the choroid plexus in vitro. *Science* **187,** 540-2.

Staples, M., Hardy, J. & Liang, E. (1992). Enzyme based assay for the quantitation of folate in serum. *Clin Chem* **38,** 1090.

Steele, B. F., Sauberlich, H. E., Reynolds, M. S. & Baumann, P. J. (1949). Media for *Leuconostoc mesenteroides* P-60 and *Leuconostoc citrovorum* 8081. *J Biol Chem* **177,** 533-44.

Stokes, J. L., Koditschek, L. K., Rickes, E. L. & Wood, T. R. (1949). Factors affecting the growth of *Lactobacillus casei*. *J Biol Chem* **178,** 93-101.

Svendson, I. B., Hansen, S. I., Holm, J. & Lyngbye, J. (1982). Amino Acid Sequence Homology between Human and Bovine Low Molecular Weight Folate Binding Protein Isolated from Milk. *Carlsberg Research Communications* **47,** 371-376.

Svendson, I. B., Hansen, S. I., Holm, J. & Lyngbye, J. (1984). The Complete Amino Acid Sequence of the Folate-Binding Protein from Cow's Milk. *Carlsberg Research Communications* **49,** 123-131.

Svendson, I. B., Martin, B., Pederson, T. G., Hansen, S. I., Holm, J. & Lyngbye, J. (1979). Isolation and Characterization of the Folate-Binding Protein from Cow's Milk. *Carlsberg Research Communications* **44,** 89-99.

Tamura, T., Mizuno, Y., Johnston, K. E. & Jacob, R. A. (1997). Food folate assay with protease, alpha-amylase, and folate conjugase treatments. *Journal of Agricultural and Food Chemistry* **45,** 135-9.

Tamura, T., Shin, Y. S., Williams, M. A. & Stockstad, E. L. R. (1972). *Lactobacillus casei* Response to Pteroylpolyglutamates. *Anal Biochem* **49,** 517-521.

Teply, L. J. & Elvehjam, C. A. (1945). The titrimetric detemination of *Lactobacillus casei* factor and folic acid. *J Biol Chem* , 303-309.

Toth, J. P. & Gregory, J. F. (1988). Analysis of Folacin by GC/MS: Structures and Mass Spectra of Fluorinated Derivatives of *para*-Aminobenzoyl Glutamic Acid. *Biomed Env Mass Spec* **17,** 73-79.

Varela-Moreiras, G., Seyoum, E. & Selhub, J. (1991). Combined affinity and ion pair liquid chromatographies for the analysis of folate distribution in tissues. *J Nutr Biochem* **2,** 44-53.

Waxman, S. & Schreiber, C. (1973). Characteristics of folic acid-binding protein in folate-deficient serum. *Blood* **42,** 291-301.

Waxman, S. & Schreiber, C. (1975a). The isolation of the folate binding protein from commercially purified bovine beta lactoglobulin. *FEBS Lett* **55,** 128-30.

Waxman, S. & Schreiber, C. (1975b). The purification and characterization of the low molecular weight human folate binding protein using affinity chromatography. *Biochemistry* **14,** 5422-8.

Waxman, S., Schreiber, C. & Herbert, V. (1971). Radioisotopic assay for measurement of serum folate levels. *Blood* **38,** 219-28.

Webber, S., Deits, T. L., Snyder, W. R. & Whiteley, J. M. (1978). The purification of rat and sheep liver dihydropteridine reductases by affinity chromatography on methotrexate-sepharose. *Analytical Biochemistry* **84,** 491-503.

Weitman, S., Anderson, R. G. W. & Kamen, B. A. (1994). Folate Binding Proteins. In *Vitamin receptors: Vitamins as ligands in cell*, pp. 107-135. University Press, Cambridge.

Whiteley, J. M., Jackson, R. C., Mell, G. P., Drais, J. H. & Huennekens, F. M. (1972). Folate antagonists covalently linked to carbohydrates: synthesis, properties, and use in the purification of dihydrofolate reductases. *Arch Biochem Biophys* **150,** 15-22.

Wilson, S. D. & Horne, D. W. (1982). Use of glycerol-cryoprotected Lactobacillus casei for microbiological assay of folic acid. *Clin Chem* **28,** 1198-200.

Wolff, R., Drouet, L. & Karlin, R. (1949). Occurence of vitamin Bc conjugase in human plasma. *Science* **109,** 612-3.

Yamada, M. (1979). Folate contents in milk. *Vitamins.* **53,** 221-227.

Zamierowski, M. & Wagner, C. (1974). High molecular weight complexes of folic acid in mammalian tissues. *Biochem Biophys Res Commun* **60,** 81-7.

Zwiener, R. J., Johnson, C. A., Anderson, R. G. W. & Kamen, B. A. (1992). Purified folate receptor-5-methyltetrahydrofolic acid interaction at neutral and acid pH. *Cancer Res Ther Control* **3,** 37-42.

Chapter Three

Folate Binding Protein Purification and Characterization

Abstract

Folate binding protein (FBP) is used as a powerful affinity tool for isolating folate from biological tissues. Highly purified FBP is desirable for competitive binding assays that rely on a high degree of specificity. Pure FBP was prepared and characterized as follows: the 40-70% ammonium sulfate cut of fat-free, casein-free fresh bovine milk was resuspended in buffer, acidified to pH 3.5 and stirred for 1 hr. Released folate was removed by overnight stirring with albumin-treated charcoal and centrifugation. After dialysis, the dialyzed material was applied to a Sepharose-4B methotrexate-affinity column, washed, and FBP eluted with acetic acid. SDS-PAGE of the eluent showed multiple bands of protein with apparent molecular weights in the 30-35 kDa and 55-70 kDa region. In-gel digestion of these bands, microsequencing and database searching of the partial amino acid sequence of these bands identified the two bands in the 30-35 kDa region as bovine FBP. Both bands had a high degree of sequence homology with the bovine FBP, and their molecular weight difference was due to the degree of glycosilation. The FBPs were further purified by DEAE-Sephadex anion-exchange chromatography or preparative isoelectric focusing. Purity and molecular weight was confirmed by SDS-PAGE and MALDI-TOF. Milligram quantities of highly purified FBP were obtained by preparative isoelectric focusing. The purified protein was coupled to agarose beads and used for isolating folate from biological samples. This procedure resulted in the highest specific binding capacity for FBP reported in the literature.

Introduction

Folate molecules typically appear at nanomolar concentrations in complex biological matrices. For reliable determination of the total folate concentration, as well as identification of individual folate molecules, standardized assay reagents, conditions and protocols are required. Procedures, however, vary from laboratory to laboratory according to available equipment, expertise and required turn-around time. This has resulted in vastly different determinations of folate concentration in reference samples. A recent round-robin study of 20 different laboratories found up to a 9-fold difference in the measured concentration of folate in test serum and red blood cell samples (Gunter, 1996). These laboratories employed either the conventional microbiological assay using *L. casei*, competitive binding assay kits from different manufacturers or affinity-isolation of folate followed by HPLC.

For routine diagnostic purposes, the competitive binding assays have become the method of choice for a majority of clinical and research laboratories. Assay kits from several manufacturers are available and provide a cost-effective and time-effective solution for determination of folate concentration in serum and red blood cells. These assays are used for clinical diagnosis of anemia and other folate-related clinical conditions. The assays differ slightly in use of labeled-folate tracer, removal of the tracer after incubation and detection of remaining tracer in the sample. These differences produce slightly different cut-off values for identification of 'low' or 'normal' folate individuals.

Although measured folate concentrations vary slightly between the assays, folate deficient individuals can be reliably identified due to the large difference in their plasma or red blood cell folate concentrations compared to normal individuals. The one common factor in these assays is the folate binder, folate binding protein (FBP), isolated from cow's milk by affinity chromatography (Salter, 1972). The purity of this protein is generally not determined since the purification procedure satisfies a critical requirement, to increase the binding capacity of the product. To further increase the specific binding capacity, the protein must be subjected to another purification step, resulting in a highly purified binding protein specific for folate and less susceptible to non-specific interferences from the sample matrix.

Although FBP is commonly used for competitive binding assays, it is also used for affinity purification of folate from biological samples for further characterization by HPLC. The cost and time associated with developing these affinity columns necessitates use of FBP with maximum specific activity.

This section describes the development of a novel preparative purification scheme for isolation of highly purified folate binding protein. The characteristics of the purified protein and its coupling to a novel affinity support matrix are also described.

Experimental Section

Materials: ^{3}H-folic acid (American Radio Chemicals). Affigel-10 agarose beads (BioRad).

Folate binding protein purification

Milk preparation: Fresh bovine and goat milk (36 L) was obtained from the campus dairy. The milk was de-creamed by centrifugation and the non-fat portion acidified to pH 4.5 with 1.0 M HCl. Precipitated caseins were strained through cheesecloth and the whey neutralized with 1 N NaOH. Ammonium sulfate (6 kg) was slowly added to 25 L of whey while stirring to give a 40% saturated solution. The mixture was left overnight at room temperature to allow settling of precipitates. The supernatant (20 L) was removed and an additional 4 kg ammonium sulfate added (70% saturation) to precipitate the proteins. After overnight settling at room temperature, the supernatant was discarded and precipitates resuspended in 3 L 0.05 M potassium phosphate, pH 7.0. To remove bound folate, the suspension was acidified to pH 3.5 with 1.0 M HCl, dialyzed in membrane tubing with a 2 kDa molecular weight cut-off (Spectrum) for 24 hours in 2 x 24 L 0.05 M citrate-phosphate buffer, pH 3.5 and then transferred to 24 L 0.05 M potassium phosphate, pH 7.0 for another 12 hours. All dialyses were performed at 4°C with gentle stirring. Folate binding proteins were isolated from this preparation by affinity chromatography.

Folate binding protein was also isolated from whey according to published methods (Salter, 1972). Briefly, 500 g whey powder purchased locally was suspended in

1 L 0.5 M potassium phosphate dibasic, pH 6.4, centrifuged for 15 minutes at 20,000g and binding proteins isolated from the supernatant by affinity chromatography.

Methotrexate-Affinity Chromatography: Sepharose-4B methotrexate affinity column (Sigma), 50 mL bed volume, was used for isolating folate binding proteins. The column was equilibrated with 0.05 M potassium phosphate, pH 7.0 and dialyzed solution (750 mL) containing folate binding proteins applied to the column at a flow rate of 2 mL/minute. The column was washed with 600 mL 2.0 M NaCl, 0.05 M sodium borate, pH 8.0 and 600 mL 0.01 M sodium borate, pH 8.0. Bound proteins were eluted with 200 mL 0.05 M acetic acid, neutralized with 1.0 N NaOH and dialyzed for 24 hours against 4 L of water at 4°C.

Anion-exchange Chromatography: Affinity purified proteins were separated by anion-exchange chromatography on a Varian Model 5000 Liquid Chromatograph HPLC system with a Rheodyne Model 7125 injector was connected to a Pharmacia Mono Q HR 5/5 anion-exchange column (Uppsala, Sweden). Absorbance was monitored at 280 nm with a Varian UV-100 detector. Buffer A contained 0.05 M ethanolamine, pH 10. Buffer B contained 0.05 M ethanolamine, 1 M NaCl, pH 9.5. Ethanolamine was added to affinity-purified protein solution and pH adjusted to give a 0.05 M ethanolamine solution, pH 10.0. Approximately 5 mg protein in 20 mL Buffer A was applied to the column with a flow rate of 1 mL/minute. The column was washed with 25 mL Buffer A and bound proteins were eluted by step-wise gradients to 15, 20 and 100% Buffer B. Three peaks

were collected, desalted and concentrated on Centricon-30 centrifugal concentrator (Amicon, MA).

Preparative Isoelectric Focusing: Affinity purified binding proteins (10 mL, 2 mg/mL) were mixed with 10 mL AMPSO and Bis-Tris (4:1) Bio-Rad RotoLyte ampholite-free buffer (Richmod, CA) and loaded onto a Bio-Rad Mini Rotofor Cell Preparative Isoelectric Focusing unit. The unit was connected to a Bio-Rad PowerPac 3000 power supply and allowed to focus for 3 hours at 10 W constant power to give a pH range of ~7.6-13.2. Twenty fractions were collected and the pH measured. Small aliquots of each fraction were separated by SDS-PAGE.

Purity determination

Amino acid microsequencing

In-gel digestion: Four distinct protein bands were resolved by gel electrophoresis in the affinity-purified sample. In-gel digestion and microsequencing confirmed the identity of these four bands. The four bands, numbered 1-4 from largest to smallest, were cut out of the gel and washed and incubated overnight at 30°C with 0.1-0.2 μg Lys-C in 0.1 M Tris, pH 7.8, 0.05% SDS. The gel chips were washed with 0.1% trifluoroacetic acid (TFA) in 80% acetonitrile and 25 μL 6 M guanidium hydrochloride 0.4 M Tris, pH 8.5, 1 mM EDTA added. The peptides were reduced by addition of 1 μL 450 mM dithiothreitol and incubated for 45 minutes at 50°C. Two microliters of 185 mM iodoacetamide was added

and the sample incubated another 15 minutes at room temperature. The peptides were ready for microbore HPLC separation.

Microbore column HPLC. An Applied Biosystems Instrument (Foster City, CA) model ABI 140B solvent delivery system was used equipped with model 112A injector and model 785 programmable absorbance detector. A C18, 100x1 mm microbore column was used to perform the separations. Solvent A was 0.1% TFA in water, Solvent B was 0.075% TFA in 70% acetonitrile. A pump was programmed with a linear gradient from 8% Solvent B to 100% Solvent B over 105 minutes. Flow rate was 100 μL per minute.

Sequence Analysis. Peptides (10-20 pmol) were collected and analyzed using automated Edman degradation by an ABI gas phase (407A) or liquid pulse (477A) peptide sequencer. FATSA and BLAST computer programs were used for rapid sequence database searching.

Protein assay: Protein concentration was measured with the Bio-Rad Protein Assay Kit (Richmond, CA) based on the method of Bradford (Bradford, 1976).

SDS-PAGE: Whey, affinity-purified, ion-exchange and isoelectric-focused binding proteins were analyzed by SDS-PAGE. Acrylamide gels were made with the following reagents: Stock acrylamide, 30% acrylamide (w/v) and 0.8% bis-acrylamide (w/v); separating buffer: 75 mL 2M Tris-HCl, 4 mL 10% SDS, 21 mL H_20; stacking buffer: 50 mL 1 M Tris-HCl, 4 mL 10% SDS, 46 mL H_2O; 10 % ammonium persulfate (APS). A

15% cross-linked separating gel was made by mixing 2.5 mL separating buffer, 2.5 mL H_2O and 5 mL stock acrylamide. The gel was formed by addition of 50 μL APS and 5 μL tetramethylene-ethylenediamine (TEMED). A stacking gel was poured above the separating gel by mixing 1 mL stacking buffer, 0.67 mL acrylamide, 2.3 mL H_2O, 30 μL APS and 5 μL TEMED. The electrophoresis buffer consisted of 3 g Tris, 14.4 g glycine, 1 g SDS and H_2O to bring the total volume to one liter. Each 20 μL protein sample was denatured by boiling for 5 minutes in 5 μL of sample buffer consisting of 0.6 mL 1 M Tris-HCl, pH 6.8, 5 mL 50 % glycerol, 2 mL 10% SDS, 0.5 mL 2-mercaptoethanol and 0.9 mL H_2O. Trypsin inhibitor (20.1 kDa), carbonic anhydrase (29 kDa), glycerophosphate dehydrogenase (36 kDa) and egg albumin (45 kDa) were used as molecular weight markers (Bio-Rad). Bands were stained for 10 minutes with a solution of 45% methanol, 45% H_2O, 10 % glacial acetic acid (v/v) containing 0.1% (w/v) Coomassie Blue R-250. The gel was then destained with a solution of 10% methanol, 10% glacial acetic acid and 80% H_2O (v/v). A Bio-Rad Mini-PROTEAN II electrophoresis system and PowerPac 300 power supply (Richmod, CA) were used for the separation.

MALDI-TOF mass spectrometry

Folate binding protein (3 mL, 0.2 mg/mL) obtained by isoelectric focusing was dialyzed in 4 L nano-pure water at 4°C using 10 kDa dialysis cassettes (Pierce), lyophilized and resuspended in 80 μL 50 % acetonitrile (v/v) saturated with sinapinic acid (3,5-dimethoxy-4-hydroxycinnamic acid) as the matrix. A Hewlett-Packard (Palo Alto, CA) G-2030A time-of-flight mass spectrometer was operated at an accelerator voltage of 28

kV. Desorption/ionization was achieved with a nitrogen laser (λ=337 nm) with a pulse width of 3 ns delivering approximately 9.59 μJ/pulse. The instrument was calibrated with an external mixture of known standards.

Polyclonal antibody production

Female New Zealand White rabbits weighing 2-3 kg were housed at the Laboratory Animal Health Clinic/Comparative Pathology Lab. A 10 mL blood sample was collected prior to the first immunization. On day 1, the animal (#2920) was injected subcutaneously with 3 mL Freund's complete adjuvant containing 1 mg FBP purified by affinity-chromatography and isoelectric focusing. On day 7 and day 21 booster shots of the antigen were administered containing 1.0 mg FBP in 3 mL Freund's incomplete adjuvant. Serum was collected on days 37, 44, 51 and 58.

Ouchterlony double diffusion plate: A 1 % (w/v) agarose solution in 100 mL was prepared containing 0.01 M Tris, pH 8.0, 0.15 M NaCl, 0.005 M EDTA, 0.02 % NaN_3, boiled and poured into 60-mm diameter Petri dishes. Between 50-70 μL sample was placed in 5-mm wells cut into the agar. One well was filled with rabbit antibody (#2920) and the other well with whole milk. The dish was covered and allowed to sit at room temperature for 24-36 hours until precipitin bands appeared.

FBP binding capacity

Albumin-coated charcoal: Four grams Norit 0.8 mesh charcoal (Aldrich) was ground to a fine powder and added to 40 mL 0.05 M potassium phosphate containing 0.88 g bovine

serum albumin (Sigma), 0.034 g NaCl and 0.004 g NaN_3. The slurry was mixed for 30 minutes at 4°C and aliquoted into 1.5 mL Eppendorf tubes and stored at 4°C.

Folate binding protein binding capacity: A 40 μM ^{3}H-folic acid working solution was prepared by adding 0.67 nmol of ^{3}H-folic acid (30 mCi/mmol, American Radio Chemicals) to 10 mL of 40 μM folic acid in 0.05 M potassium phosphate, pH 6.1, 1% ascorbic acid. Folate binding capacity was measured by mixing 100 μL binding protein with 500 μL 0.05 M potassium phosphate buffer, pH 7.0 and 20 μL ^{3}H-folic acid. Parallel samples containing 100 μL buffer in place of protein were used to adjust for non-specific binding. The solution was mixed and incubated for 15 minutes at room temperature. Albumin-coated charcoal (100 μL) was added and mixed by vortexing for 30 seconds and immediately centrifuged at 12,000 rpm for 5 minutes at room temperature. A 400 μL aliquot of the supernatant was mixed with EcoLite scintillation fluid (ICN) and activity measured with a Wallac 1410 liquid scintillation counter (Gaithersburg, MD). Folic acid binding capacity was expressed as nmol folic acid bound/mg protein.

Immobilization of folate binding protein

FBP-agarose coupling: Purified folate binding protein was dialyzed in 10K dialysis cassettes (Pierce) against 4 L nanopure H_2O for 24 hours at 4°C. The dialyzate was lyophilized and resuspended in 0.05 M HEPES, pH 7.3 (1.5 mg/mL). Protein was coupled either saturated with or free from folic acid to see if protein saturated with folic acid would orient the protein in a manner that would increase the gel's binding capacity.

Folate binding protein, 4.2 mg (0.14 nmol), was incubated with 300 nmol folic acid for 1 hour at 4°C. The solution was then dialyzed in 10 K dialysis cassettes against 4 L 0.05 M HEPES, pH 7. Folate binding protein free of folic acid was prepared as a control. Five milliliters N-hydroxysuccinimide esters of a derivatized cross-linked agarose gel, (Affigel® 10, Bio-Rad), was washed with 3 bed volumes cold 0.05 M HEPES, pH 7 and 4.2 mg folate binding protein added. After four hours of gentle mixing at 4°C, 0.1 mL 1 M ethanolamine-HCl was added and mixed for another 30 minutes to block the remaining active esters. The solution was then poured over a disposable plastic column and washed with 20 mL 0.05 M HEPES, pH 7.3 followed with 20 mL of 0.01 M sodium acetate, pH 4.5. Both gels were then washed with 20 mL of 0.02 M trifluoroacetic acid to remove folic acid from the saturated protein gel followed by 20 mL 0.05 M potassium phosphate, pH 7.0. Fractions were collected and measured for protein concentration to determine coupling efficiency.

FBP-agarose binding capacity: In an Eppendorf tube, 100 μL agarose beads and 4 nmol ^{3}H-folic acid (53.9 Ci/mol) were mixed gently in 500 μL of 0.05 M potassium phosphate, pH 7.0 for 15 minutes at 4°C. The solution was poured into a narrow disposable plastic column (BioRad) and washed with 2 mL 0.05 M potassium phosphate, pH 7.0 and 2 mL 0.05 M potassium phosphate, pH 7.0, 1 M NaCl. Bound ^{3}H-folic acid was collected by elution with 2 mL 0.02 M TFA and measured by liquid scintillation. Binding capacity was expressed as nanomoles folic acid per milligram protein.

Results

Purification of folate binding protein

Freshly prepared milk and whey powder were used for the affinity purification of folate binding protein according to previously published methods with slight modifications in the preparation of the whey (Salter, 1972; Waxman, 1975). The end-products from these procedures were checked for purity by SDS-PAGE. The gel showed four major protein bands appearing as two pairs with apparent molecular weights of 60-70 kDa and 30-33 kDa. The identity of the proteins with the higher molecular weights was not known. To determine the identity of the four bands, the partial amino acid sequences of the proteins were identified by in-gel digestion and microbore column HPLC. A search of the partial sequence was performed using the Swiss-Prot Database, Release 31.0. Table 1 shows the partial amino acid sequence of each band and the best match found in the database. Band 1 had a best match with a rabbit immunoglobulin. This match had a 67% score and was obviously not a rabbit immunoglobulin. The degree of homology between the two sequences indicated that the protein was a lactoglobulin whose sequence had not yet been determined. A match was found for the sequence of Band 2 with a homology score of 61%. The matching sequence was from the gamma-2A subunit of mouse immunoglobulin (IgG). Again, the Band 2 protein was obviously not a mouse protein, but had a high enough homology to indicate that it belonged to the immunoglobulin or lactoglobulin family of proteins. The sequences from Band 3 and Band 4 had a 100% homology with the sequence of bovine milk folate binding protein (Svendson, 1984). This information was used to develop strategies for further purification of FBP.

Table 1. Affinity-purified proteins were separated by SDS-PAGE and four major bands observed. Band 1 migrated the least and Band 4 the most. Bands were cut out and partially sequenced by in-gel digestion and microbore HPLC. Proteins were identified by searching for the partial sequences on the SWISS-PROT database, Release 31.0.

Band #	Best-Match Sequence	Identity
Band 1	1 10 LICQATDFSP |||||..||| LPPEVSGFIPPRDAFFGBPRKSQLICQASGFSPRQVWSLR 110 120 130 140	Mucm_Rabbit Ig
Band 2	1 18 PAXEPQVYVLAPPQEELS |...|||||.||.||.. PVRAPQVYVLPPPAEEMT 230 247	GCAB_Mouse Ig gamma-2A
Band 3	1 15 DISYLYRFNWDHCGK ||||||||||||||| WRKNACCSVNTSIEAXKDISYLYRFNWDHCGKMEPACKRH 50 60 70 80	Fol1_Bovin Milk Folate Binding Protein
Band 4	1 15 DISYLYRFNWDHCGK ||||||||||||||| WRKNACCSVNTSIEAXKDISYLYRFNWDHCGKMEPACKRH 50 60 70 80	Fol1_Bovin Milk Folate Binding Protein

Anion-exchange chromatography

Folate binding protein was successfully purified from the mixture of affinity-purified proteins by anion-exchange chromatography. Figure 1 shows a chromatogram of the separation using step-wise gradient elution. Three peaks were collected, dialyzed and measured for folate binding capacity.

Peak 1 had a binding capacity 2.5 times the capacity of Peak 2, while peak 3 had minimal binding capacity. Peak 1 was electrophoresed by SDS-PAGE and showed bands

with apparent molecular weights in the 30-33 kDa region. Figure 2 shows the comparison of proteins obtained by the three different methods. Lanes 1 and 6 were molecular weight markers. Lane 2 contained proteins isolated from whey powder by affinity-chromatography as described previously (Salter, 1972). Lane 3 contained proteins obtained from fresh bovine milk using affinity-chromatography as described earlier. Both procedures yielded proteins with MW in the 30-33 kDa and 50-60 kDa region. Lane 4 contained highly purified folate binding protein obtained after addition of an anion-exchange procedure. Lane 5 contained a mixture of proteins present in the whey preparation after precipitation with 70 % ammonium sulfate and resuspension in buffer. The gel was slightly overloaded with protein to allow visualization of minor impurities more apparent. The two-step purification procedure resulted in a significant improvement in the purity of the folate binding protein.

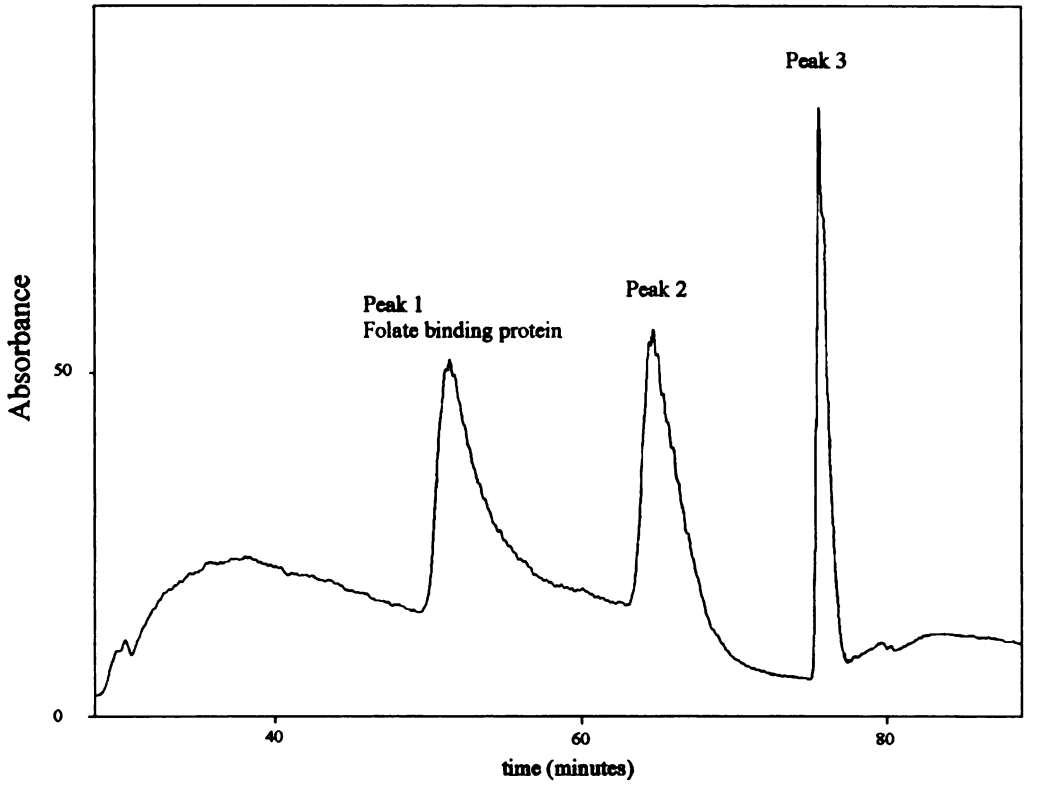

Figure 1. Anion-exchange chromatography of affinity-purified binding proteins. Proteins were applied to column and washed with 0.05 M ethanolamine, pH 10 for 10 minutes. The mobile phase was adjusted to 0.05 M ethanolamine, pH 9.5, 0.15 M NaCl by a stepwise gradient to elute folate binding protein. Peak 2 eluted by a stepwise gradient to 0.2 M NaCl and Peak 3 was washed off the column by increasing the salt concentration to 1.0 M. Flow rate was 1 mL/minute. Absorbance was measured at 280 nm.

Fractions were collected from each step along the purification scheme and assayed for specific folate binding activity. Folic acid binding capacity was determined with a ^{3}H-folic acid binding assay using albumin-coated charcoal for removal of ^{3}H-folic acid. The total protein concentration was determined by the method of Bradford (Bradford, 1976).

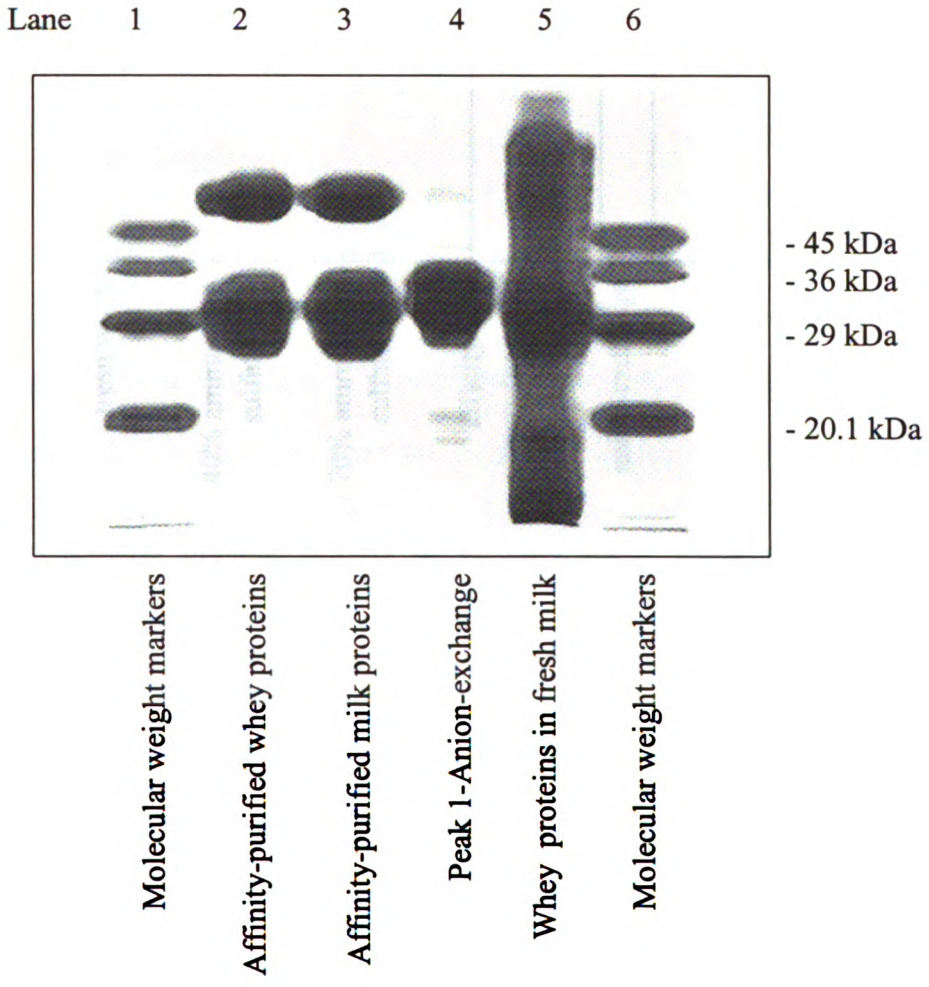

Figure 2. SDS-PAGE of fractions collected along the purification scheme. Lanes 1 and 6: molecular weight markers; Lane 2: proteins obtained by affinity-purification of whey powder according to previous methods (Salter, 1972); Lane 3: proteins obtained by affinity purification of fresh bovine milk; Lane 4: proteins obtained by a combination of affinity-chromatography and anion-exchange chromatography (Peak 1 from Figure 1); Lane 5: proteins in fresh bovine whey obtained by ammonium sulfate precipitation. Note: a larger amount of protein was loaded in Lanes 2-4 to emphasize any minor proteins that might be present as impurities.

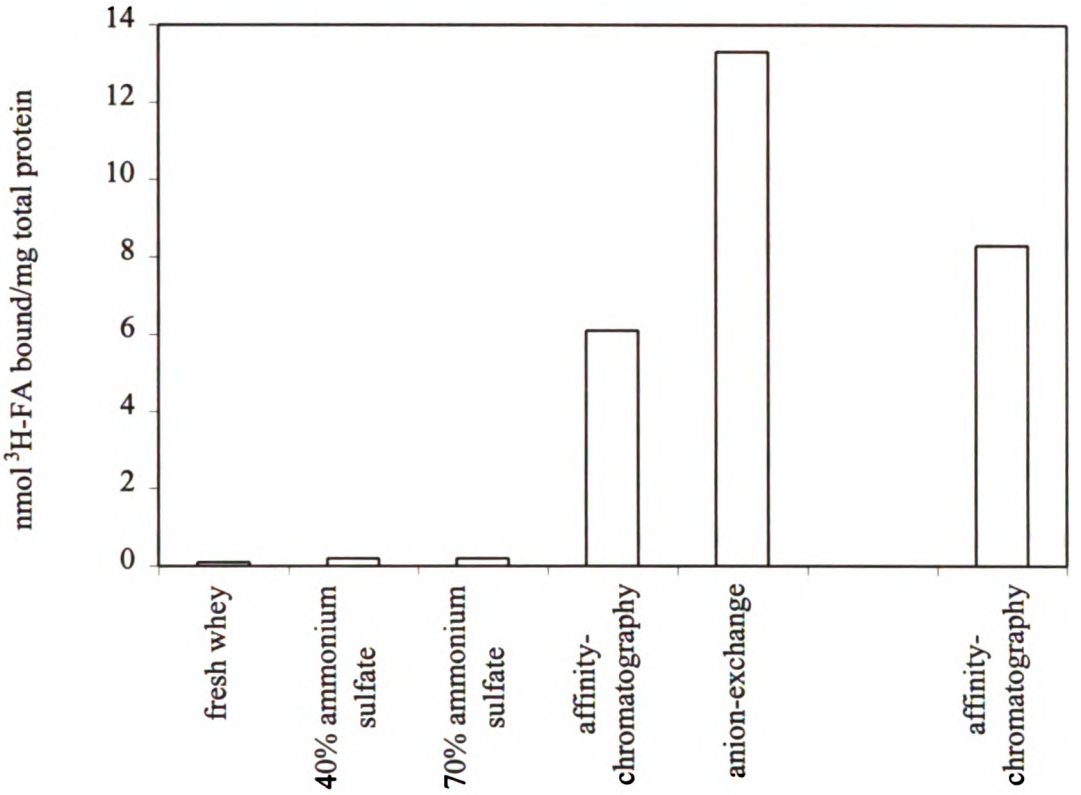

Figure 3. The specific binding activity of samples taken along each step of the purification procedure is shown. Activity increased as the purity of the folate binding protein increased. The column on the right shows the specific binding activity of a folate binding protein solution prepared according to previously published methods (Selhub, 1980).

The specific binding activity was calculated by dividing the binding capacity with total protein concentration and was expressed as nmol folic acid bound/mg protein. The specific binding capacity of major fractions in the purification scheme are shown in Figure 3. The fresh whey and the ammonium sulfate fractions had very low specific activity. There was a significant enrichment of folate binding proteins after the affinity-chromatography procedure. Maximum enrichment was achieved after ion-exchange chromatography resulting in a specific activity of 13.3 nmol ^{3}H-folic acid/mg protein.

The specific binding capacity of folate binding protein prepared according to previously published methods was nearly half the activity of the protein prepared according to the methods in this study. If one mole of folate binding protein bound to one mole of folic acid, the expected maximum specific activity would be 33.3 nmol folic acid/mg protein. The current procedure achieved 40% of this maximum activity perhaps due to protein degradation or other losses of binding activity.

Preparative isoelectric focusing

For large-scale purification a preparative isoelectric focusing procedure was used which allowed purification of milligram quantities of folate binding protein. A preparative isoelectric focusing unit consisting of a cylindrical chamber divided into 20 sections by permeable membranes. The samples and buffer were added and allowed to focus for ~3 hours. Each of the 20 fractions was then harvested and analyzed by SDS-PAGE to identify fractions containing FBP. Fractions 1-5 and 18-20 contained no protein. Figure 5 shows a gel of fractions 6 though 17. The high molecular weight globulin proteins had a lower pI and were found in fractions 6-10. Folate binding protein had a higher pI (more basic) and focused across fractions 8-17. Fractions containing pure folate binding protein (11 through 17) were pooled and dialyzed in water to remove the buffer. The protein solution was lyophilized and stored at –20°C. The system gave rapid and reproducible results suitable for purification of milligram quantities of folate binding protein.

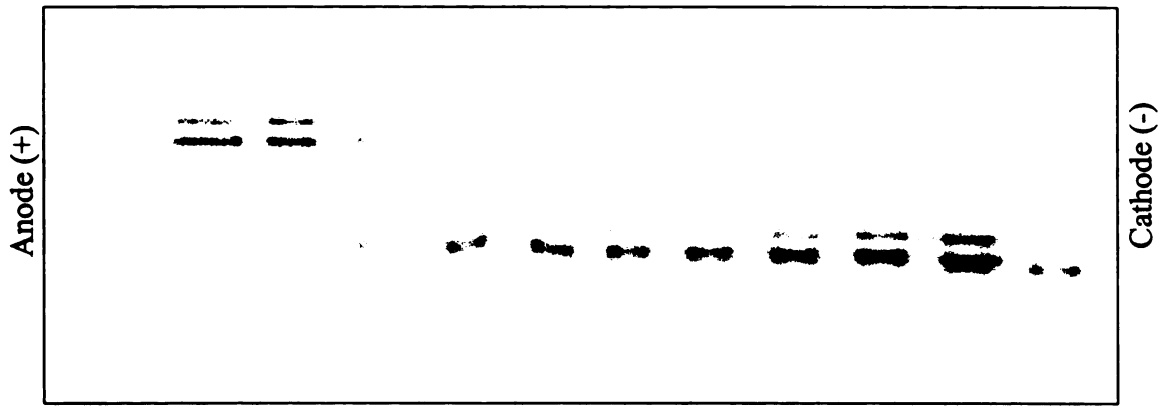

Lane	6	7	8	9	10	11	12	13	14	15	16	17
pH	7.6	7.9	8.0	8.1	8.2	8.3	8.5	8.8	9.5	10.5	10.7	11.6

Figure 4. Affinity-purified proteins (10 mL, 2 mg/mL) were separated by isoelectric focusing into 20 fractions ranging in pH from 7.6-13.2. The pH of each 2 mL fraction was measured before analyzing 20 μL of the fraction by SDS-PAGE. Fractions 6 through 17 contained protein. Folate binding protein appeared in fractions 8 through 17 and the interfering immunoglobulin proteins appeared in fractions 6-10. Fractions 11-17 were pooled and used for MALDI-TOF mass spectrometry and coupling to agarose beads.

Antibody characterization

Several milligrams of the purified protein were used to raise antibodies against folate binding protein. A female New Zealand white rabbit was immunized subcutaneously with 1 mg of protein in 3 mL Freund's complete adjuvant. Booster shots containing 1 mg protein in 3 mL Freund's incomplete adjuvant were given on days 7 and 21. Serum (2 mL) was collected on days 37 and 41 and assayed for antibody activity.

Heterogeneity of the antibody response was determined by a double-diffusion precipitation assay. If the antigen was pure a single homogenous immune response would be expected. If multiple proteins were present in the antigen, polyclonal antibodies against each of the proteins would be expected. A small well was cut out of an

agarose gel and filled with 50 μL of bovine milk. An adjacent well was filled with 50 μL rabbit antiserum. Proteins in the milk and serum samples migrated out of the wells by diffusion for 36 hours. Interactions between antibodies and antigen resulted in a single precipitation band providing further evidence that the antigen contained highly purified protein eliciting a single immune response.

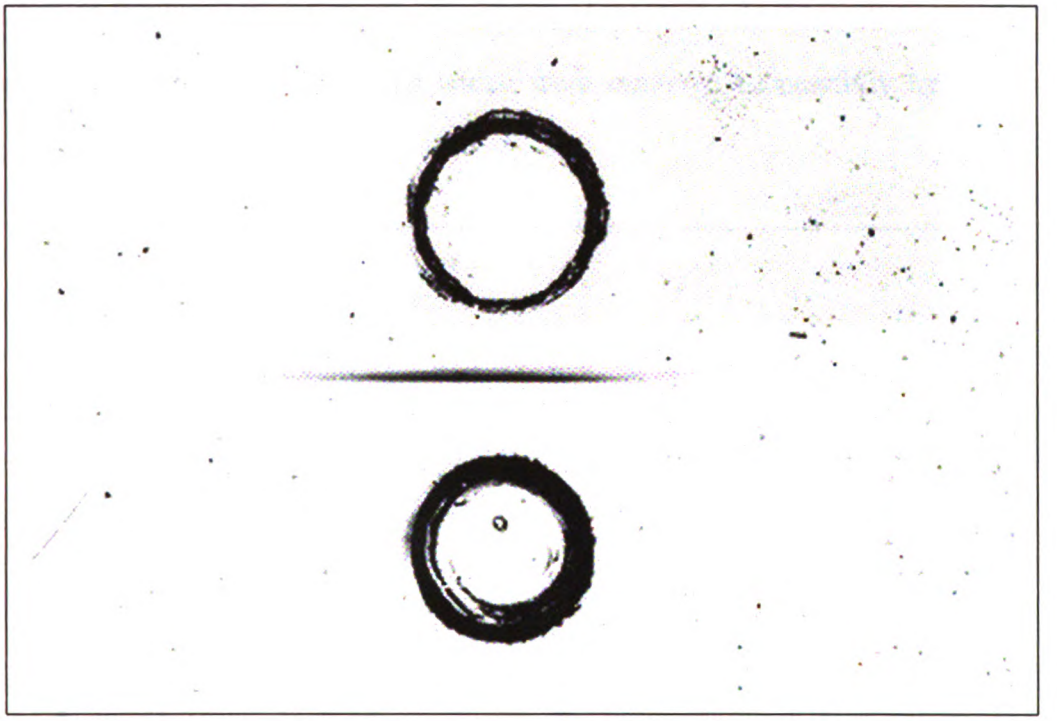

Figure 5. Ouchterlony double diffusion plate of antibodies raised against FBP purified by affinity-chromatography and isoelectric focusing. The wells were filled with 50 μL rabbit antiserum (top) and 50 μL whole milk (bottom). A single precipitation band appeared after 36 hours indicating a highly pure FBP antigen.

MALDI-TOF

Folate binding protein was further characterized by MALDI-TOF mass spectrometry. This instrument is useful for the analysis of macromolecules such as proteins and provides valuable information on the purity and molecular weight of samples. Figure 6

shows the mass spectrum of folate binding protein using sinapinic acid as the matrix. A relatively high laser energy was used to desorb the protein, as has been reported previously for glycoproteins (Yang & Orlando, 1996). The major peak had a molecular weight of 29.09 kDa with a range of 27-31 kDa. This relatively broad range of masses was attributed to varying degrees of glycosylation. The heterogeneous population of glycoproteins produced the observed broadening of the peak. There were no peaks in the region of the milk globulin proteins which were removed successfully by isoelectric focusing.

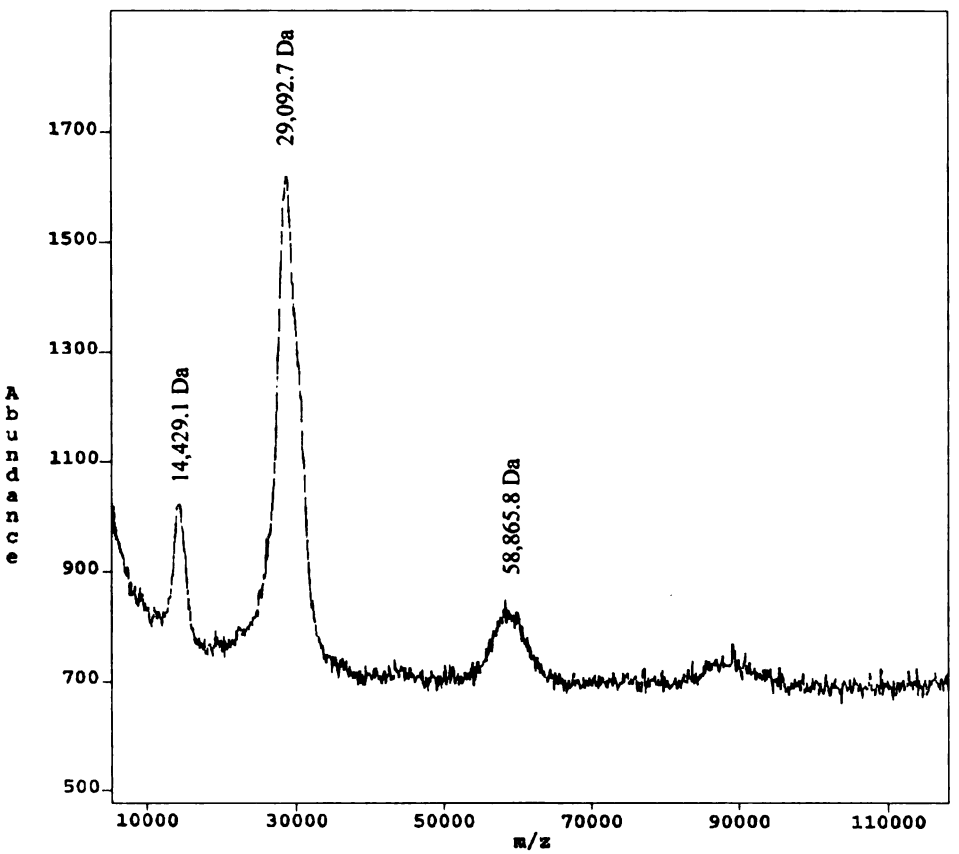

Figure 6. MALDI-TOF mass spectrum of milk folate binding protein purified by affinity chromatography and isoelectric focusing. The minor peaks at 14.4 and 58.9 kDa represented doubly-charged and dimers of the binding protein, respectively.

The purified protein was used as an affinity ligand to isolate folate from biological samples. Binding protein was coupled to agarose beads by the N-hydroxysuccinimide active ester method which coupled activated agarose gel beads to

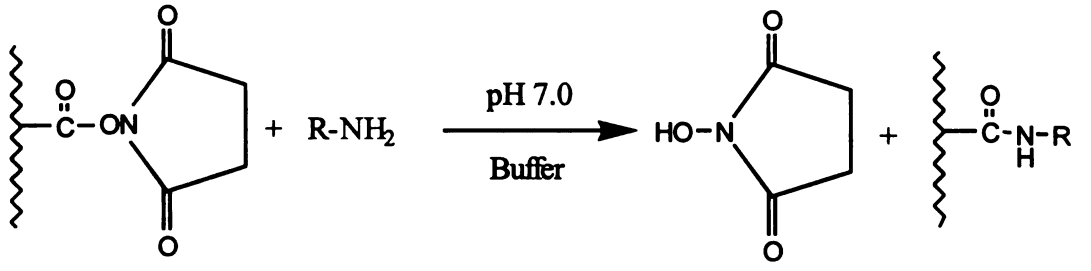

Figure 7. Coupling chemistry of protein primary amines to N-hydroxysuccinimide esters of derivatized crossed-linked aggarose gel beads.

primary amines of the ligand (Figure 7). The amide bond between the protein and the terminal carboxyl of the 10-carbon spacer arm was stable in acid and base (pH 2-11) (BioRad Bulletin 1085).

The binding capacity of the folate binding protein coupled to the agarose beads was determined by resuspending the beads in a buffered solution containing excess ^{3}H-folic acid. After 15 minutes of gentle mixing the solution was poured into a small disposable column and washed to remove unbound ^{3}H-folic acid. The binding capacity, calculated by the amount of ^{3}H-folic acid that did bind, was 4.6 nmol ^{3}H-FA/mg protein. This value suggested that about 14% of the proteins coupled to the beads were binding folic acid. The protein used for the coupling had a binding capacity of 13.3 nmol ^{3}H-FA /mg protein (Figure 3). A decrease in the binding capacity of immobilized protein could be expected since the coupling reaction might randomly block the binding site.

Coupling reactions were performed using binding protein saturated with folic acid. Table 2 shows the results of the coupling reaction using either saturated or free folate binding protein. The binding capacity of the free binding proteins was 5.6 nmol ^{3}H-FA/mg protein, similar to earlier results. Protein saturated with folic acid had a binding capacity of 2.9 nmol ^{3}H-FA /mg protein. Nearly a 50% reduction in binding capacity was observed indicating that only about one-fifth of the proteins were binding. This was in contrast to the folic acid free proteins where one-half of the binding capacity was retained after immobilization. As a result, further coupling reactions were performed using the free (apo) protein. This method allowed easy and efficient coupling of proteins and avoided the chemical hazards associated with methods that use cyanogen bromide.

Table 2. Folate binding protein affinity column properties. Identical conditions were used to couple agarose beads with FBP saturated with or free from folic acid. The column was washed and binding properties assessed (see methods).

	+ Folic acid	- Folic acid
Folate binding protein used (mg)	4.2	4.2
Agarose beads used (mL)	5.0	5.0
% protein coupled to beads	52	45
Specific folic acid binding activity		
(nmol ^{3}H-FA /mg protein)	2.9	5.6
(nmol ^{3}H-FA /nmol protein)	0.087	0.168

Discussion

Milk is a common source of folate binder used in competitive binding assays and as an affinity ligand for isolating folate from biological samples. Folate binding protein (FBP) is commonly purified from milk by methotrexate-affinity chromatography as has been described previously (Salter, 1972). The purity of the resulting product was rarely determined since the protein's binding capacity increased sufficiently for use as a folate binder. In this study, folate binding protein was purified from fresh bovine milk and whey powder. The resulting products were shown to contain contaminating proteins which were removed by the addition of a secondary purification step. Characterization of the final product determined the protein to be highly pure. This degree of purity has not been reported for FBP in the literature to our knowledge.

It was found that fresh milk was not necessary as the source for FBP. Indeed, commercial sources of β-lactoglobulin contain fair amounts of FBP and can be a good source for purifying FBP (Waxman, 1975). The protein was stable under a wide range of pHs. The purified protein was lyophilized and stored for more than six months at –80°C with no significant loss of activity.

Milk folate binding protein molecular weight had been reported to be about 30 kDa (Svendson, 1984), 35 kDa (Salter, 1981), 37 kDa (Rubinoff, 1977) and 38 kDa (Ford, 1969). These determinations were based on electrophoretic separations and know standards. In this study, MALDI-TOF mass spectrometry revealed a molecular weight of 29 kDa, with a range of 27-31 kDa, representing a heterogeneous population of FBP glycoproteins. This closely matched some past reports but also demonstrated the

imprecision of electrophoretic techniques for determining the molecular weight of glycoproteins.

The purified protein was immobilized to a novel support matrix with good efficiency while avoiding the use of toxic cyanogen bromide. The bound proteins were used as an affinity tool to isolate folate from biological samples. One milliliter of FBP-affinity beads was sufficient to isolate folate from one milliliter of plasma and red blood cells for further analysis. Other researchers have used affinity-purified FBP to isolate folate from plasma and characterize the product by HPLC or GC/MS (Gregory, 1990; Gregory, 1984; Santhosh-Kumar, 1995; Seyoum, 1993; von der Porten., 1992). In these protocols, the affinity step concentrated folate from biological samples while a second chromatographic step further separated the various folate forms.

Affinity-purified folate binding protein is also used in competitive binding assays. These one-step assays do not have a secondary separation step to further isolate folate or other competing compounds. The danger exists that contaminating proteins that were co-isolated with FBP during affinity-chromatography could interfere with the competitive assays. These proteins have affinity for folate and could compete for folate in the sample. Since the binding properties of these proteins have not been characterized compounds other than folate in the samples could interfere with the assay in an unpredictable manner. For example, measurement of plasma folate by competitive binding assays in subjects taking methotrexate is contraindicated (Technical Bulletin, Lederle Labs, NY). Other dietary or endogenous compounds may also interfere with this assay since the binder is not in pure form.

Results of a recent round-robin evaluation of the reproducibility of folate assays demonstrated a 9-fold difference between estimations of folate concentration in plasma and red blood cells (Gunter, 1996). The procedures described in this study for isolating FBP to purity may help to lower this variability by increasing the specificity of the binder used in the assay.

The stability of FBP-immobilized beads makes them suitable for routine measurement of folate in biological samples. The beads can be packed into a small column and placed in-line with a solvent and sample delivery system. Conceivably, an autoinjector could apply a sample to the column at slow flow rates, wash the column with a suitable buffer and then apply a known amount of radiolabeled folic acid. Competition for a limited number of binding sites would result in radiolabeled folic acid flowing through the column without binding. These could be quantified by in-line radiometric detection and would represent the amount of folate in the sample. Plasma folate concentration could then be quantified using a set of calibration standards. The system could be automated for routine, sensitive and reproducible measurements.

Literature Cited

Bradford, M. M. (1976). A rapid and sensitive method for the quantitation of microgram quantities of protein utilizing the principle of protein-dye binding. *Analytical Biochemistry* **72,** 248-54.

Gregory, J. F., Bailey, L. B., Toth, J. P. & Cerda, J. J. (1990). Stable-isotope methods for assessment of folate bioavailability. *Am J Clin Nutr* **51,** 212-5.

Gregory, J. F., Sartain, D. B. & Day, B. P. (1984). Fluorometric determination of folacin in biological materials using high performance liquid chromatography. *J Nutr* **114,** 341-53.

Gunter, E. W., Bowman, B. A., Caudill, S. P., Twite, D. B., Adams, M. J. & Sampson, E. J. (1996). Results of an international round robin for serum and whole-blood folate. *Clin Chem* **42,** 1689-94.

Salter, D. N., Ford, J. E., Scott, K. J. & Andrews, P. (1972). Isolation of the Folate-Binding Protein from cow's milk by the use of Affinity Chromatography. *FEBS Letters* **20,** 302-6.

Salter, D. N., Scott, K. J., Slade, H. & Andrews, P. (1981). The preparation and properties of folate-binding protein from cow's milk. *Biochem J* **193,** 469-76.

Santhosh-Kumar, C. R., Deutsch, J. C., Hassell, K. L., Kolhouse, N. M. & Kolhouse, J. F. (1995). Quantitation of red blood cell folates by stable isotope dilution gas chromatography-mass spectrometry utilizing a folate internal standard. *Anal Biochem* **225,** 1-9.

Selhub J., Ahmad O., Rosenberg I.H. (1980). Preparation and use of affinity columns with bovine milk folate-binding protein (FBP) covalently linked to Sepharose 4B. *Methods Enzymol* **66,** 686-90.

Seyoum, E. & Selhub, J. (1993). Combined Affinity and Ion Pair Column Chromatographies for the Analysis of Food Folate. *Journal of Nutritional Biochemistry* **4,** 488-94.

Svendson, I. B., Hansen, S. I., Holm, J. & Lyngbye, J. (1984). The Complete Amino Acid Sequence of the Folate-Binding Protein from Cow's Milk. *Carlsberg Research Communications* **49,** 123-131.

von der Porten, A. E., Gregory, J. F., Toth, J. P., Cerda, J. J., Curry, S. H. & Bailey, L. B. (1992). In vivo folate kinetics during chronic supplementation of human subjects with deuterium-labeled folic acid. *Journal of Nutrition* **122.**

Waxman, S. & Schreiber, C. (1975). The isolation of the folate binding protein from commercially purified bovine beta lactoglobulin. *FEBS Lett* **55,** 128-30.

Yang, Y. & Orlando, R. (1996). Identifying the glycosylation sites and site-specific carbohydrate heterogeneity of glycoproteins by matrix-assisted laser desorption/ ionization mass spectrometry. *Rapid Comm. in Mass Spectrometry* **10,** 932-6.

Chapter Four

Literature review:

Folic acid Bioavailability and Kinetics

Introduction

Folate requirement can be estimated in humans by determining folate bioavailability and turnover. Determination of bioavailability permits calculation of the amount of folate that is actually absorbed. Determination of turnover permits calculation of the amount of folate that is lost over a period of time. The amount of folate required to maintain nutrient balance can then be calculated. Estimations of folate requirement, in concert with reliable estimations of actual folate intake, can help measure any differences between required and actual intake that may lead to adverse health effects. This chapter reviews the scientific literature where previous estimations of folate bioavailability and turnover have been attempted.

Assessment of the bioavailability and turnover of folate in an organism can be performed using labeled folate so that its movement can be traced in various tissues and samples. Folate is commonly labeled with stable or radioactive isotopes of carbon or hydrogen. Traditionally, radioisotope-labeled folate has been used in animals and certain human studies. Recently, mass spectrometric analysis of stable-isotope labeled folate compounds has made it possible to study folate kinetics in healthy humans. The current study describes the application of accelerator mass spectrometry (AMS) to determine the kinetics of folic acid in a healthy subject. The study overcame many of the current methodological limitations and allowed significant advancement of our knowledge and understanding of folate metabolism in humans by establishing protocols for measuring the bioavailability and turnover of folic acid under physiologic conditions. A review of the biological applications of AMS is also provided in this chapter.

Major advances in our understanding folate kinetics were made possible by the availability of chemically synthesized folic acid using radiolabeled precursors (Krumdieck, 1969; Plante, 1980). Radiocarbon or tritium labeled folic acid have been used in animals and humans to determine folic acid bioavailability and turnover.

Animal studies

Animal models of folic acid metabolism used radiolabeled folic acid to assess bioavailability, route of excretion and whole-body turnover rates. Murphy, *et al.* had elucidated the mechanism of folate catabolism in the rat and its subsequent excretion in urine (Murphy, 1976). However, it was not known whether the labeling position of the radioisotope affected interpretation of the excretion data due to selective loss or retention of catabolites of folic acid.

To clarify this, [2-^{14}C]- and [3',5',9-^{3}H]-folic acid were used individually and together in rats (Barford, 1978). Since the pteridine ring was labeled with ^{14}C, differences in excretion of the pteridine ring and the *para*-aminobenzoylglutamate moieties could be identified. Rats received an intraperitoneal dose of the mixture and urine, feces and liver radioactivity were measured over a 6-day period.

Tritium recovered in the urine was almost twice as great as radiocarbon. Little difference was observed in feces while liver showed higher retention of radiocarbon. This suggested that label in the pteridine ring of folic acid underwent recycling after catabolism or was retained to a greater extent than the *para*-aminobenzoylglutamate portion of catabolized folic acid. Others confirmed this using radiolabeled 10-formylfolate, folic acid and 10-formylfolate tetraglutamate (Connor, 1977; Connor,

1979). It became apparent that folate should not be labeled in the pteridine ring alone if catabolites were to be measured in the urine.

The fate of radiolabeled folic acid was followed in urine, feces and organs of animals. Murphy *et al.* administered physiologic amounts of [3',5',9-^{3}H]-folic acid to rats and measured urinary losses of unmetabolized tracer as well as metabolites in the form of 5-methyltetrahydrofolate, 10-formyldihydrofolate and catabolites in the form of pteridines, *para*-aminobenzoylglutamate and acetamidobenzoylglutamate (Murphy, 1979). Pheasant *et al.,* studied the metabolism and disposition of [2-^{14}C]folic acid and 10-formyl-pteroylglutamate in rats at levels ranging from 10-100 μg/kg body weight (Pheasant, 1981). Tracers detected in urine, feces and organs within the animal were separated chromatographically and a descriptive model was developed that showed the routes of distribution and elimination of the tracer. The model suggested polyglutamate derivatives were retained whereas monoglutamate derivatives were recycled through enterohepatic circulation and eventually excreted in the urine as catabolites. Bhandari, *et al.* followed tritium labeled folic acid, 5-methyltetrahydrofolate, and 5-formyl-tetrahydrofolate in rats over an 8-day period after an intragastric dose of 50 pmol folate/100 gram body weight (Bhandari, 1992). All three forms of folate showed close to complete absorption after 8 hours. Urine and feces were the major routes of elimination exhibiting biphasic excretion half times of 0.11 days and 13.4-15.9 days.

In another study, ^{3}H-labeled folic acid administered to rats intragastrically was followed in urine, feces, liver, kidney, spleen, heart and blood for 32 days (Scott , 1996). Cumulative urinary losses showed an early fast loss that slowed over the following 32 days. Cumulative fecal losses showed an early slow excretion rate for the first four days

that increased to a steady level over the next 28 days. Approximately 35% of the dose, half of which were catabolites, was recovered in the urine after 32 days, and 15% of the dose was recovered in the feces. Half of the dose was retained by the rats after 32 days, mostly in the liver and muscle.

Rats have been used to discern the major pathways of folate distribution and elimination. The discovery and identification of various folate molecules in bile suggested that bile may play a significant role in folate homeostasis (Shimoda, 1994; Shin, 1993a; Shin, 1993b; Shin, 1994). Folate distribution and cycling in bile was studied by intravenous infusion of various folate molecules in rats. Plasma folate concentration dropped rapidly after bile diversion indicating significant secretion into bile and reabsorption in the intestine (Shin, 1995). The authors concluded that folate cycling in bile may be important in the reduction and methylation of oxidized folate.

Interpretation of animal data to human nutrition and physiology must be made cautiously. Rodent gastrointestinal physiology and metabolism differs from humans in many aspects which make these animals a poor model for studying folate absorption and disposition.

Folate bioavailability and pharmacokinetics have been studied in pigs which are a better model of human folate metabolism than rodents (Kokue, 1994). Two-month-old female pigs were administered 1 mg folic acid/kg body weight by intravenous and intramuscular injections and 50 mg/kg by gavage. The bioavailability was determined by a conventional manner that compared areas under the plasma concentration curve (AUC) after intravenous and extravascular routes of administration. Folic acid had an extremely low 1% bioavailability by oral administration and 95% by intramuscular injection.

Active transport mechanisms involved in folic acid absorption may have become saturated resulting in low bioavailability of a high folic acid dose. Plasma folate was analyzed by HPLC and confirmed tetrahydrofolic acid to be the major folate metabolite in pig plasma rather than 5-methyltetrahydrofolate found in human plasma (Natsuhori, 1991). The authors used this knowledge to develop strategies for maintaining high plasma folate concentrations by intramuscular injections which have been shown to improve reproductive performance (Matte, 1984).

Pigs have also been used as a model to study the effects of alcohol on folate absorption (Reisenauer, 1986; Reisenauer, 1989; Villanueva, 1994). Animal studies have been valuable for estimating folate distribution and disposition rates, however, studies performed directly on humans often provide the most valuable information regarding nutrient metabolism.

Human studies

Results from experiments performed on animals usually serve as a guideline for designing experiments that ought to be repeated or validated in humans. However, human nutrition research has limitations that require the researcher to make certain assumptions and compromises not made by animal researchers. Genetic heterogeneity, uncontrollable environmental factors, illness, accessibility to samples and ethical issues are limitations animal researchers do not commonly encounter. Cost and limited subject number add further difficulty to conducting and interpreting human research. However, in most cases, research conducted in humans would be the first choice if results are to advance understanding of human nutrition and health. For these reasons, results obtained

from human studies, regardless of limitations in scope and design, are invaluable parts of the puzzle.

Due to the many complications inherent in human nutrition research, sometimes the simplest experiments are the most elegant. Almost four decades ago one such experiment provided insights which to this day influence much of our understanding of human folate requirement (Herbert, 1962). The study entailed a healthy adult consuming foods that were boiled three times in water to extract water-soluble vitamins. With the exception of folic acid, all other vitamins were reintroduced into the diet by supplementation. Nutritional and hematological parameters were monitored while the subject consumed approximately 5 μg folic acid daily. Serum folate concentration, measured by *L. casei* microbiological assay, dropped to less than 5 ng/mL and remained low for most of the depletion period.

Red blood cell folate, a long-term indicator of folate status, dropped steadily over the entire study reaching a low of <20ng/mL. Hypersegmentation of neutrophils was observed after 10 weeks and megaloblastic anemia after 19 weeks. The subject then consumed 250 μg folic acid orally resulting in a rapid rise in serum folate concentration and a return of red blood cell folate above 20 ng/mL after four days. The study indicated that folate reserves in the subject were adequate for a little more than one month and provided a means for defining minimum daily intakes which was suggested to be in the range of 50 μg.

Absorption and elimination of folic acid in humans has been studied by measuring folic acid concentration in serum and urine after oral ingestion of folic acid (Butterworth, 1957; Chanarin, 1958; Cox, 1958; Girdwood, 1953). These early studies provided only

qualitative data since it had been shown earlier that significant amounts of microbially produced folate can interfere with quantitation of folate balance (Denko, 1946).

Use of radioisotope-labeled folic acid resolved this confounding factor. A wide array of radiolabeled folate molecules were available from animal experiments but their use in humans was justified in only a few cases where the benefits outweighed the risks associated with radiation exposure. Anderson *et al.* administered single doses of 0.2 mg ^{3}H-folic acid (20-40 μCi), generated by exchange with tritiated water, to 23 patients with a variety of clinical and hematological disorders ranging from idiopathic steatorrhea and tropical sprue to pernicious and megaloblastic anemias and 36 healthy individuals (Anderson, 1960).

Measurement of fecal tritium indicated absorption for control and cases of between 40-90% and 9-90% of the dose, respectively. Twenty-four hour urinary excretion ranged from 1.5-16% of the dose in controls and 1.5-12.4% in cases. These values jumped to 30-65% in controls and 4-52% when the oral dose was preceded with a 15 mg folic acid intramuscular injection, indicating a saturation effect. The study demonstrated reduced folic acid bioavailability in these clinical and hematological conditions as well as a large variability in folic acid absorption in control individuals.

The plasma kinetics and urinary excretion of folic acid was studied in 16 healthy subjects receiving 1, 15 and 150 μg/kg body weight ^{3}H-folic acid (<25 μCi total) by intravenous injection (Johns, 1961). Plasma clearance of ^{3}H-folic acid, given at a dose of 1 μg/kg body weight, was very rapid, with 2% of the dose per liter plasma remaining after 3 minutes and 0.1-0.2% after 30 minutes. This rapid elimination from plasma was not

due to renal clearance since less than 2% of the injected dose appeared in urine after two hours.

When ^{3}H-folic acid was given with larger amounts of non-labeled folic acid, such as 15, 150 or 1430 μg/kg body weight, an increasing proportion of the dose, 25-50% of the dose was excreted in the urine. These results suggested rapid distribution of folic acid into body tissues at all dosing levels with significant urinary excretion at doses greater than or equal to 15 μg/kg body weight. Pharmacokinetic parameters describing plasma clearance were not presented.

Butterworth *et al.* studied absorption and excretion of folic acid and folylpolyglutamates after oral ingestion of ^{14}C-labeled folate. Five patients with chronic lymphatic leukemia or Hodgkin's disease were studied. Four of the patients were in complete or partial remission, while a fifth patient with leukemia remained untreated for the condition at the time of the study. Patients received 0.4 or 4.4 mg folate as either folic acid or folylpolyglutamate labeled with 10-20 μCi ^{14}C either in the pteridine or glutamate moieties.

Feces was the major route of excretion in two patients who received ^{14}C-folylpolyglutamate labeled in the pteridine or first glutamate position accounting for 25% and 50% of the oral dose. The patient receiving 10 μmoles lost 8% of the dose in the first 24-hour urine collection while the patient receiving 1 μmole lost 1.5% of the dose in urine. Two patients received folylpolyglutamates labeled in the second glutamate position. In the first patient, an 81-year-old low income female, no radioactivity could be found in urine, feces or plasma. The second patient lost 2.5% of the dose in feces. Expired air was collected for 30 minutes after dosing in this patient and found to contain

a estimated 60% of the radioactivity in the dose, presumably as CO_2. The fifth patient received ^{14}C-folic acid labeled in the pteridine ring and lost 10% of the dose in feces and 44% in urine after 24 hours. A marginal response in plasma radioactivity was observed during the first four hours in the patient receiving 0.4 mg folate, whereas much more apparent plasma responses where observed in patients receiving 4.4 mg folate.

In a long-term study, a 36-year old woman with Hodgkin's disease and in remission for three years, received 320 μg folic acid as four doses of 10 μCi 2-^{14}C-folic acid at 12 hour intervals. Complete urine was collected for the first eight days and at intervals over four months. Urine and feces were collected for the first week of the study and at intervals over a four month period.

Urine radioactivity reached a maximum on day 2 and declined slowly for the remainder of the study. Feces radioactivity reached a maximum in the second collection and declined slowly for the remainder of the study similar to urine. Bioavailability was calculated as the sum of losses in feces over the first six days and equaled 92% of the dose. Urine showed a two-phase elimination pattern with half-lives of 31.5 hours and 100 days. This study and the human studies described earlier helped, in part, to shape recommendations for daily allowances of folate.

Radiolabeled folic acid tracers also had clinical applications for divulging folic acid absorption capacity in children (Hjelt, 1989). Fractional folic acid absorption was studied in 66 patients aged 2-16 years with celiac disease, partial small intestine resection or Crohn's disease. Forty-five of the children served as controls once they had recovered from their condition. The patients and controls were administered 50 μg [3',5',7,9-^{3}H]folic acid and the following stool sample collected. The dose contained ~20 μCi

activity equivalent to 4.8 mrad of radiation. Unabsorbable $^{51}CrCl_3$ (1.2 μCi) was given at the same time to correct for partial stool collection.

The bioavailability of folic acid ranged from 28-98% with a mean of 81%. Less than 4% of the ^{3}H-folic acid was excreted in urine after 48 hours. The authors concluded that the radiation exposure, equivalent to about two weeks of exposure from background sources, was a safe and ethical exposure with minimal risk. Also, the small physiologic dose of 50 μg folic acid was suitable for studying folate bioavailability since it was below the saturation level of specific, carrier mediated, intestinal folic acid absorption mechanisms (Halsted, 1980).

In the studies presented so far, radiolabeled folate compounds were used as a tracer for studying bioavailability, distribution and excretion in urine. Detection of the tracer was made by scintillation counting and required minimal or no sample preparation. Complex sample matrices, such as feces, were measured by simple extraction in acid or base. In some cases chromatographic separation and identification of the folate molecule in plasma and urine was performed. This clearly showed the advantage of using tracer labeled with a radioisotope. However, administration of radioisotopes as routine diagnostic tests to healthy subjects, even at ~20 μCi levels, posed difficulties that made their acceptance unlikely. In the absence of more sensitive methods for detection of radioisotopes, which would have allowed exposure to much smaller amounts of radioisotopes, techniques were developed that used folate tracers labeled with stable isotopes.

Stable isotope experiments became possible once schemes for synthesis of deuterium-labeled folate molecules and methods for their isolation and detection by mass

spectrometry were developed (Gregory, 1988a; Gregory, 1988b; Hachey, 1978). Studying folate bioavailability with stable isotope-labeled folate typically involves administration of the tracer followed by detection of excreted tracer in the urine. Since measurement of the isotope requires tracer isolation and purification from a complex feces matrix, feces tracer is not measured.

Concentration of tracer in the urine is used as an indirect measure of bioavailability, especially if the subject has been consuming pharmacological doses of nonlabeled folic acid prior to tracer administration. This saturation protocol ensures that most of the absorbed tracer is diverted to urine since all folate pathways and carrier-mediated processes are saturated. In theory, absorbed tracer would immediately be excreted in urine where it can be quantified.

In one study, d_2-folic acid was ingested orally and d_4-folic acid simultaneously injected intravenously (Gregory, 1991). The healthy volunteers had been saturated by consumption of 2 mg folic acid/day for seven days prior to the study. Measurement of urine d_2/d_0 and d_4/d_0 ratios by GC/MS and total folate by microbiological assay allowed calculation of tracer elimination in urine. The first trial (n=7) resulted in recovery of 37 and 25% of the d_2- and d_4-tracers, respectively, in the first 48 hour urine samples.

A second trial resulted in recovery of 14% of the d_2-folic acid and 21% of d_4-folic acid over the same period. Since the ratios of d_2/d_4 in urine were different than d_2/d_4 ratios of administered folic acid, there was selective elimination due to route of administration. This precluded the use of intravenously administered tracer for calculating bioavailability of orally ingested tracer.

In a second report by the same authors using a similar protocol, the losses of d_2- and d_4-folic acid after 48 hours were 5.8 and 5.2%, respectively (Gregory, 1990). No explanation was given to reconcile the significant difference observed in the two studies for urinary loss of the tracer. The authors concluded that the similarity in percentage loss of the d_2- and d_4-folic acid administered by different routes, although in contrast to an earlier study, enabled calculation of absolute bioavailability.

Urine represented a major route of folate elimination from the body. This was either intact folate, in cases when the subject is supplemented daily with greater than ~ 1 mg folate, or catabolites such *para*-aminobenzoylglutamate or acetamido-benzoylglutamate when tissue stores of folate are being turned over (Geoghegan, 1995; McPartlin, 1992).

Using deuterium-labeled folate, seven male subjects received 600 μg of an equal mixture of d_2- and d_4-folic acid after a seven day 2 mg/day saturation regimen. Urine was collected for 48 hours and analyzed by GC/MS for tracer appearance into the intact folate or catabolic pools. Total catabolite excretion increased less than two-fold as a result of supplementation, whereas intact folate excretion increased 10-fold. Approximately 14-15% of the labeled folic acid appeared in the urine as intact folate (equal proportions of folic acid and 5-methyltetrahydrofolate) and 0.98-1.15% as catabolites. The saturation effect of the seven-day supplementation period forced a significant amount of the tracer to be eliminated as intact folate and only a minor portion as catabolites.

This indicated that a large portion of the labeled folic acid did not equilibrate with body folate and was eliminated. The catabolites represent labeled-folic acid that might

have been subjected to folate catabolic pathways after equilibration with endogenous pools. It would be difficult to make physiological inferences from this data since mechanisms for absorption, metabolism and elimination of folate in these subjects were at or near saturation. The authors concluded that the quantitative significance of urinary folate catabolites in this study decreased as a result of supplementation. However, since quantitation of deuterium-labeled folic acid into any biological pool was not attainable under physiologic conditions, the authors continued to use a protocol if administering a large test dose after a saturation period.

The saturation protocol permitted estimation of bioavailability to be made, albeit under non-physiologic conditions. Even under these large dosing and saturating conditions, only about 15% of the administered dose was recovered in the urine after 48 hours. The remainder was either not absorbed, or absorbed but not eliminated in urine (retained). For this reason, urine cannot be used to estimate absolute bioavailability, unless an intravenous folate tracer is also administered whose kinetics parallels absorbed folate. Contradictory evidence existed regarding the validity of this protocol (Gregory, 1990; Gregory, 1991).

This dilemma could be resolved if the kinetics of folic acid within body pools, such as plasma, could be quantified. This was difficult since the isotope-labeled folic acid tracer given as a bolus represented a very small proportion of body folate stores. The percent enrichment of isotope into the plasma folate pool would be well below the detection limits of GC/MS protocols (Rogers, 1997).

To overcome this limitation, a chronic supplementation protocol was used that required daily supplementation with 1.6 mg d_2-folic acid for 28 days (von der Porten,

1992). This large daily influx of isotope-labeled folic acid resulted in maximum isotope enrichments of 69% in urine and ~10% in red blood cells. Quantitation of plasma isotope enrichment was not attempted since low folate concentrations in plasma would have required collection of large blood samples. Chronic supplementation resulted in a 2.5-fold increase in total plasma folate, a two-fold increase in red blood cell folate and a 20-fold increase in urinary folate, as determined by the microbiological assay.

Kinetic modeling of total plasma folate concentrations showed a two-phase decay after the 28 day supplementation period. The half-lives for these decay rates were $t_{1/2}$ <1 day (could not be calculated precisely due to long sampling frequency) and $t_{1/2}$ of 18.7 days. A two-pool compartment model was proposed which indicated a 43.7 mg total body folate pool and a 4.5% daily turnover of total body folate. Since the kinetic modeling was based on total folate concentrations determined by the microbiological assay, modeling could have been performed on subjects supplemented with non-labeled folate to eliminate the high cost of deuterium labeled folic acid.

Results from the saturation protocols described above were not physiologically relevant to normal folate bioavailability or kinetics in humans. The protocols, however, have been used to determine the relative bioavailability of deuterated folic acid mixed in various food matrices. Seven healthy male subjects were supplemented daily with 10 mg folic acid for seven days (Wei, 1996). Each subject was administered 300 μg of d_2-pteroylglutamate (folic acid) and 300 μg of d_4-pteroylhexaglutamate mixed in water (control) and orange juice, tomato juice, lima bean homogenate and in citrate buffer, pH 4.1. Since polyglutamates must be cleaved by intestinal pteroylpolyglutamate hydrolase

to a monoglutamate for absorption, the relative bioavailability of the two folate forms could be determined by measuring d_2/d_4 ratios by GC/MS in 48 hour urine collections.

A significantly lower ratio of d_2/d_4 was observed when the two tracers were mixed in orange juice compared to the other samples and controls. When the pH of orange juice was adjusted to 6.1 with NaOH the ratio increased to control levels, indicating that the low pH of orange juice reduced the enzymatic efficiency for conversion of pteroylpolyglutamate to pteroylpolyglutamate and thus, reduced its absorption and bioavailability relative to controls.

It is important to note that this study determined relative bioavailability of labeled folate, but not intrinsically incorporated, into various food matrices. Food folate bioavailability might not be reflected by tracer bioavailability. Also, since the subjects were saturated with large amounts of folic acid, the interpretation of these data and the conclusions regarding tracer-folate bioavailability are valid only under these non-physiologic conditions. Application of these data to the population at large would be inappropriate.

Supplementation with non-physiologic doses of folic acid has prevented the adoption of the saturation protocol by other researchers. In an attempt to overcome this limitation, two recent studies were conducted using stable isotope-labeled folate in subjects consuming physiologic amounts of folate.

One study used d_2-folic acid and $^{13}C_5$-folic acid labeled in the glutamate moiety (Rogers, 1997). Four subjects consumed 220 μg of each folate tracer in 50 mL water and 24-hour urinary excretion of each isotope was measured by GC/MS. Total folate loss in urine increased from 3.9 to 56.5 nmol as a result of the oral dose. The ratio of $^{13}C_5/d_2$ was

0.96 indicating equal absorption and elimination of the two folate tracers. Less than 2% of the dose appeared in urine after 24 hours.

In a second trial, 1010 nmol $^{13}C_5$-folic acid was administered orally and 226 nmol d_2-folic acid by intravenous injection. Nine plasma samples were taken over a nine hour period and d_2/d_0 and $^{13}C/d_0$ ratios measured. Intravenously administered d_2/d_0 ratios increased rapidly and reached a maximum of ~5.5 at 1 hour and returned to near baseline at 2 hours postdose. Orally administered $^{13}C/^{12}C$ ratios reached a plateau of ~0.5 from 30 minutes to 3 hours and returned to near baseline by 4 hours postdose. Comparison of areas under the curve indicated a 15- to 20-fold difference in the response of the ratios between the two routes of administration.

The authors concluded that the low response in the isotope ratios observed in the orally administered ^{13}C-folic acid was due to low absorption, and to a greater extent, fast clearance from plasma as a result of liver uptake during the first pass in portal blood. Since the clearance rate of folate administered by the different routes varies, orally administered folate is required for a reliable assessment of bioavailability.

The most recent application of stable isotope-labeled folic acid was to develop a compartmental model of folate metabolism in humans (Stites, 1997). Four subjects were supplemented with 200 μg folic acid daily for two weeks. They were then administered 50 μg d_2-pteroylhexaglutamate daily for the next seven days as well as 100 μg d_2-folic acid daily for the next 56 days. Urine was collected at intervals over 125 days, folate isolated by affinity chromatography and isotope enrichment of the pABG derivative measured by GC/MS. Urinary folate isotope enrichment increased during the

supplementation period and decreased with a two-phase pattern after d_2-folic acid was withdrawn.

The only kinetic data available for modeling were urinary excretion of deuterated-folate which constituted ~2% of ingested dose. Bioavailability of the deuterated-folate was assumed to be 67% for purposes of calculating amount of dose entering body pools. The model consisted of fast and slow turnover pools, a urine excretion pool and a pool for all other losses such as fecal urinary catabolites. Rate constants were derived for flux of the tracer between pools, but the authors conclude 'that caution must be taken in interpreting the quantitative results of this kinetic model, which is based solely on isotopic enrichment of urinary excretion of folate'.

Urinary folate isotope data representing less than 2% of the administered dose and 'exhibiting considerable scatter' was used to develop a model of folate kinetics. Whole-body turnover was determined to be <1% based on urinary folate excretion, however, it is premature to make this conclusion since fecal and urinary catabolites were not measured. The 1-2% loss as intact folate in urine led the authors to conclude that 'the other 98-99% if the dietary folate was presumably excreted in the urine and feces as a mixture of catabolites and intact folate or as catabolites excreted in urine', but fail to mention that a significant portion of the deuterated-folate could have been retained by the body. The slow whole-body turnover of folate corresponded to a mean residence time of approximately 100 days.

The studies described above represent the sum of our knowledge regarding folate bioavailability and kinetics in humans. The classic study of Herbert, although simple in design, remains as perhaps the most relevant study in a healthy adult (Herbert, 1962).

The radioisotope studies of Krumdieck and Butterfield, although quantitative, were conducted in clinically impaired subjects (Butterworth, Baugh & Krumdieck, 1969; Krumdieck, 1978). The stable isotope studies of Gregory *et al.* have added little to our understanding of folate dynamics, mainly due to non-physiologic experimental protocols and analytical limitations (Gregory, 1990; Gregory, 1992; Pfeiffer, 1997; Rogers, 1997; Stites, 1997).

The common thread in all these studies was the lack of suitable analytical protocols that would allow the study of true folate dynamics in healthy humans under physiologic conditions. This has forced compromises to be made in the study subjects and experimental design (i.e. sick individuals, large dosing regimens, sampling urine instead of plasma). To truly understand the dynamics of folate metabolism significant advances have to be made in our analytical capabilities that will usurp such compromises. Accelerator mass spectrometry has provided this capability.

Accelerator mass spectrometry

Accelerator mass spectrometry (AMS) sensitivity permits the design of experimental protocols that can significantly improve our understanding of nutrient dynamics in humans. The first requirement in any nutrient kinetic study is the availability of a labeled nutrient tracer. The nutrient can be labeled with stable or radioactive isotopes or even conjugated to molecules with fluorescent properties. The second requirement is the existence of reliable methodologies for detection of the tracer at concentrations present in relevant biological samples. As outlined earlier, current methodologies fail to meet one

or both of these requirements. AMS meets both of these requirements and has far reaching implications for the future studies of nutrient dynamics.

Radiocarbon (^{14}C) is commonly detected by the β-particles it emits as the atoms decay. The half-life of ^{14}C is 5760 years. This long half-life necessitates detection of β-particles over a long period, or more practically, use of relatively large amounts of ^{14}C with shorter detection times. This necessity has precluded use of radiocarbon-labeled nutrients in human studies for ethical reasons. In contrast to decay counting, AMS measures ^{14}C in a sample without the need for a decay event to occur.

The technique is based on the mass-to-charge (m/z) difference between carbon isotopes (^{12}C, ^{13}C and ^{14}C). Carbon atoms are ionized by a negative ion source, accelerated through an 8 MV electrostatic accelerator and ^{14}C selected by high-energy mass spectrometers. Quadropole lenses focus the beam while a gas ionization detector measures ^{14}C after it passes through an electrostatic and magnetic filter (Vogel, 1995). The instrument can detect ^{14}C with attomole sensitivity (10^{-18}) and is 10^6 more sensitive than conventional decay counting methods.

The extreme sensitivity gives AMS two significant advantages. Firstly, much smaller doses of ^{14}C-labeled compounds, that are both physiologically relevant and safe, can be given to human subjects. Secondly, since very small samples are required, sampling frequency can be very high. This is an important issue in modeling since nutrient kinetic curves can be drawn with much more confidence. Another reason why AMS is so well suited for these studies is that background ^{14}C is extremely low ($^{12}C/^{14}C$ ratio is 1.18×10^{-14}). AMS also permits measurement of the radioisotope without any sample clean up. This is especially important in samples with complex and difficult

biological matrices such as feces. AMS permits easy measurement of unabsorbed ^{14}C-labeled nutrients in feces and is the most direct method for measuring nutrient bioavailability.

Only recently has biomedical research profited from the many advantages of AMS. Several recent animal studies have applied AMS to toxicological research (Creek, 1997; Kautiainen, 1997; White, 1997). Examples of the use of AMS in human biomedical research is extremely scant and is a testament to the novelty of the technique. DNA adduct formation has been studied as a result of exposure to low doses of toxicant (Turteltaub, 1997).

Other researchers have measured $^{14}CO_2$ concentration in the expired breath of four elderly male volunteers after ^{14}C-triolein ingestion (Stenstrom, 1996; Stenstrom, 1997). ^{14}C-triolein is used for assessment of fat malabsorption as a breath test in clinical settings (Newcomer, 1979). The risks associated with long-term exposure to relatively high doses of absorbed ^{14}C-triolein are unknown. Three subjects consumed 2 μCi ^{14}C-triolein and breath $^{14}CO_2$ was measured by liquid scintillation counting while a fourth subject consumed 40 nCi ^{14}C-triolein and breath $^{14}CO_2$ was measured by AMS. $^{14}CO_2$ was easily detected in the expired breath by AMS for several months a single dose. About 30% of the triolein was catabolized rapidly with a half-life of about two days while the remaining 70% exhibited a slow turnover with a half-life of several hundred days.

Literature cited

Anderson, B., Belcher, E. H., Chanarin, I. & Mollin, D. L. (1960). The urinary and faecal excretion of radioactivity after oral doses of ^{3}H-folic acid. *Brit J Haemat* **6,** 439.

Barford, P. A., Staff, F. J. & Blair, J. A. (1978). The metabolic fate of (2-^{14}C)folic acid and a mixture of (2-^{14}C)- and (3',5',9-^{3}H)-folic acid in the rat. *Biochemical Journal* **174,** 579-83.

Bhandari, S. D. & Gregory, J. F. (1992). Folic acid, 5-methyl-tetrahydrofolate and 5-formyl-tetrahydrofolate exhibit equivalent intestinal absorption, metabolism and in vivo kinetics in rats. *Journal of Nutrition* **122,** 1847-54.

Butterworth, C. E., Jr., Baugh, C. M. & Krumdieck, C. (1969). A study of folate absorption and metabolism in man utilizing carbon-14-labeled polyglutamates synthesized by the solid phase method. *Journal of Clinical Investigation* **48,** 1131-42.

Butterworth, C. E., Nadel, H., Perez-Santiago, E., Santini, R. & Gardner, F. H. (1957). Folic acid absorption, excretion and leukocyte concentrations in tropical sprue. *J lab clin med* **50,** 673.

Chanarin, I., Anderson, B. B. & Mollin, D. L. (1958). The absorption of folic acid. *Brit J Haemat* **4,** 156.

Connor, M. J., Blair, J. A. & Barford, P. A. (1977). Isolation, purification, characterization and metabolism of high-molecular-weight folate from rat liver. *Biochem Soc Trans* **5,** 1319-20.

Connor, M. J., Pheasant, A. E. & Blair, J. A. (1979). The identification of p-acetamidobenzoate as a folate degradation product in rat urine. *Biochem J* **178,** 795-797.

Cox, E. V., Meynell, M. J., Cooke, W. T. & Gaddie, R. (1958). The folic acid excretin test in the steatorrhea syndrome. *Gastroenterology* **35,** 390.

Creek, M. R., Mani, C., Vogel, J. S. & Turteltaub, K. W. (1997). Tissue distribution and macromolecular binding of extremely low doses of [C-14]-benzene in B6C3F1 mice. *Carcinogenesis* **18,** 2421-2427.

Denko, C. W., Grundy, W. E., Wheeler, N. C., Henderson, c. R., Berryman, G. H., Friedemann, T. E. & Youmans, J. B. (1946). The excretion of B-complex vitamins by normal adults on a restricted intake. *Arch Biochem* **11,** 109.

Geoghegan, F. L., McPartlin, J. M., Weir, D. G. & Scott, J. M. (1995). para-acetamidobenzoylglutamate is a suitable indicator of folate catabolism in rats. *J Nutr* **125,** 2563-70.

Girdwood, R. H. (1953). A folic acid excretion test in the investigatio of intestinal malabsorption. *Lancet* **ii,** 53.

Gregory, J. F. & Toth, J. P. (1988). Preparation of folic acid specifically labelled with deuterium at the 3',5'-positions. *J Labelled Comp Radiopharm* **25,** 1349-59.

Gregory, J. F., Bailey, L. B., Toth, J. P. & Cerda, J. J. (1990). Stable-isotope methods for assessment of folate bioavailability. *Am J Clin Nutr* **51,** 212-5.

Gregory, J. F., Bhandari, S. D., Bailey, L. B., Toth, J. P., Baumgartner, T. G. & Cerda, J. J. (1991). Relative bioavailability of deuterium-labeled monoglutamyl and

hexaglutamyl folates in human subjects. *American Journal of Clinical Nutrition* **53,** 736-40.

Gregory, J. F., Bhandari, S. D., Bailey, L. B., Toth, J. P., Baumgartner, T. G. & Cerda, J. J. (1992). Relative bioavailability of deuterium-labeled monoglutamyl tetrahydrofolates and folic acid in human subjects. *American Journal of Clinical Nutrition* **55**. 1147-53.

Gregory, J. F. & Toth, J. P. (1988). Chemical synthesis of deuterated folate monoglutamate and in vivo assessment of urinary excretion of deuterated folates in man. *Anal Biochem* **170,** 94-104.

Hachey, D. L., Palladino, L., Blair, J. A., Rosenberg, I. H. & Klein, P. D. (1978). Preparation of pteroylglutamic acid-3',5'-^{2}H by acid catalyzed exchange with deuterium oxide. *J Labelled Com Radiopharm* **14,** 479-86.

Halsted, C. H. (1980). Intestinal absorption and malabsorption of folates. *Annual rev med* **31,** 79-87.

Hjelt, K. (1989). Folic acid absorption determined by a single stool sample test-a double-isotope technique. The folic acid absorption capacity in children. *Journal of Pediatric Gastroenterology and Nutrition* **9,** 335-41.

Herbert, V. (1962). Experimental nutritional folate deficiency in man. *Trans Assoc Am Physicians* **75,** 307-20.

Johns, D. G., Sperti, S. & Burgen, A. S. V. (1961). The disposal of tritiated folic acid injected intravenously in man. *Canad Med Ass J* **84,** 77.

Kautiainen, A., Vogel, J. S. & Turteltaub, K. W. (1997). Dose-dependent binding of trichloroethylene to hepatic DNA and protein at low doses in mice. *Chemico-Biological Interactions* **106,** 109-121.

Kokue, E., Sekiya, T., Shimoda, M. & Natsuhori, M. (1994). Pharmacokinetics and bioavailability of folic acid and plasma levels of bioactive folates after folic acid administration to pigs. *Veterinary Quarterly* **16,** 91-4.

Krumdieck, C. L. & Baugh, C. M. (1969). The solid phase synthesis of polyglutamates of folic acid. *Biochemistry* **8,** 1568-72.

Krumdieck, C. L., Fukushima, K., Fukushima, T., Shiota, T. & Butterworth, C. E., Jr. (1978). A long-term study of the excretion of folate and pterins in a human subject after ingestion of ^{14}C folic acid, with observations on the effect of diphenylhydantoin administration. *American Journal of Clinical Nutrition* **31,** 88-93.

Matte, J. J., Girard, C. L. & Brisson, G. J. (1984). Folic acid and reproductive performance in sows. *J Anim Science* **59,** 1020-5.

McPartlin, J., Courtney, G., McNulty, H., Weir, D. & Scott, J. (1992). The quantitative analysis of endogenous folate catabolites in human urine. *Anal Biochem* **206,** 256-61.

Murphy, M., Keating, M., Boyle, P., Weir, D. G. & Scott, J. M. (1976). The elucidation of the mechanism of folate catabolism in the rat. *Biochem Biophys Res Commun* **71,** 1017-24.

Murphy, M. & Scott, J. M. (1979). The turnover catabolism and excretion of folate administered at physiological concentrations in the rat. *Biochim Biophys Acta* **583,** 535-9.

Natsuhori, M., Shimoda, M., Kokue, E., Hayama, T. & Takahashi, Y. (1991). Tetrahydrofolic acid as the principal congener of plasma folates in pnpigs. *Am J Physiol* **261,** R82-6.

Newcomer, A. D., Hofmann, A. F., DiMagno, E. P., Thomas, P. J. & Carlson, G. L. (1979). Triolein breath test: a sensitive and specific test for fat malabsorption. *Gastroenterology* **76,** 6-13.

Pfeiffer, C. M., Rogers, L. M., Bailey, L. B. & Gregory, J. F.. (1997). Absorption of folate from fortified cereal-grain products and of supplemental folate consumed with or without food determined by using a dual-label stable-isotope protocol [see comments]. *American Journal of Clinical Nutrition* **66,** 1388-97.

Pheasant, A. E., Connor, M. J. & Blair, J. A. (1981). The metabolism and physiological disposition of radioactively labelled folate derivatives in the rat. *Biochem Med* **26,** 435-50.

Plante, L. T., Williamson, K. L. & Pastore, E. J. (1980). Preparation of folic acid specifically labeled with carbon-13 in the benzoyl carbonyl. *Methods in Enzymology* **66,** 533-5.

Reisenauer, A. M., Buffington, C. A., Villanueva, J. A. & Halsted, C. H. (1989). Folate absorption in alcoholic pigs: in vivo intestinal perfusion studies. *Am J Clin Nutr* **50,** 1429-35.

Reisenauer, A. M., Chandler, C. J. & Halsted, C. H. (1986). Folate binding and hydrolysis by pig intestinal brush-border membranes. *Am J Physiol* **251,** G481-6.

Rogers, L. M., Pfeiffer, C. M., Bailey, L. B. & Gregory, J. F. (1997). A dual-label stable-isotopic protocol is suitable for determination of folate bioavailability in humans:

evaluation of urinary excretion and plasma folate kinetics of intravenous and oral doses of [$^{13}C_5$] and [$^{2}H_2$]folic acid. *Journal of Nutrition* **127,** 2321-7.

Scott, K. C. & Gregory, J. F., III. (1996). The fate of (^{3}H)folic acid in folate-adequate rats. *Journal of Nutritional Biochemistry* **7,** 261-269.

Shimoda, M., Shin, H. C. & Kokue, E. (1994). Simultaneous determination of tetrahydrofolate, 10-formyltetrahydrofolate and 5-methyltetrahydrofolate in rat bile by high-performance liquid chromatography with electrochemical detection. *J Vet Med Sci* **56,** 701-5.

Shin, H. C., Shimoda, M. & Kokue, E. (1994). Identification of 5,10-methylenetetrahydrofolate in rat bile. *J Chromatogr B Biomed Appl* **661,** 237-44.

Shin, H. C., Shimoda, M., Kokue, E. & Takahashi, Y. (1993a). Identification of 10-formyltetrahydrofolate, tetrahydrofolate and 5-methyltetrahydrofolate as major reduced folate derivatives in rat bile. *J Chromatogr* **620,** 39-46.

Shin, H. C., Shimoda, M., Kokue, E. & Takahashi, Y. (1993b). Identification of endogenous tetrahydrofolate and 10-formyltetrahydrofolate as major folates in rat bile. *Adv Exp Med Biol* **338,** 737-40.

Shin, H. C., Takakuwa, F., Shimoda, M. & Kokue, E. (1995). Enterohepatic circulation kinetics of bile-active folate derivatives and folate homeostasis in rats. *Am J Physiol* **269,** R421-5.

Stenstrom, K., Leidesvegborn, S., Erlandsson, B., Hellborg, R., Mattsson, S., Nilsson, L. E., Nosslin, B., Skog, G. & Wiebert, A. (1996). Application Of Accelerator Mass Spectrometry (AMS) For High-Sensitivity Measurements Of (CO_2)-C-14 In Long-Term Studies Of Fat Metabolism. *Applied Radiation and Isotopes* **47,** 417-422.

Stenstrom, K., LeideSvegborn, S., Erlandsson, B., Hellborg, R., Skog, G., Mattsson, S., Nilsson, L. E. & Nosslin, B. (1997). A programme for long-term retention studies of C-14-labelled compounds in man using the Lund AMS facility. *Nuclear Instruments & Methods In Physics Research Section B-Beam Interactions With Materials and Atoms* **123,** 245-248.

Stites, T. E., Bailey, L. B., Scott, K. C., Toth, J. P., Fisher, W. P. & Gregory, J. F. r. (1997). Kinetic modeling of folate metabolism through use of chronic administration of deuterium-labeled folic acid in men [see comments]. *Am J Clin Nutr* **65,** 53-60.

Turteltaub, K. W., Mauthe, R. J., Dingley, K. H., Vogel, J. S., Frantz, C. E., Garner, R. C. & Shen, N. (1997). MeIQx-DNA adduct formation in rodent and human tissues at low doses. *Mutation Research-Fundamental and Molecular Mechanisms Of Mutagenesis* **376,** 243-252.

Villanueva, J., Chandler, C. J., Shimasaki, N., Tang, A. B., Nakamura, M., Phinney, S. D. & Halsted, C. H. (1994). Effects of ethanol feeding on liver, kidney and jejunal membranes of micropigs. *Hepatology* **19,** 1229-40.

Vogel, J. S., Turteltaub, K. W., Finkel, R. & Nelson, D. E. (1995). Accelerator Mass Spectrometry - Isotope Quantification At Attomole Sensitivity. *Analytical Chemistry* **67,** A353-A359.

von der Porten, A. E., Gregory, J. F. d., Toth, J. P., Cerda, J. J., Curry, S. H. & Bailey, L. B. (1992). In vivo folate kinetics during chronic supplementation of human subjects with deuterium-labeled folic acid. *J Nutr* **122,** 1293-99.

Wei, M. M., Bailey, L. B., Toth, J. P. & Gregory, J. F. r. (1996). Bioavailability for humans of deuterium-labeled monoglutamyl and polyglutamyl folates is affected by selected foods. *Journal of Nutrition* **126,** 3100-8.

White, I. N. H., Martin, E. A., Mauthe, R. J., Vogel, J. S., Turteltaub, K. W. & Smith, L. L. (1997). Comparisons of the binding of [C-14]radiolabelled tamoxifen or toremifene to rat DNA using accelerator mass spectrometry. *Chemico-Biological Interactions* **106,** 149-160.

Chapter Five

^{14}C-Folic Acid Bioavailability and Dynamics Determined by Accelerator Mass Spectrometry and Mathematical Modeling

Abstract

Recent advances in mass spectrometry and the availability of stable isotope-labeled compounds have made kinetic tracing of nutrients a powerful tool for understanding nutrient metabolism in humans. The quality of the data generated by such studies was dictated to a large degree by limitations due to sample preparation and analysis. Accelerator mass spectrometry (AMS) provided an alternative approach to study tracer kinetics by measuring ^{14}C-labeled in human samples at attomole concentrations. AMS measured isotope concentrations to parts per 10^{13-15} on milligram-sized samples making it 10^6 more sensitive than decay counting. The increased sensitivity combined with an extremely low background allowed tracing of ^{14}C-folic acid in a healthy human subject under physiologic conditions. The methodological considerations necessary for determining the kinetics of ^{14}C-folic acid in human subjects are presented. A male volunteer consumed an oral dose of 100 nCi ^{14}C-folic acid in 35 μg unlabeled folic acid. Plasma, red blood cells and complete urine and feces were collected and ^{14}C concentration measured by AMS. The values were converted to femtomoles ^{14}C-folic acid by measuring and adjusting for total carbon concentration in each sample. The kinetic data was analyzed by various mathematical modeling techniques including compartmental modeling. This method is applicable to the study of any organic compound for assessment of bioavailability and kinetics at physiologic doses in healthy volunteers.

Introduction

Folate plays an important role in the etiology of many diseases. This relationship encompasses pathology of multiple organs occurring at different stages during development (Wadsworth, 1997). This increases the challenge faced by researchers aiming to identify the mechanisms underlying many of these pathologies. Many biological processes are involved in the coordination of folate homeostasis and metabolism. Folate balance is also influenced to a great degree by environmental factors such as dietary intake. The interplay between biological regulation determined at the genetic level (genotype), and environmental factors, produce the observed state of the organism (phenotype). Kinetic modeling can identify the metabolic phenotype of the organism. Genetic and/or environmental factors that contribute to the observed phenotype can then be determined. This will help to identify the etiology of folate-related diseases and to develop rational therapies. No reliable method has ever been developed to model folate kinetics in humans under physiological conditions. In this study, the extreme sensitivity of accelerator mass spectrometry permitted the modeling of folate kinetics in a healthy adult male for the first time. The instrument will be useful for scientists as a biomedical research tool and for clinicians as a diagnostic tool.

Although accelerator mass spectrometry (AMS) has been used in the past for environmental, geologic and archeological research, only recently has it been applied to the biomedical sciences. Animal and human toxicological research has yielded novel insights into interactions between macromolecules and toxicants (Creek, 1997; Kautiainen, 1997; Turteltaub, 1997; White, 1997). A recent investigation revealed

femtomole quantities of $^{14}CO_2$ in the expired breath of humans after ingestion of 40 nCi ^{14}C-triolein (Stenstrom, 1996). No biomedical AMS research has ever been attempted with the sampling density and quantitative precision required by this study. Many of the experimental protocols and design considerations were novel and specific to this study. These considerations were based on current understanding of folate kinetics in humans. Important parameters such as dosing level and sampling schedule were planned specifically to aid the mathematical modeling of the data.

The experimental procedures for the first quantitative human biomedical study using AMS are described. The results and their mathematical interpretation are presented. The implications to folate nutrition, disease prevention and the future of AMS biomedical research are also discussed.

Experimental Procedures

Materials: L-Glutamic acid [^{14}C (U)] (250 mCi/mmol) was purchased from Moravek Biochemicals. Folic acid, 5-methyltetrahydrofolic acid and folinic acid standards were purchased from Sigma. Acetonitrile and water were OPTIMA grade from Fisher.

Methods

Radiolabeling of folic acid: Pteroyl-[^{14}C(U)]-glutamic acid (folic acid) was synthesized according to the method of Plante (Plante, 1980) with some modifications (Clifford, 1998). The concentration was measured by UV-VIS spectrometry after separation by reverse-phase HPLC. Radioactivity was measured by scintillation counting and specific

activity calculated at 1.24 mCi/mmol. The specific activity of the final product was lower than the specific activity of the ^{14}C-glutamic acid because of dilution with non-labeled glutamic acid.

Blood sampling schedule: The small volume of sample required for AMS measurement allowed frequent sampling of blood in the first 24 hours of the study. The early dynamic stage of folate absorption and distribution was determined by collection of ~8 mL blood at 10 minute intervals postdose. Sampling frequency was reduced to 20-minute intervals after one hour and to 30-minute intervals after 3 hours. A total of 24 samples were collected in the first 24 hours. Sampling of ~ 24 mL blood continued for the next 200 days at weekly to monthly intervals.

^{14}C-Folic acid dose: A healthy informed male volunteer weighing 85 kg consumed 50 mL water orally containing 35 μg ^{14}C-folic acid (80 nmol, specific activity 1.24 mCi/mmol) in the morning followed by a light breakfast. Residual dose in the container was rinsed with approximately 100 mL water and ingested. All procedures were approved by Institutional Review Boards at the University of California, Davis and Lawrence Livermore National Laboratory.

Sample collection and processing

Blood: Whole blood was collected prior to administration of the oral dose and postdose through a catheter for the first week and by venipuncture thereafter. Red blood cells were separated from whole blood within an hour after collection by centrifugation at 3,500

RPM for 5 minutes. Plasma was removed, the buffy-coat discarded and red blood cells washed four times with an approximately equal volume of isotonic buffer (150 mM sodium chloride, 10 mM potassium phosphate, pH 7.2, 0.05 mM EDTA, 2 % ascorbate). Plasma and red blood cells were stored at –20°C for AMS, folate and carbon measurements.

Urine: Complete urine samples were collected in 3 L plastic urine collection containers (Fisher). A 24-hour sample was collected a day before ingestion of the dose. Four 6-hour collections were made immediately after the dose and complete 24-hour collections were made for the next 41 days. Each collection was weighed and aliquots taken for AMS, carbon and folate analysis and stored at –20°C.

Feces: Fecal samples were collected in plastic containers. One collection was made prior to ingestion of the dose and complete collections made over the next 42 consecutive days. Samples were weighed in their tared containers and digested in a hood with 1 L 0.5 M potassium hydroxide for 4 hours at room temperature. A spatula was used to break-up larger pieces and a disposable magnetic stir bar facilitated mixing over a stir plate. Aliquots were taken for AMS, carbon and folate analysis and stored at –20°C.

AMS sample preparation

Screening for radioactivity: Samples collected in the first week of the study were screened for radioactivity by conventional scintillation counter prior to analysis by AMS. Samples, 50 μL of plasma, 10 μL of red blood cell homogenate, 50 μL of fecal extract

(supernatant) or 50 μL urine were each mixed with 10 mL of scintillant (UniverSol, ICN) and counted for 30 minutes on a Wallac 1410 liquid scintillation counter (Gaithersburg, MD).

Packaging: Triplicates of each plasma (20 μL), RBC (20 μL), urine (100 μL) and fecal (15 μL) sample were placed in individual quartz tubes and graphitized according to published methods (Vogel, 1992). In samples where the total carbon content was less than one milligram, additional carbon was added as a carrier to facilitate isotope measurement. Tributyrin was used as the carrier and adjustments were made in the calculation to account for the carrier carbon (calculations shown in Appendix I).

Plasma HPLC-AMS

Acetonitrile extraction: Plasma folates were extracted and chromatographed to identify which folates were labeled with radiocarbon. Plasma (200 μL) was spiked with 10 μL of unlabeled 5-methyltetrahydrofolate (5MTFA) and folic acid (FA) standards in potassium phosphate 5 mM, pH 8.6, 2% (w/w) ascorbic acid and extracted with 1.5 mL buffer (potassium phosphate 5 mM, pH 8.6, 50 mM tetrabutylammonium dihydrogen phosphate (TBAP), 2% (w/w) ascorbic acid) by boiling for 10 minutes. The samples were cooled on ice, centrifuged at 3500 RPM for 5 minutes and the supernatant removed. Pellets were washed with an additional 1 mL buffer, spun and the supernatants pooled.

Solid-phase extraction: Disposable solid phase extraction cartidges (50 mg C18, Varian) were conditioned with 2 mL acetonitrile followed by 2 mL potassium phosphate 0.05 M,

pH 8.6, 50 mM TBAP. Plasma extracts were applied to the column at a flow of 0.2 mL/minute and washed with 2 mL buffer. Folate was eluted with 1 mL acetonitrile, dried under nitrogen at room temperature and resuspended in 1 mL potassium phosphate 5 mM, pH 8.6 and purified by folate binding protein-affinity chromatography.

Affinity-chromatography: Affinity matrix was poured into a disposable plastic column (BioRad) to give a bed volume of 200 μL. FBP-agarose beads were equilibrated with 4 mL 0.05 M potassium phosphate, pH 7.0, and the sample applied and allowed to flow by gravity. The column was washed with 4 mL 0.05 M potassium phosphate, pH 7.0, 1 M NaCl followed with 4 mL 0.05 M potassium phosphate, pH 7.0. Bound folate were eluted with 1 mL 0.02 M trifluoroacetic acid, mixed with 2 mL potassium phosphate 0.05 M, pH 8.6, 50 mM TBAP and applied to C18 extraction cartridges as described earlier. Folate was eluted with 1 mL acetonitrile, dried under nitrogen at room temperature and resuspended in 0.2 mL HPLC mobile phase.

HPLC-AMS: Affinity-purified plasma folate was chromatographed using a C18 reverse-phase (Alltech) column on a Hewlett-Packard 1100 HPLC system pumping an isocratic mobile phase (90% 0.05 mM potassium phosphate, pH 5.0, 3.5 mM TBAP, 10% acetonitrile) at 0.8 mL/minute. Detection was monitored at 292 nm. One-minute fractions were collected in Eppendorf tubes for AMS analysis. Mobile phase was collected prior to each injection and measured by AMS to ensure the $^{14}C/^{12}C$ ratio had returned to baseline.

Total carbon

The total carbon concentration in each sample (75-100 μL) was measured by freezing the sample over liquid nitrogen in individual Costech tin capsules (Ventura, CA) followed by overnight lyophilization. Each capsule was then placed inside a second tin capsule, rolled into a ball and analyzed for total carbon concentration using a Carlo-Erba carbon analyzer (Pella, 1990). Calculations were based on sample weights measured to four decimal places.

Total folate

Total folate was measured by the standard microbiological assay in microtiter plates. Plasma, urine and feces extract were thawed and assayed for total folate. Red blood cell suspensions were thawed and diluted 1:27 with cold 0.05 M potassium phosphate buffer, pH 7.0, 1% ascorbic acid. Chicken pancreas acetone-washed conjugase (Sigma) was prepared according to the method of Martin *et al.* (Martin, 1990). One milliliter of the enzyme solution and 2 mL of red blood cell preparation were mixed in screw capped digestion tubes and incubated in a 37°C water bath for 4 hours with gentle shaking. Tubes were removed, 1 mL of ascorbate buffer added, and proteins precipitated by boiling at 100°C for 10 minutes. Precipitates were pelleted by centrifugation at 2500 RPM for 5 minutes and the supernatant removed and assayed in triplicates.

Hemoglobin in red blood cell suspensions

Red blood cell folate values were normalized to hemoglobin to correct for differences in dilution. Hemoglobin in lysed red blood cell suspensions was measured with a

hemoglobin assay kit (Sigma). To 5 mL Drabkin's solution (Drabkin's reagent No. 252-2, 1 L deionized water, 0.5 mL 30 % Brij-35) 20 μL red blood cell suspension was added and absorbance measured at 550 nm. Hemoglobin standards were used to generate a standard curve. Hemoglobin was expressed as grams hemoglobin per milliliter red blood cell suspension.

Calculations and data reduction

Dose: ^{14}C-Folic acid had a specific activity of 1.24 mCi/mmol. Exactly 441.4 μL of the synthesized preparation was used for the dose with an activity of 222,000 DPM (5.028 DPM/μL). This corresponded to 100 nCi of activity and 80.6 nmol of folic acid. This amount (35.6 μg) was approximately equivalent to 1/6th the current RDA for folic acid.

Time: The dose was mixed with ~ 150 mL water and ingested at 7:12 AM. The first blood sample was taken after 10 minutes the time of subsequent samples recorded in minutes after the dose and expressed as days (after ingestion of dose). A 24-hour urine sample was collected before ingestion of the dose followed by 6-hour collections for the first day and 24-hour collections thereafter. All values were expressed at the end-point of each collection. A pre-dose fecal sample was collected 24 hours before ingestion of the dose. The time of each collection was recorded and values for that sample are expressed at that time point.

^{14}C-Folate: The modern value (defined in Appendix I) for each sample was determined three times by accelerator mass spectrometry and the mean value used to calculate ^{14}C-

folic acid concentration. The modern value, carbon concentration of each sample and specific activity of the dose were used to calculate the concentration of ^{14}C-folate in each sample. Since the identity of the folate molecule was not determined, this value was expressed as a molar quantity to eliminate ambiguities between different folate molecules due to differences in molecular weight. The same approach was taken in expressing ^{14}C-folate concentration in urine and feces. These samples contained catabolites of folate but concentrations were expressed as moles of ^{14}C-folate since one mole of catabolite was derived from exactly one mole of ^{14}C-folic acid. The equations for calculating ^{14}C-folate concentrations are shown in Appendix I.

Results

The subject successfully fulfilled the requirements of the study and provided the necessary samples with no complications. All samples were collected at locations known to be free of radiocarbon contamination and were processed and stored in a dedicated laboratory with no previous exposure to radiocarbon. As a result, no contamination was observed in the hundreds of samples analyzed by AMS. Modern values for each sample were converted to moles of ^{14}C-folate and the entire data set is presented in Appendices.

The subject maintained a daily log of his diet and activities. The diet was consistent with a typical American diet containing mainly convenience foods and prepared food items. Food consumed over a two-day period was collected, homogenized and analyzed for macronutrient and energy content. Mean daily intake was 127 g fat (determined by ether extraction), 112 g protein (nitrogen determined by the Kjeldahl

procedure and converted to protein by multiplication with 6.25), 387 g carbohydrate (determined by difference) and 3,139 kilocalories (determined by bomb calorimetry). The subject experienced no weight gain or loss throughout the study period by maintaining a regular diet and physical activity level. Food records revealed a mean folate intake of 270 μg/day based on food folate databases (FoodProcessor).

Carbon and folate balance

Evidence that the subject was in steady-state was provided by the carbon concentration in the blood and carbon losses in urine and feces. The carbon concentration of each sample was measured using a modified protocol that simplified pipetting and packaging samples prior to analysis. The results, shown in Table 1, provided evidence that carbon homeostasis was maintained over the 200-day study period. Figure 1 shows the carbon concentration in plasma and red blood cells (top) and urine and feces (bottom) over a 42-day period.

Table 1. Carbon in samples collected over a 200-day period

Sample	Mean ± Standard deviation
Plasma (n=59)	4.42 ± 0.14 g/dL
Red blood cells (n=59)	0.60 ± 0.04 g/g hemoglobin
Urine (n=63)	9.68 ± 1.9 g/day
Feces (n=39)	9.09 ± 1.5 g/day

Total folate in all samples was measured in triplicate by the *Lactobacillus casei* microbiological assay. Plasma, urine and feces extracts were measured directly while red blood cell folate was enzymatically cleaved to folate monoglutamates before folate measurement. The results are shown in Figures 2 and 3.

Plasma HPLC-AMS

Folate was extracted from plasma using C18 solid phase extraction cartridges and folate binding protein-affinity chromatography. The extracted folate molecules were separated by reverse-phase HPLC with detection at 292 nm. Folate from 100 μL plasma did not produce a detectable signal because the endogenous folate concentration was below the limit of detection. Folate standards were added to the plasma as internal standards before extraction to check for recovery and to mark the retention of folate under the HPLC conditions. Folic acid (FA) and 5-methyltetrahydorfolate (5MTFA) standards were added since plasma folate was in the form of 5MTFA and the administered dose was in the form of FA. Folate standards, extraction buffers and HPLC solvents were screened by AMS to ensure there would be no ^{14}C contamination. Fractions were collected every minute, lyophilized and carbon carrier added prior to AMS measurement.

The results for recovery of folate using this procedure are shown in Table 2. The first step in the extraction procedure involved an acetonitrile precipitation of plasma proteins and subsequent removal of folate in the supernatant. To check for recovery, ^{3}H-folic acid was added to fasting and postprandial plasma samples since there were significant differences in their lipid content. Acetonitrile extraction resulted in complete recovery of the spiked ^{3}H-folic acid.

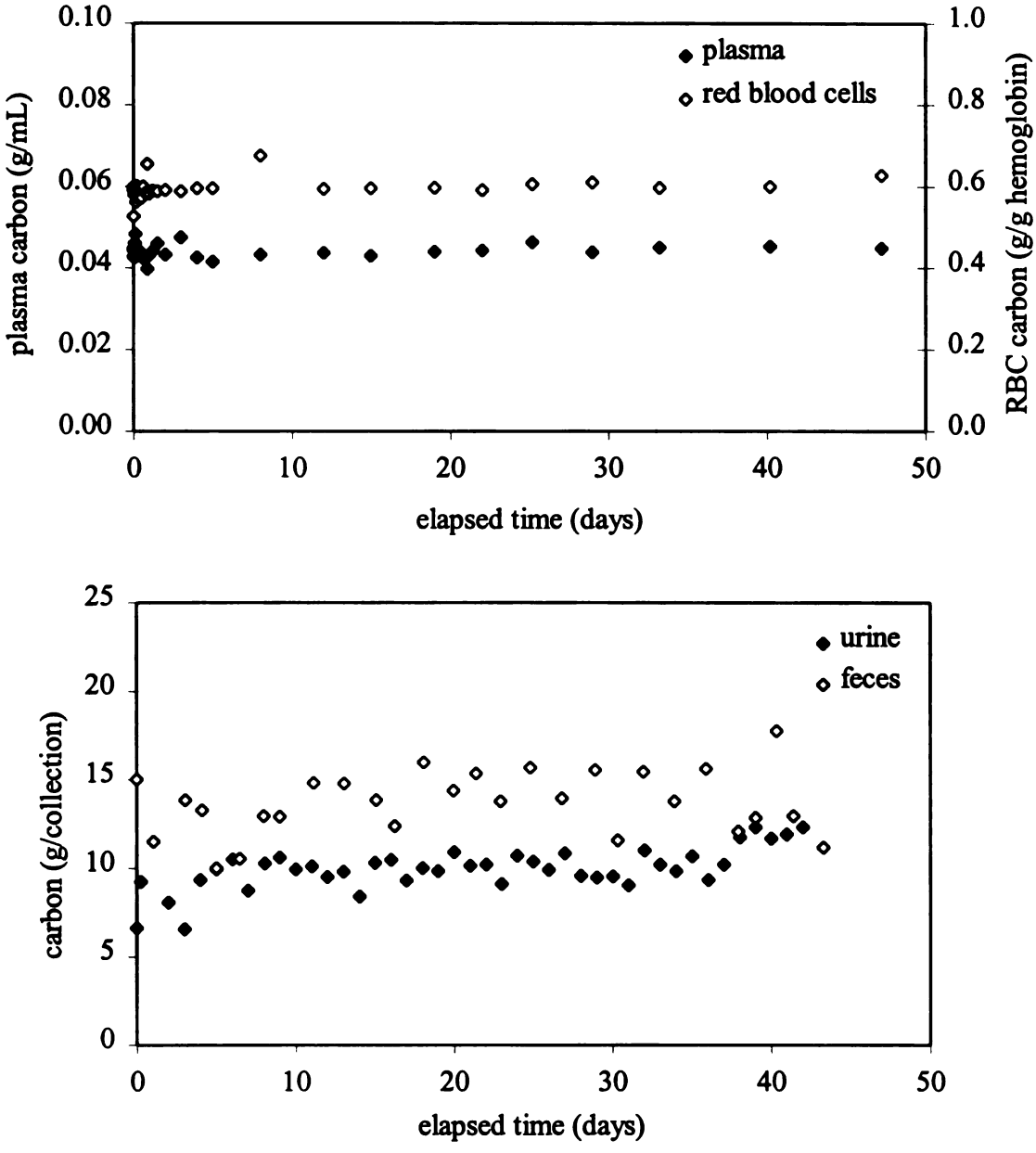

Figure 1. Carbon concentration in plasma and red blood cells (top) and total losses per collection in urine and feces over the first 42-day period.

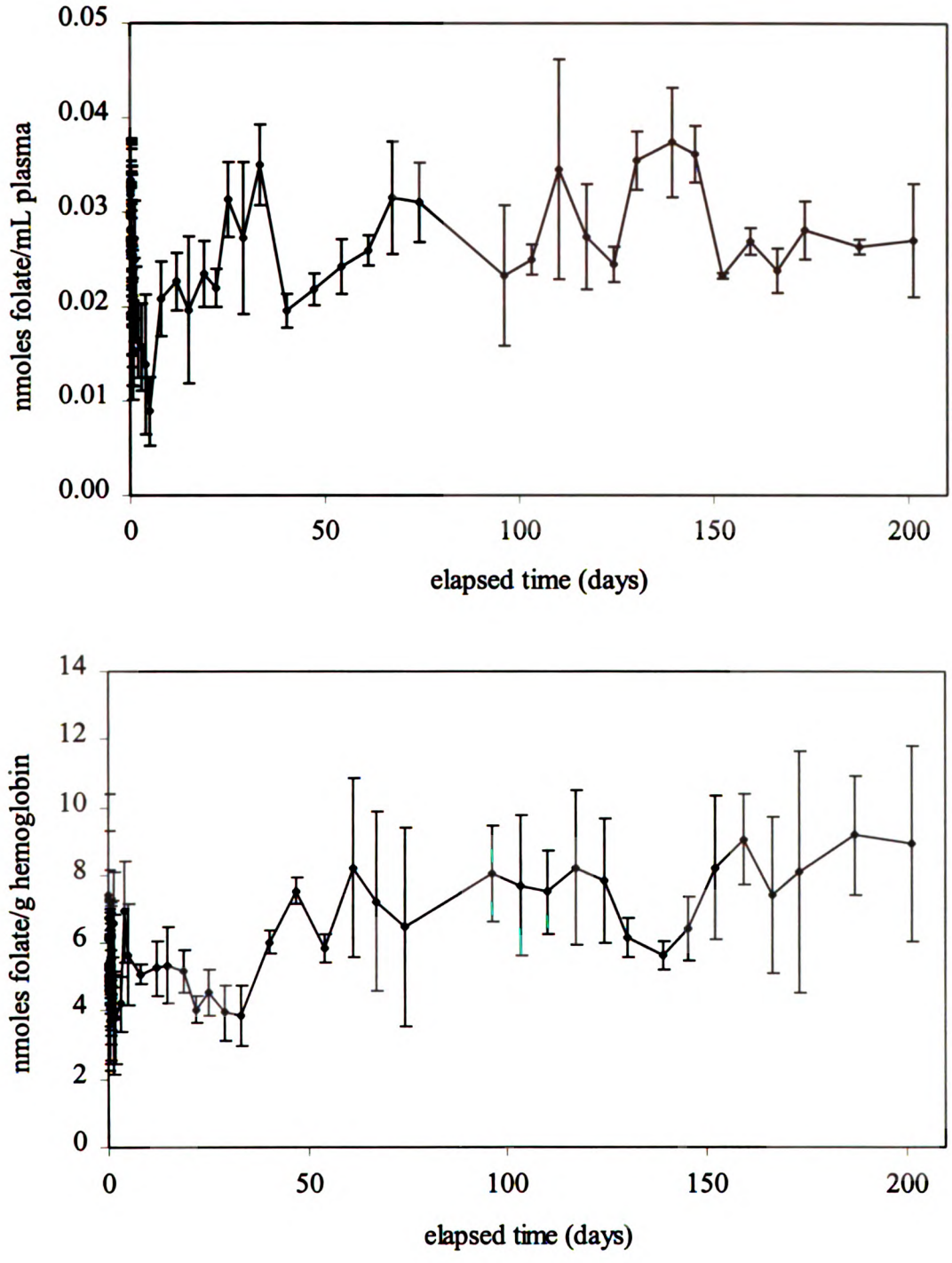

Figure 2. Total folate concentration in plasma (top) and red blood cells (bottom) over a 200-day period. Error bars represent standard deviation of triplicate microbiological assay determinations.

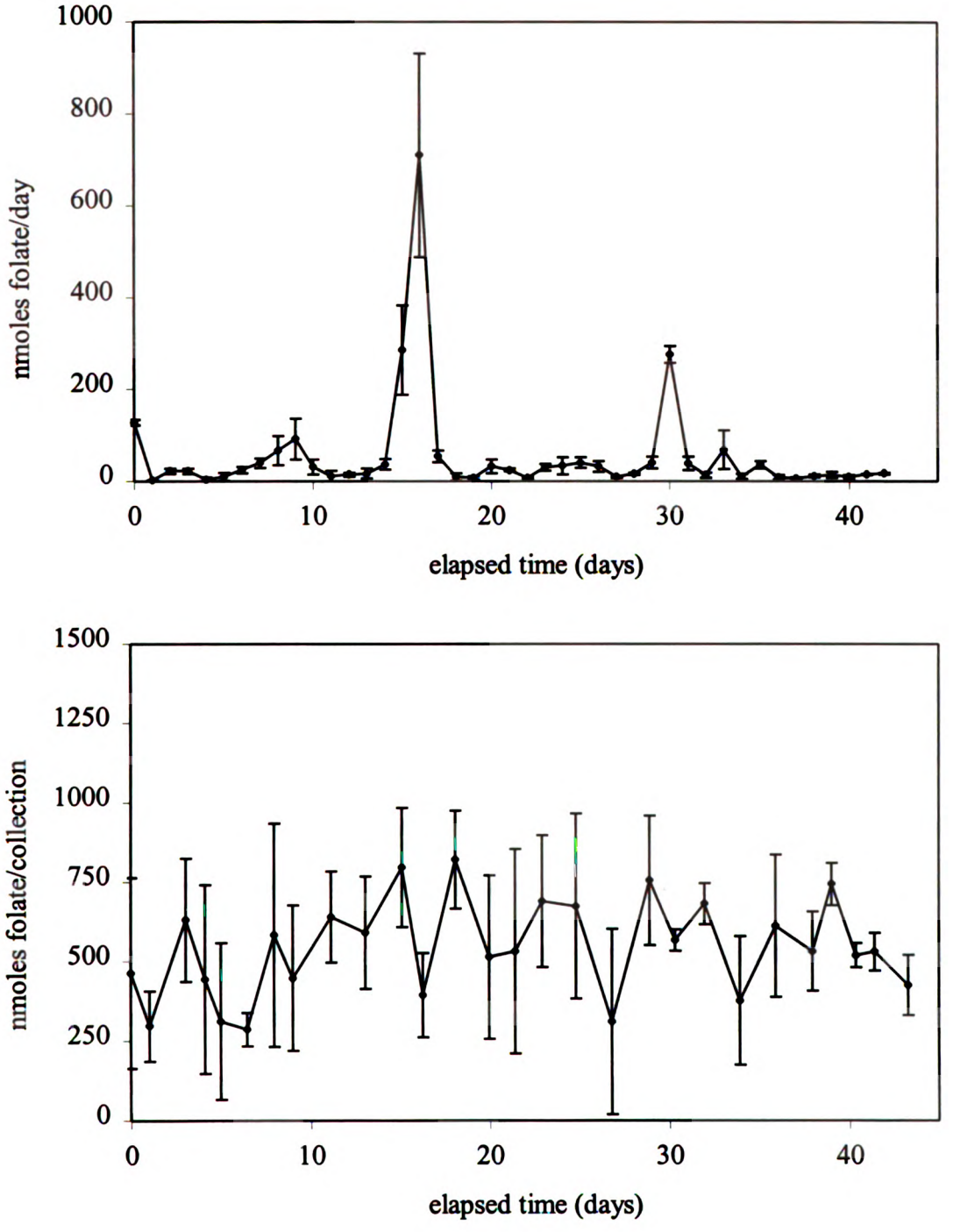

Figure 3. Total folate losses in urine (top) and feces (bottom) over a 42-day period. Error bars represent standard deviation of triplicate microbiological assay determinations.

To check for recovery of FA and 5MTFA after an affinity-chromatography step, plasma was spiked with known amounts of FA and 5MTFA, extracted with acetonitrile, purified by FBP-affinity chromatography and identified and HPLC. Endogenous plasma folate compounds were below the detection limit and did not contribute to the absorbance signal. The lower portion of Table 2 shows the recovery of FA and 5MTFA from spiked plasma. A recovery of approximately 60% was achieved under the conditions described. Some losses may have occurred as a result of affinity-column saturation, however, the recoveries were sufficiently high to isolate and fractionate plasma for AMS.

AMS-HPLC results of plasma collected one hour after the dose is shown in Figure 4. The large early peak of absorbance was due to ascorbic acid added to the sample to protect against oxidation. Retention times for FA and 5MTFA were 5.5 and 7 minutes, respectively. The ^{14}C concentration, in units of moderns, is shown with a dashed line. Baseline moderns were around 0.1 moderns, corresponding to natural radiocarbon concentration in the tributyrin carrier. An increase in ^{14}C concentration occurred at four minutes coinciding with the small peak in the absorbance. This may have been due to a small amount of degraded or oxidized 5MTFA (from the standard and ^{14}C-5MTFA). Catabolic products of 5MTFA, such as *para*-aminobenzoylglutamate, have retention times in this range under these HPLC conditions. There was no increase in the ^{14}C concentration in the FA fraction while there was a significant increase in ^{14}C concentration in the 5MTFA fraction. The chromatogram shows the vast majority of ^{14}C were in the 5MTFA fraction.

The remaining AMS plasma, urine and feces samples were measured with little or no extraction or processing. ^{14}C-Folic acid was labeled in a manner that ensured the radiocarbon would always remain with folic acid or its catabolites. ^{14}C concentrations measured by AMS were converted to ^{14}C-folate concentration that included folate metabolites and catabolites in a sample. Major folate molecules in plasma (5-methyltetrahydofolate), red blood cells (polyglutamates of reduced folic acid), urine (*para*-aminobenzoylglutamate, or their acetamido- derivatives) and feces (combination of metabolites and catabolites) were therefore expressed as moles of ^{14}C-folate, facilitating the kinetic tracing and distribution of the original dose. This was a reasonable approach since mathematical modeling of the data treated various folate metabolites and catabolites as one.

^{14}C-Folic acid bioavailability and kinetics

Plasma ^{14}C-folate concentrations are shown in Figure 5. The top figure shows plasma ^{14}C-folate concentrations in the first sixteen hours after the dose and the bottom figure shows the concentrations over the entire 200-day study period. ^{14}C-Folate was detected in the first plasma sample taken just ten minutes after oral ingestion of the radiolabeled dose. Plasma ^{14}C-folate concentrations continued to climb rapidly and reached a peak at one hour after the dose. ^{14}C-Folate concentration remained at this peak for two hours before declining rapidly. ^{14}C-Folate exhibited a biphasic elimination process from plasma comprised of fast and slow elimination processes. This data was analyzed mathematically to describe the dynamics of ^{14}C-folate in plasma and is described later in the chapter.

Table 2a. Recovery of ^{3}H-folic acid added to plasma and extracted by solid-phase extraction. Fasting and post-prandial plasma recoveries were determined independently.

Sample	^{3}H-FA Spike (DPM)	Fasting plasma (DPM)	Recovery (%)	Post-prandial plasma (DPM)	Recovery (%)
1	7334.8	7503.7	102.3	8703.6	118.7
2	7334.8	7664.5	104.5	7500.4	102.3
3	7334.8	8220.2	112.1	6265.3	85.4
4	7334.8	8289.4	113.0	7368.7	100.5
5	7334.8	9555.6	130.3	6705.1	91.4
Mean		8246.7	112.4	7308.6	99.6
S.D.		807.3	11.0	927.2	12.6

Table 2b. Recovery of folic acid (FA) and 5-methyltetrahydrofolate (5MTFA) added to plasma and extracted by solid-phase extraction and affinity-chromatography. Recovery was determined by HPLC with detection at 292 nm.

	FA spike (AU)	FA recovered (AU)	FA recovery (%)	5MTFA spike (AU)	5MTFA recovered (AU)	5MTFA recovery (%)
P2	1248.136	670.46	53.7	1353.46	768.53	56.8
P5	1248.136	754.09	60.4	1353.46	835.25	61.7
P11	1248.136	779.96	62.5	1353.46	849.03	62.7
P30	1248.136	805.80	64.6	1353.46	943.17	69.7
Mean		752.58	60.30		848.99	62.73
S.D.		58.67	4.70		71.95	5.31

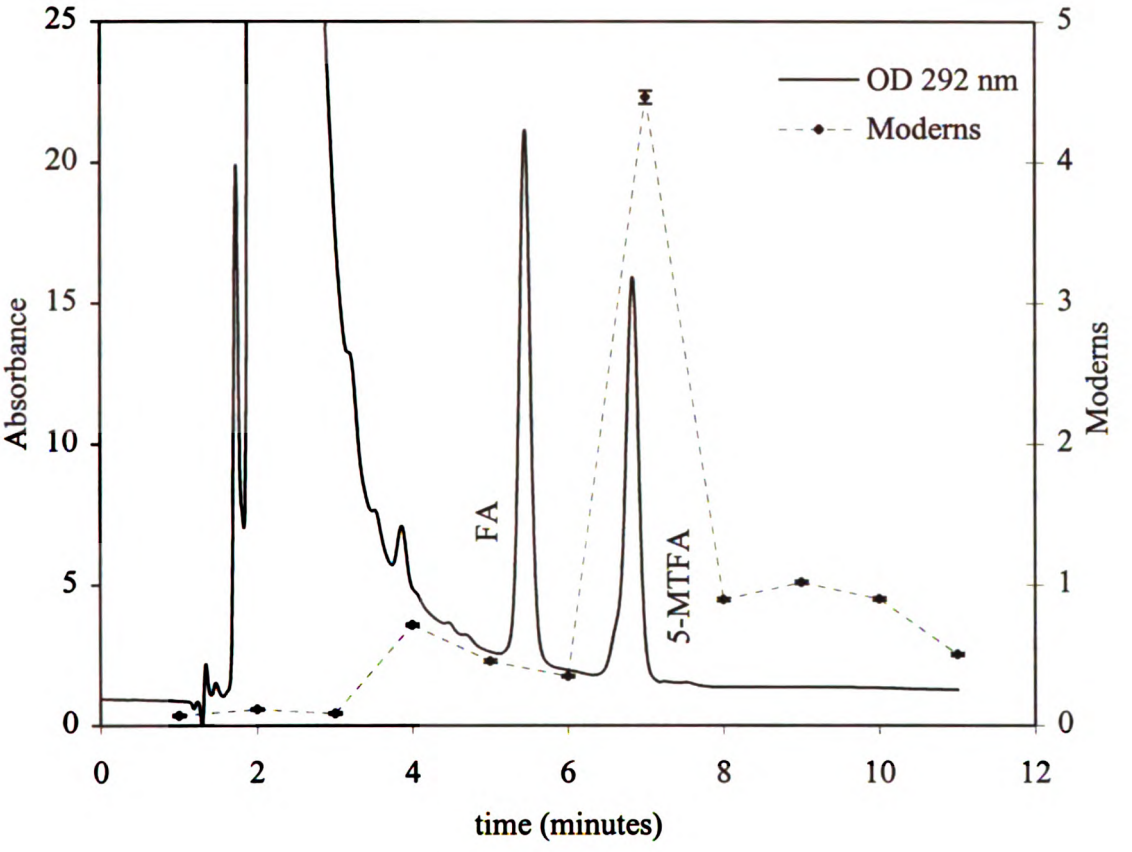

Figure 4. HPLC-AMS chromatogram of plasma sample collected one hour after ingestion of ^{14}C-folic acid. Absorption was monitored at 292 nm (solid line) and 14C concentration was measured by AMS and expressed as moderns (dashed line). The large early peak was due to ascorbic acid added to the sample to protect against oxidation. Folic acid (FA) and 5-methyltetrahydrofolate (5MTFA) standards were added to the plasma before extraction to check for recovery and to mark folate retention times.

The unabsorbed portion of the dose appeared in the first two feces samples. The first two feces samples, collected one day and three days after ingestion of the dose, contained 4.7 and 4.2 nmol ^{14}C-folate, respectively (Figure 6). This value dropped to 0.27 nmol ^{14}C-folate in the third sample and continued to drop thereafter. The sum of the first two samples represented the portion of the dose that was not absorbed.

The bioavailability of ^{14}C-folate administered as folic acid in ~150 mL water was calculated as the difference between the dose administered and the amount recovered in the first two feces samples. The bioavailability was determined to be 89%. The complete collection of feces for 42 continuous days allowed presentation of feces ^{14}C-folate data as cumulative loss. The bottom portion of Figure 6 shows the cumulative losses in feces. Unabsorbed tracer contributed to the majority of the ^{14}C-folate recovered in the feces, while much smaller amounts, representing endogenous losses, were recovered in the feces after the fourth day. After day seven, ^{14}C-folate excretion in the feces reached a steady-state loss of 0.033 nmol ^{14}C-folate/day.

^{14}C-Folate in urine exhibited an early spike in the first day amounting to 0.635 nmol ^{14}C-folate. This corresponded to 0.9% of the absorbed dose. ^{14}C-Folate recovered in the urine remained low for the remainder of the study with minor peaks on days 9, 15 and 16. The cumulative recovery of ^{14}C-folate in urine is shown in the bottom of Figure 7. An average daily loss of 0.16 nmol of ^{14}C-folate was observed resulting in a total loss of 6.9 nmol ^{14}C-folate by day 42. Urine and feces represented the major routes of tracer elimination because the folate radiocarbon could not be exhaled in the breath as $^{14}CO_2$. The cumulative recovery (urine and feces) of ^{14}C-folic acid from the body by day 42 was 17.7 nmol ^{14}C-folate, representing 22% of the administered dose.

Red blood cell ^{14}C-folate concentration was measured by AMS and the data expressed as fmol ^{14}C-folate/gram hemoglobin. This approach eliminated differences in cell dilution after washing in buffer by normalizing folate values against the hemoglobin concentration. The data for the first eight days and for the entire study period are shown in the top and bottom of Figure 8, respectively. Samples collected in the first 24 hours possessed a small amount of ^{14}C above the background. However, this returned to background by 36 hours after the dose and remained low until day 3. Samples collected after day 4 showed a rapid rise in red blood cell ^{14}C-folate concentration and reached a maximum of 1650 fmol ^{14}C-folate/gram hemoglobin by day 19.

Using the subject's hemoglobin concentration and reference values for total blood volume, the total amount of hemoglobin in circulation was estimated to be 6.6 g (13.3 g hemoglobin/dL, 5 L blood). The total amount of ^{14}C-folate in red blood cells by day 19 was approximately 10.9 pmol ^{14}C-folate or about 0.014 % of the administered bolus. This value corresponded to 2.18 fmol ^{14}C-folate/mL blood, well above the detection limit of AMS.

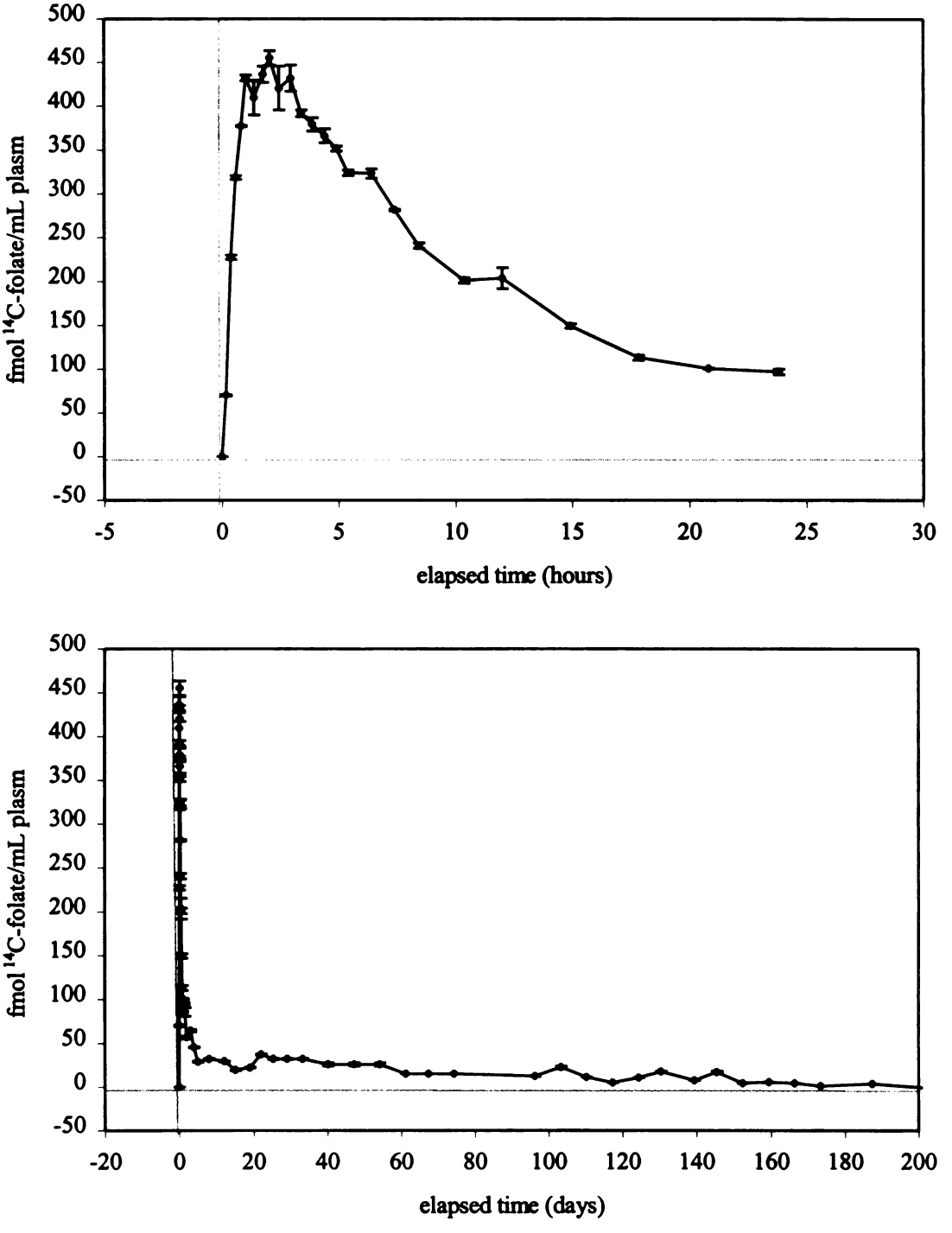

Figure 5. Plasma ^{14}C-folate concentration 24 hours (top) and 200 days (bottom) after ingestion of tracer. Error bars represent ± 1 standard deviation of triplicate determinations of ^{14}C by AMS.

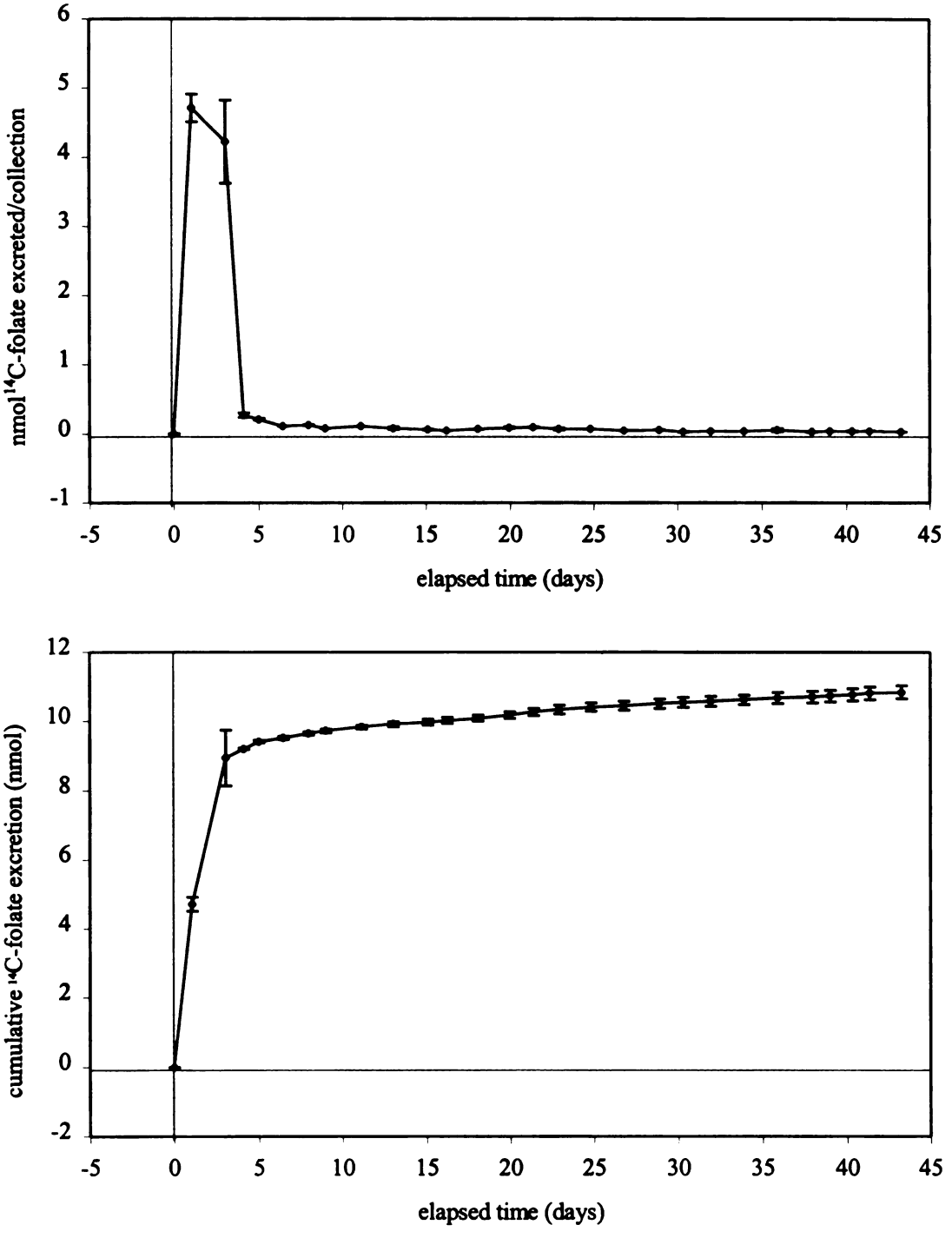

Figure 6. ^{14}C-Folate recovered in each feces collection (top) and cumulative excretion for the first 42 days postdose(bottom). Recovery in the first two samples represented unabsorbed ^{14}C-folic acid. Error bars represent ± 1 standard deviation of triplicate determinations of ^{14}C by AMS and cumulative standard deviation of unabsorbed and endogenous ^{14}C-folate losses.

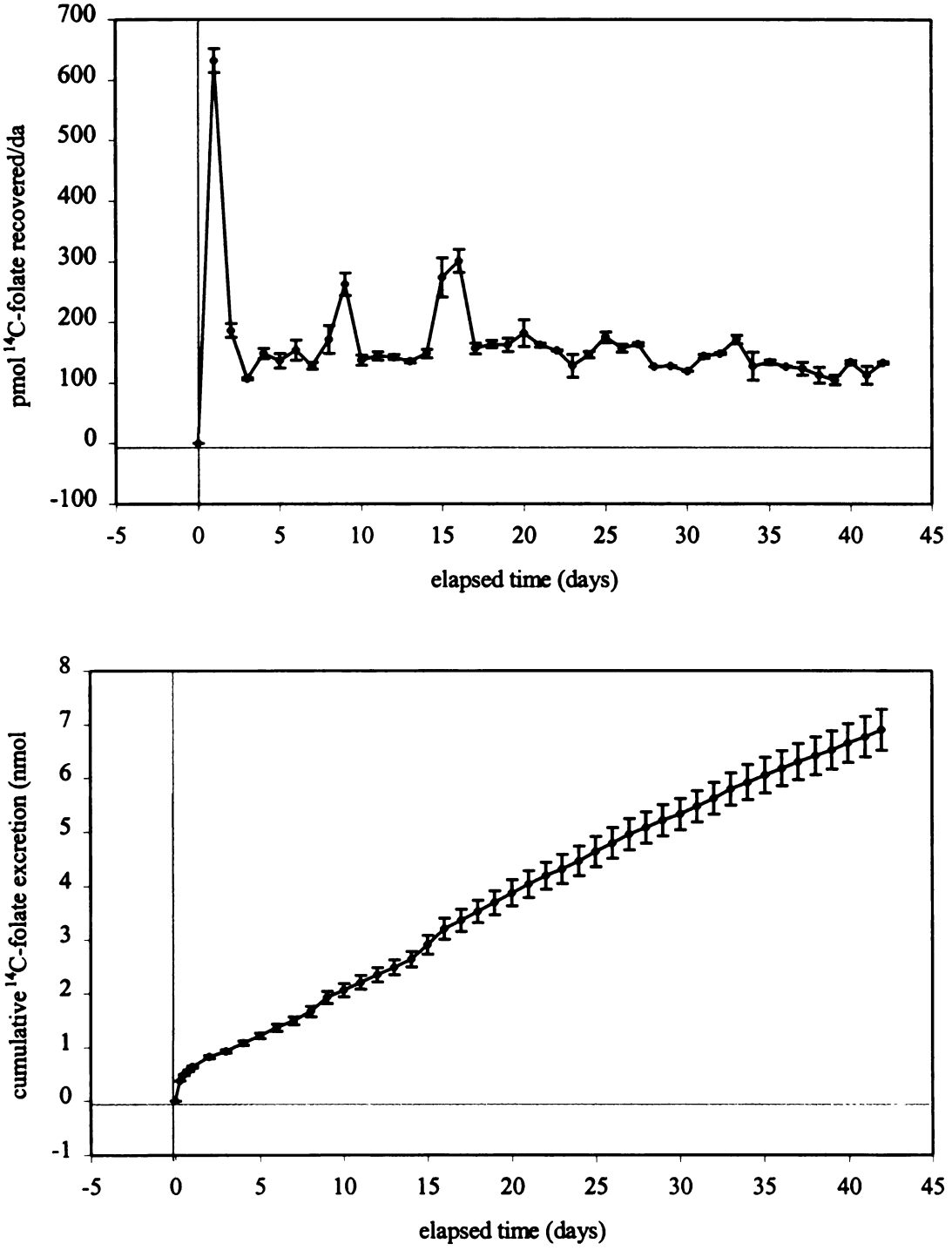

Figure 7. ^{14}C-Folate recovered in daily urine collections (top) and cumulative recovery for the first 42 days postdose(bottom). Error bars represent ± 1 standard deviation of triplicate determinations of ^{14}C by AMS and cumulative standard deviation.

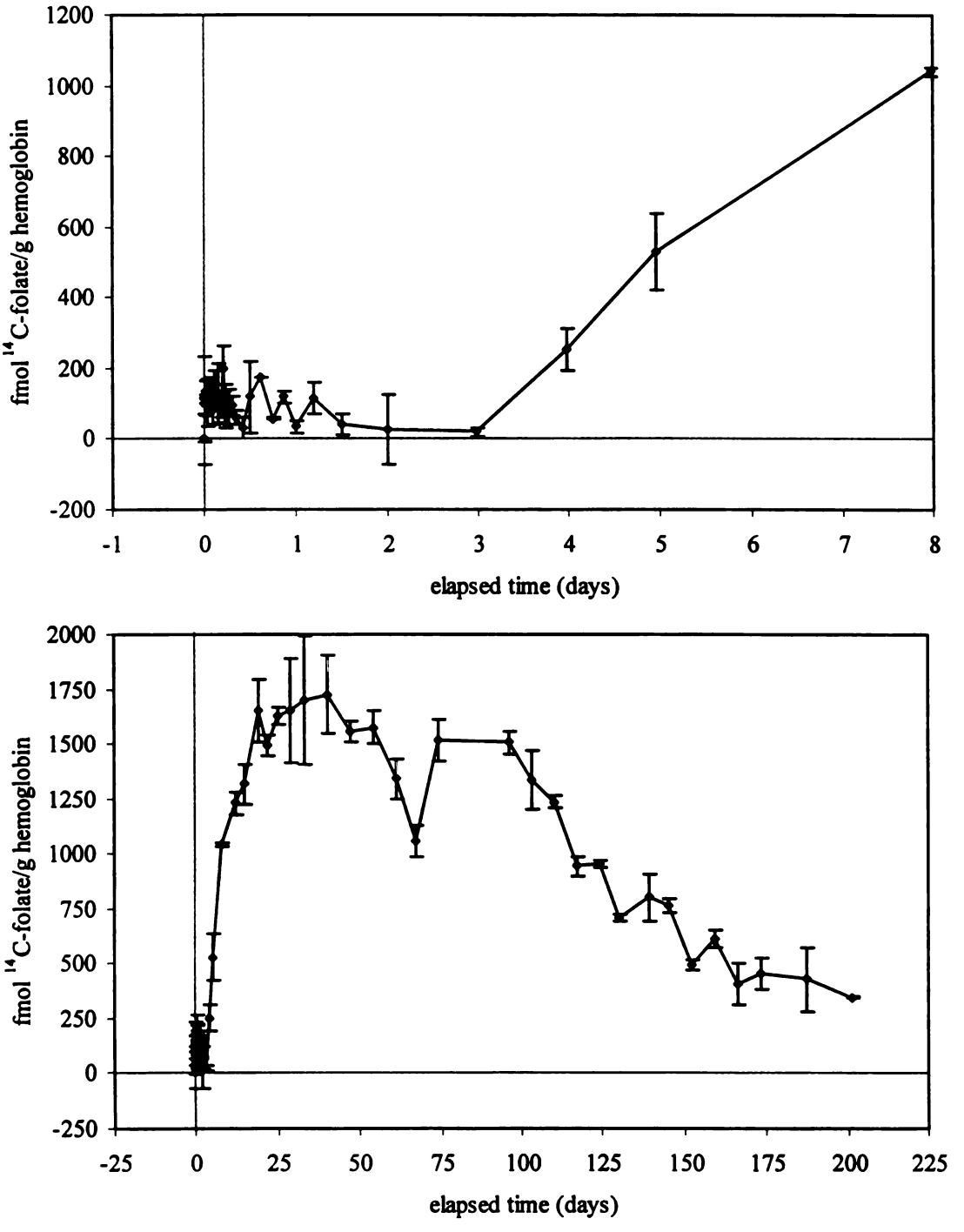

Figure 8. Red blood cell ^{14}C-folate concentration for the first 8 days (top) and 200 days (bottom) postdose. The three-day delay before appearance of ^{14}C-folate represented the time required for ^{14}C-folate incorporation into cells in the marrow during maturation. Error bars represent ± 1 standard deviation of triplicate determinations of ^{14}C by AMS.

Linear models

Plasma ^{14}C-folate concentration and cumulative losses in urine and feces were analyzed by linear models using linear regressions of the data. Plasma folate kinetics exhibited an early absorption phase and fast and slow elimination phases. Each phase was fitted using a linear regression model and is shown in Figure 9. ^{14}C-Folate was absorbed rapidly into plasma at a rate of 434 fmol ^{14}C-folate/mL/hr. After one hour there was a decline in plasma concentration at a rate of 31 fmol ^{14}C-folate/mL/hr. This elimination remained linear for seven hours after which it exhibited a slower phase of elimination. The rate of increase was about 14 times greater than the rate of the fast elimination phase. A slow elimination phase followed with a rate of 0.15 fmol ^{14}C-folate/mL/day and lasted for the remainder of the study. The linear fit of the slow phase had the lowest regression coefficient since there was greater uncertainty regarding plasma values after about 50 days.

^{14}C-Folate recovered in the feces comprised unabsorbed tracer as well as endogenous losses, possibly of biliary origin. ^{14}C-Folate excretion reached a steady rate by day 9. A linear regression of cumulative fecal excretion after day 9 is shown in the top portion of Figure 10. ^{14}C-Folate was excreted in the feces at a rate of 0.033 nmol ^{14}C-folate/day.

Cumulative ^{14}C-folate excretion in the urine exhibited a linear pattern for the entire 42 days of collection with the exception of a larger amount being excreted in the first day. The cumulative excretion rate in the urine, shown in the top portion of Figure 10, was 0.157 nmol ^{14}C-folate/day. This predicted a total excretion of 6.66 nmol ^{14}C-

folate by day 42. The actual measured excretion in urine after 42 days was 6.4 nmol ^{14}C-folate and compared well with the linear model prediction.

Red blood cell ^{14}C-folate concentration exhibited a pattern governed by the red blood cell lifespan. Linear regressions models were used to describe the rise and fall of red blood cell ^{14}C-folate concentration, representing the introduction of labeled cells into circulation and their removal as they aged, respectively. Values from days 3 through 19 were used for the rise period and days 96 to 173 for the fall period. After an initial 3-day delay, red blood cells ^{14}C-folate concentration increased at a rate of 94.4 fmol ^{14}C-folate/g hemoglobin/day and reached a plateau of about 1.5 pmol fmol ^{14}C-folate/g hemoglobin. After about 100 days, the concentration fell with a rate of 13.4 fmol ^{14}C-folate/g hemoglobin/day. After 200 days the ^{14}C-folate concentration was still above the baseline, possibly due to recycling of the tracer, or introduction of labeled red blood cells after the initial surge on day 4. A summary of the linear regression model parameters is shown in Table 2.

Table 2. Kinetic parameters of the linear model

Parameter	Slope	R^2	Units
Plasma absorption	434.8	0.96	fmol/mL/hr
Plasma elimination (fast)	-31.16	0.97	fmol/mL/hr
Plasma elimination (slow)	-0.153	0.79	fmol/mL/day
Urine cumulative loss	0.160	0.99	nmol/day
Feces cumulative loss	0.033	0.98	nmol/day
Red blood cells (rise)	94.4	0.91	fmol/g Hb/day [3]
Red blood cells (decline)	-13.3	0.91	fmol/g Hb/day [3]

[3] Hb-hemoglobin

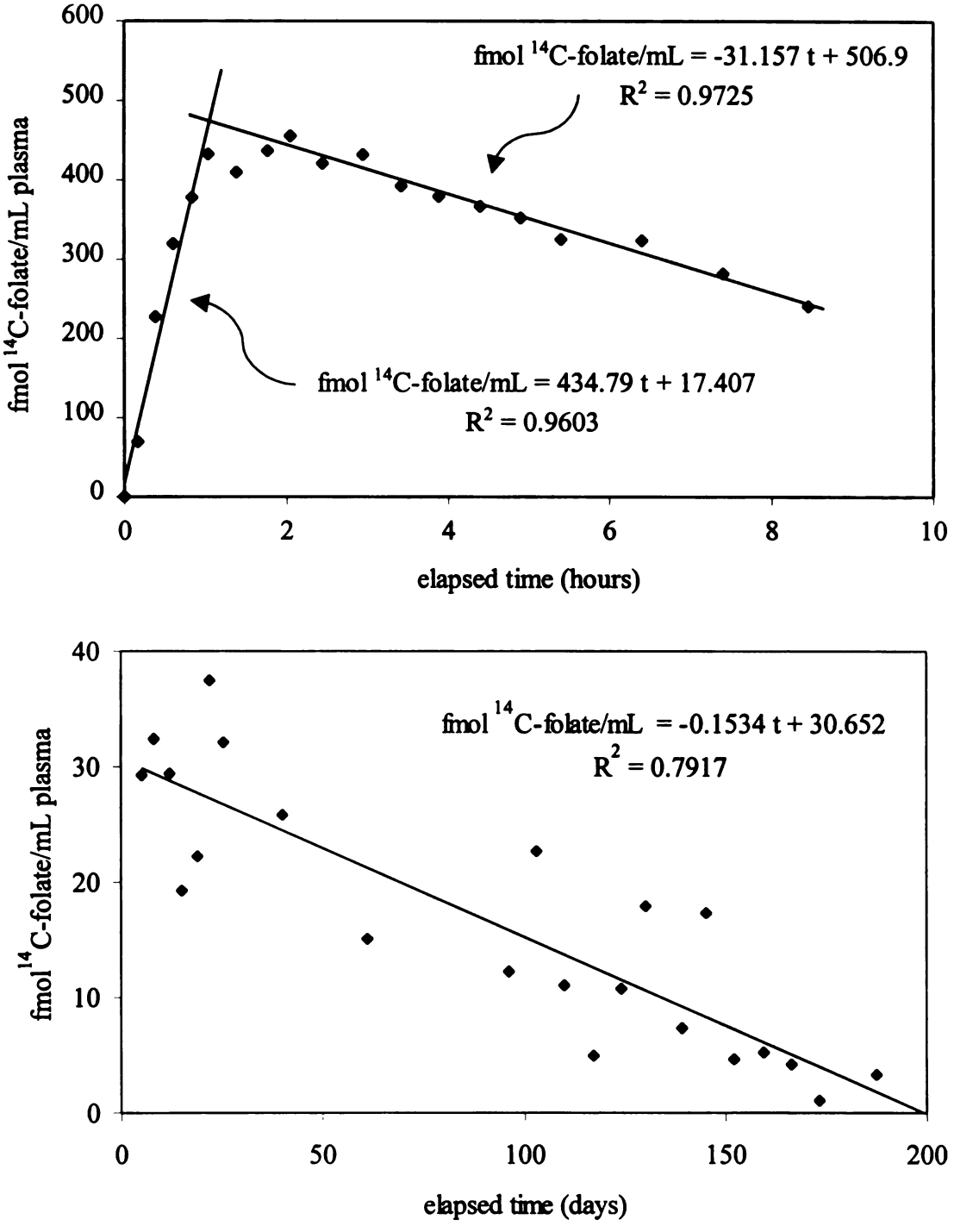

Figure 9. Linear regression models of ^{14}C-folate concentration in plasma. The three equations describe the absorption and fast and slow elimination phases observed after a single oral dose.

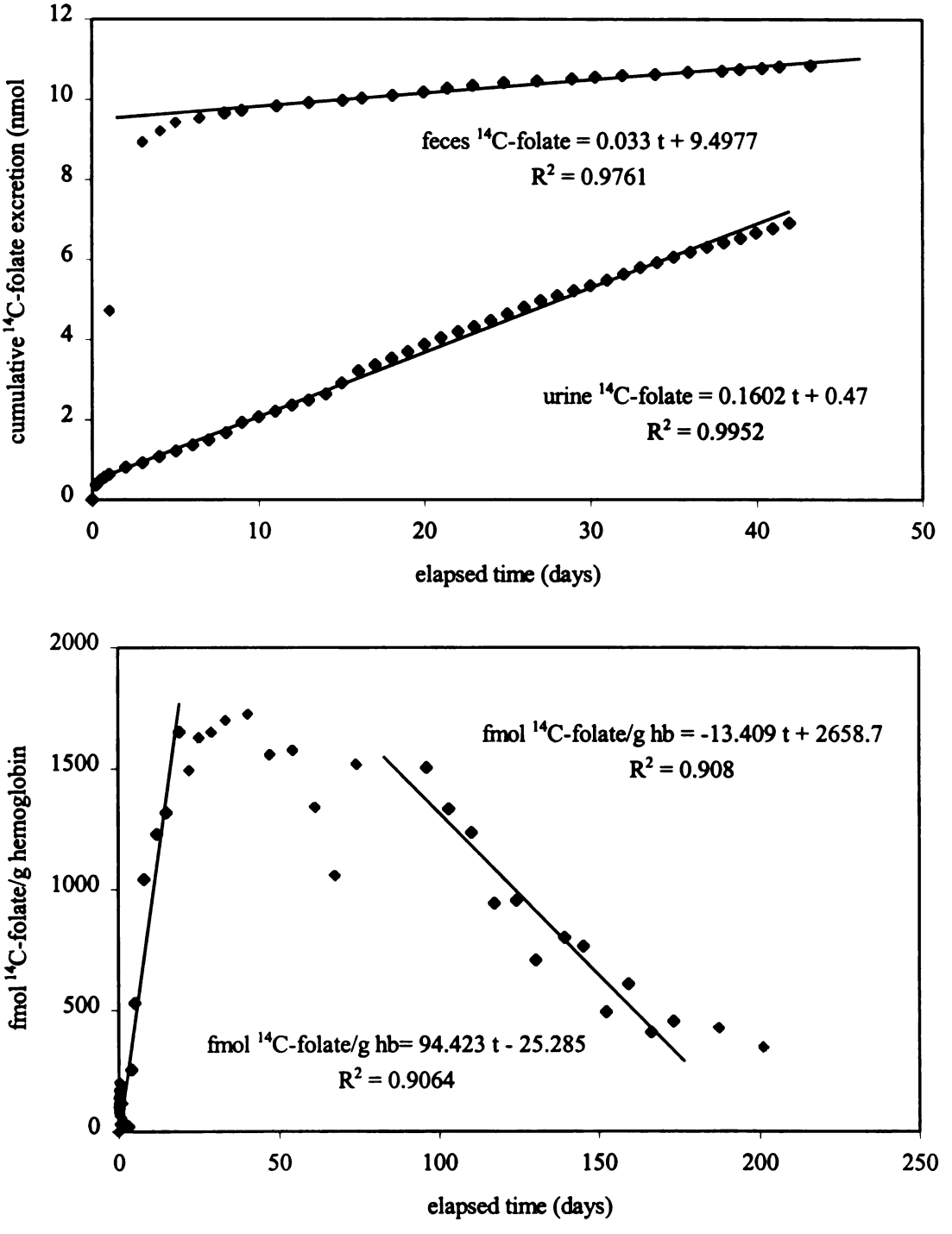

Figure 10. Linear regression models of cumulative excretion of ^{14}C-folate in urine and feces (top) and concentrations in red blood cells (bottom). Data points shown in gray were not used in the regression analysis.

Non-linear models

Complete urine and feces were collected for 42 days after the initial dose. These samples provided a solid basis for determining total excretion from the body over that time period. Several urine and feces samples were also collected 75 days and 175 days postdose. All had detectable amounts of the tracer. Excretion data for the 175-day period was modeled using non-linear regressions and the results are shown in Figure 11. Urinary excretion was described by the following exponential equation: pmol ^{14}C-folate excreted/day = 187.2 $e^{-0.0109\,t}$. Feces excretion was described by the following equation: nmol ^{14}C-folate excreted/collection = 0.0809 $e^{-0.0124\,t}$. When the slopes of these equations were divided into 0.693, half-lives of 63 and 55 days were obtained for urine and feces, respectively.

Non-linear modeling of the daily excretion over a long period provided $t_{1/2}$ values that linear modeling of cumulative excretion over a 42-day period could not provide. However, these models allowed calculation of whole-body turnover and half-lives. Although urine and feces excretion amounts differed by as much as five-fold, their half-lives were quite similar. This suggested that feces and urine were drawing on the same pool of body ^{14}C-folate and that this pool was being depleted with a half-life close to 60 days.

Although the linear regression models provided a quick means for describing the data, including rates of appearance and disappearance from plasma and losses from the body, little information could be extracted regarding dynamic processes over longer periods. Nevertheless, these simple linear models provided valuable information regarding bioavailability and whole-body turnover rates. A simple improvement to this initial approach was to describe the plasma data using non-linear regression models.

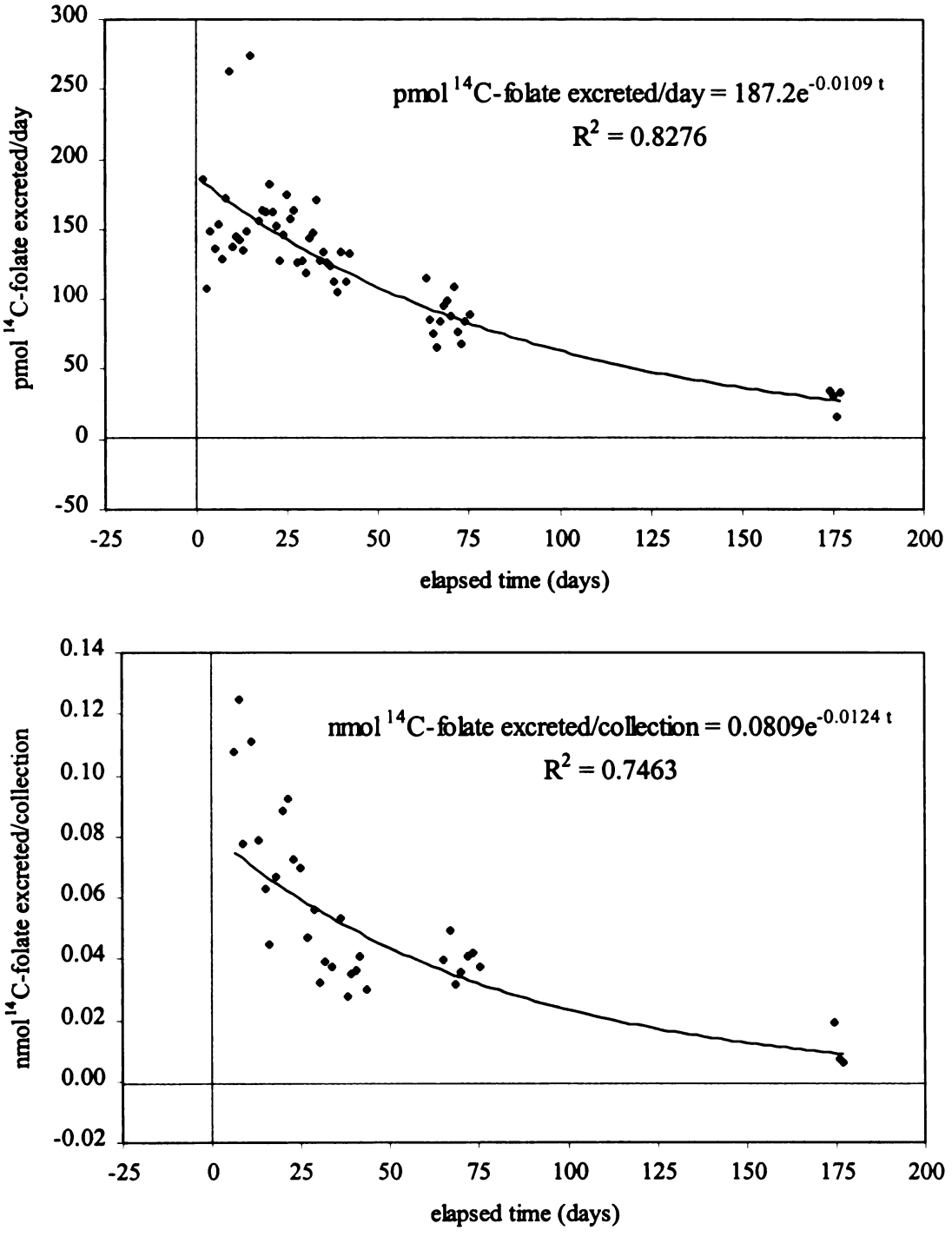

Figure 11. Non-linear regression models of ^{14}C-folate excreted in urine (top) and feces (bottom) over the entire study period.

Using a simple one pool model, plasma data were fitted to a non-linear model using the method of residuals (Bourne, 1986). This approach is commonly used in pharmacokinetics to fit drug kinetic data (Bourne, 1995). The appearance and disappearance of drugs in plasma resembled the kinetics of ^{14}C-folate in this study (Rowland, 1995). When plasma data were expressed as a logarithm of the concentration, the fast elimination phase became a straight line whose slope could be determined by exponential regression analysis. The intercept and slope of this line were used to define a two-term exponential equation that described the data for the first sixteen hours. The process, depicted in Figure 12, predicted absorption and fast elimination rates of 1.692 and –0.0917 fmol ^{14}C-folate/mL/hour, respectively. These terms were divided into 0.693 resulting in $t_{1/2}$ values of 0.4 hours for absorption and 7.5 hours for fast elimination. These terms were more representative of folate plasma kinetics than the linear model since inherent in rates of absorption and elimination were decay elements that a linear model could not describe. The two-term exponential model, therefore, described the data points better than the linear model. Interestingly, absorption and fast elimination half-lives in this model and their slopes in the linear model differed by about the same factor of 15, reinforcing the results obtained by each model.

The residual method to fit a two-term exponential equation to the data was only valid for the first sixteen hours. After that time the logarithmic plot of plasma concentration was no longer linear and the model was unable to predict the experimentally determined values. Since the simple one-pool two-term model could not describe the plasma data beyond sixteen hours a more sophisticated model was necessary.

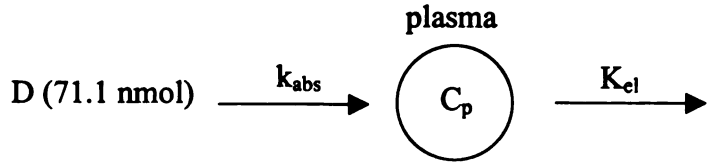

$$C_p = \frac{D \cdot K_{abs}}{V \cdot (K_{abs} - K_{el})} \cdot (e^{-k_{el} \cdot t} - e^{-k_{abs} \cdot t})$$

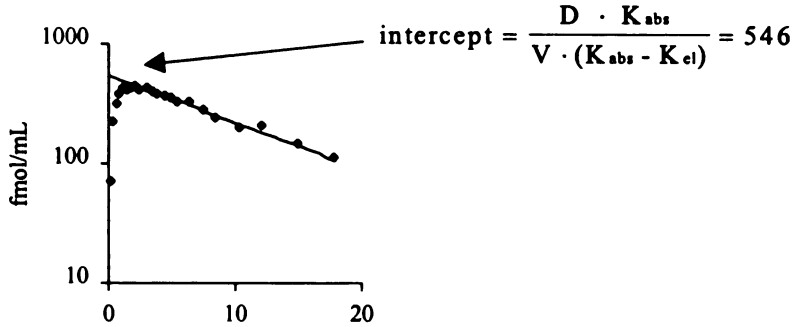

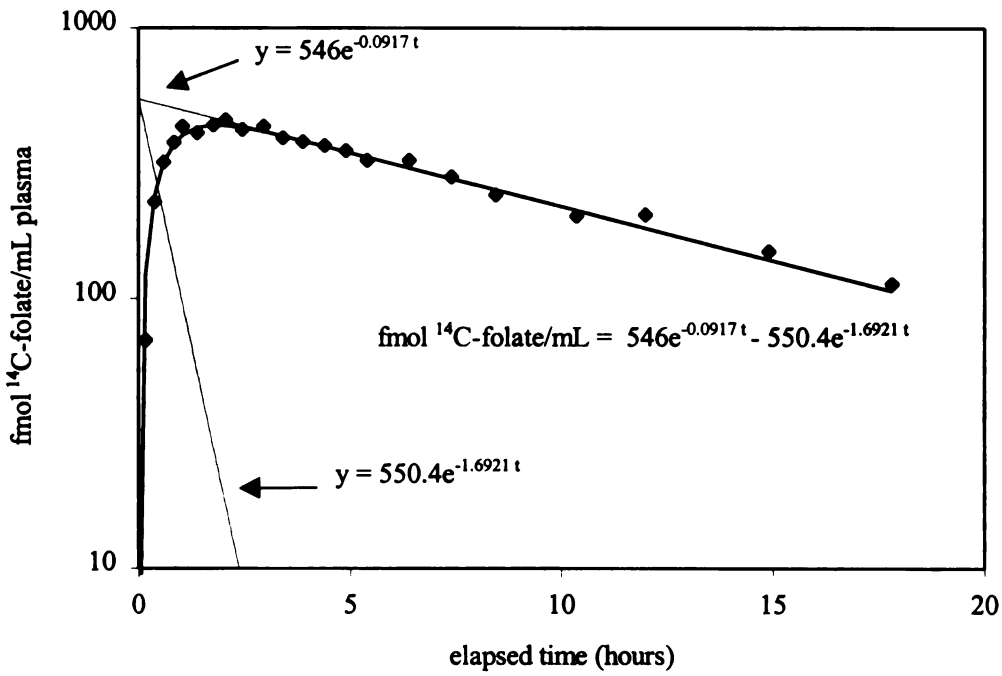

Figure 12. Single compartment model of the absorption and elimination of ^{14}C-folate in plasma. K_{abs}-absorption rate constant, K_{el}-elimination rate constant, C_p-plasma concentration, D-dose absorbed, V-volume of distribution (see text).

Plasma data were modeled beyond sixteen hours by adding a third term to the equation. Using a data analysis software package (SigmaPlot) the plasma data were fitted to give the following equation: fmol ^{14}C-folate/mL = $511.3e^{-0.1078\,t} - 584.8e^{-1.664\,t} + 49.52e^{-0.0006422\,t}$. This three-term equation described the plasma data for the entire 200-day sampling period and is shown in Figure 13. This equation predicted the plasma concentration of ^{14}C-folate but provided little information about exchanges between body pools and excretion rates of ^{14}C-folate from the body. Compartmental modeling was employed to provide these parameters.

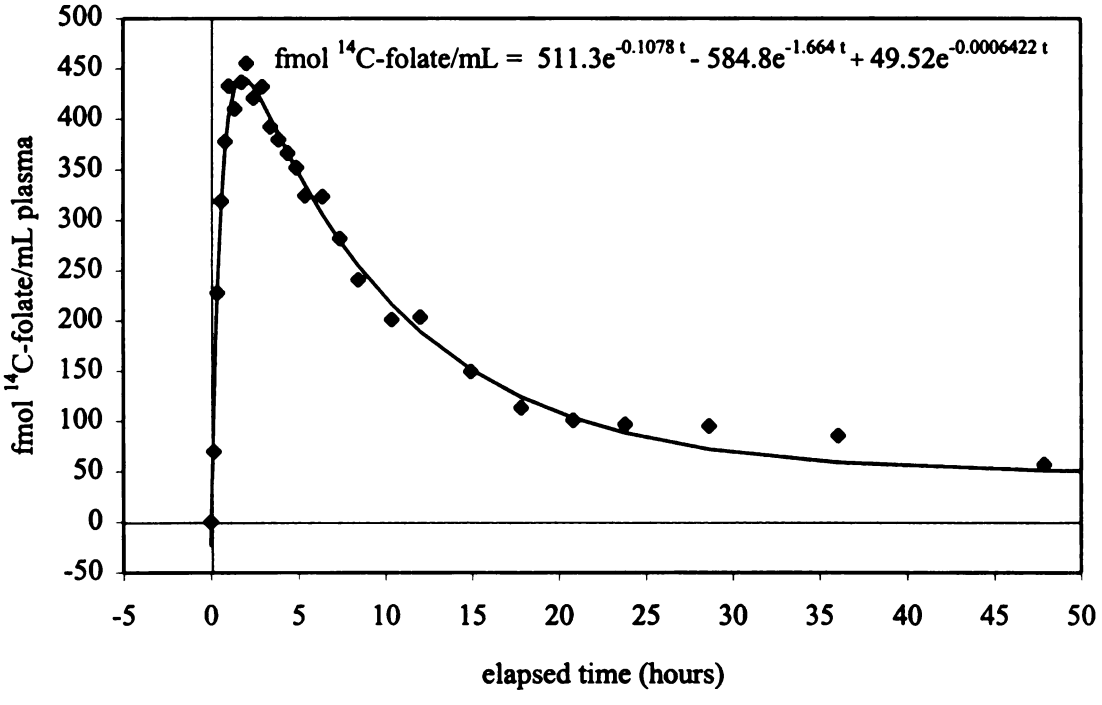

Figure 13. Three-term polyexponential model describing ^{14}C-folate concentration in plasma. The equation described the data obtained over the entire 200-day study period (data for the first 50 days is shown).

Compartmental model: components, provisions and assumptions

A compartmental model determines the transfer rates between body compartments by dividing the body into discrete pools. These pools may or may not represent actual organs with biological correlates. The model was built on the simple schematic depicted in Figure 14. The simplest model consisted of a single body pool with input for the tracer and an output for all excretions. It was essential to know the amount of tracer administered. The bioavailability of the tracer, however, complicated quantification

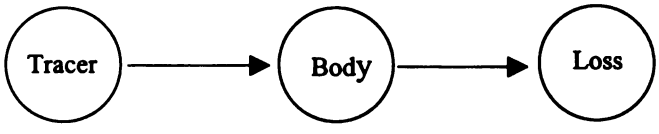

Figure 14. A simple model depicting the uptake and loss of tracer

of the amount of tracer that actually entered the body pool. This problem has been traditionally resolved by intra-venous administration of a second tracer to determine the bioavailability and make the appropriate adjustments. The bioavailability of the tracer in this study was measured directly and no such adjustments were necessary. Once the tracer was absorbed it was distributed to various tissues and eventually excreted from the body in the urine and feces. If the tracer could be lost through the lungs, expired air should also be collected and included as a route of excretion. Skin may could also represent a route of excretion for some compounds. In this study, urine and feces were considered to be the major routes of folate excretion from the body (Krumdieck, 1978).

Blood is an easily accessible pool in the body. Whole blood was sampled frequently and separated into plasma and red blood cells, each representing a discrete pool. Red blood cells represented a tissue pool that could be easily sampled. The main components of the model are shown in Figure 15. This schematic depicts major pools involved in folate metabolism. The amount of tracer was measured in all pools shown with a solid line. The tissue pool, shown with a dotted line, was the only pool whose ^{14}C-folate concentration was not measured. Compartmental modeling allowed the distribution of the tracer into this pool to be determined by simple difference.

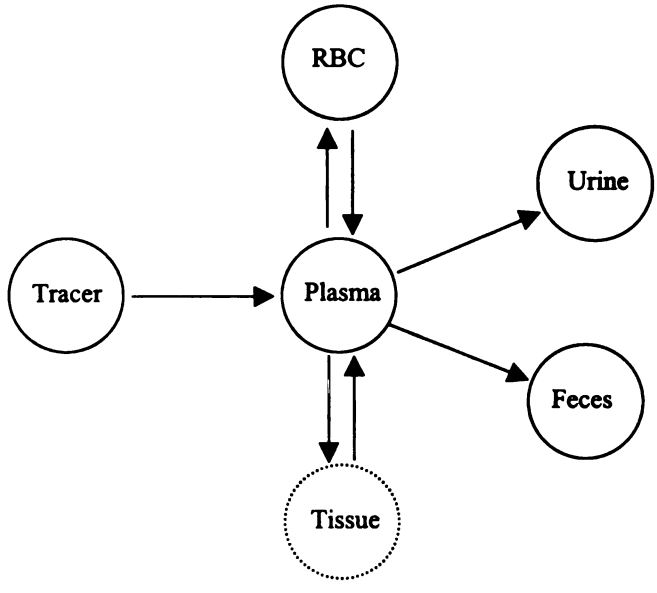

Figure 15. A multi-compartment model of folate distribution in humans. Compartments that were measured are shown with solid lines, and the inaccessible tissue compartment is shown with a dotted line.

Once the main components of the model were identified, biologically relevant components were added. These components were based on current knowledge of folate

metabolism in humans and animals. For example, ^{14}C-folic acid in the gut had to pass through intestinal cells before entering the plasma. An intestinal pool was added to account for this process. It was known that maturing red blood cells in the marrow incorporated folate before being released into circulation (Bills, 1992). A compartment representing the marrow was added as well as a delay element to provide the necessary delay observed experimentally (Strumia, 1968). Since the red blood cell folate dynamics was governed by the cell's lifespan in circulation, a delay element was added to provide for this biological process. The 24-hour transit time of material through the gastrointestinal tract also necessitated a delay element to be incorporated into this portion of the model.

Compartmental modeling made certain assumptions regarding fluxes of the tracer between compartments. Initially, the model assumed that all fluxes were governed by first-order processes, mathematically represented as flux(2,1)=k(2,1)*q1, where 1 was the donating pool, 2 was the receiving pool, k(2,1) was the transfer coefficient between the pools, and q1 was the concentration of the tracer. The flux, therefore, varied as the concentration in pool 1 changed. In most cases, the assumption that a first-order process governed flux was valid, however, the equation could be altered to meet the system's needs.

Another assumption made in the modeling was that the tracer paralleled the behavior of the endogenous compound being studied. Isotopically labeling folate permitted discrimination of the tracer from endogenous sources. The assumption was made that biological processes, such as absorption, protein binding and enzymatic conversion to metabolites, were not affected by isotope labeling. In this study, ^{14}C-

labelling of folic acid ensured minimal or no isotope effects. In previous models of nutrient kinetics the ratio of labeled and nonlabeled nutrient was used to derive the specific activity of the tracer. This value was then used to model the nutrient dynamics between various compartments since the specific activity was a measure of tracer enrichment in that compartment. In this study, ^{14}C-folate concentration alone was used to build the compartmental model. The assumption that ^{14}C-folate dynamics represented folate dynamics is discussed later.

Since modeling treated body compartments as pools, the concentration data in plasma and red blood cells were converted to total amounts of ^{14}C-folate in each pool using reference values for plasma volume and total grams of hemoglobin in circulation. These amounts, as well as cumulative ^{14}C-folate excreted in the urine and feces, were associated with their respective pools in the model. All values, in femtomoles ^{14}C-folate, were assigned a fractional standard deviation of 0.025 to represent the uncertainty in the AMS measurements.

The time of collection for each sample was converted to hours after ingestion of the bolus. The gut compartment received a bolus of 8.0×10^7 fmol ^{14}C-folic acid at time zero. The colon compartment received the experimentally measured portion of the bolus that was not absorbed equaling 9.39×10^6 fmol ^{14}C-folate. The colon to feces transfer contained a delay element of 24 hours. The marrow to red blood cells transfer contained a delay element of 100 hours while the degradation delay was one hour. Compartments were added to represent tissue folate distribution consisting of fast and slow turnover pools. The fast turnover tissue contained a delay element of 20 hours. The model was

generated using the SAAM II software package (Saam Institute, University of Washington).

The model, shown in Figure 16, was an expansion of the basic model shown earlier. The entire 80 nmol ^{14}C-folate bolus entered the gut compartment at time zero. Exactly 9.39 nmol ^{14}C-folate of this was lost to the colon compartment and represented the portion of the bolus that was not absorbed, as determined experimentally. The remainder of the bolus entered the intestine compartment. This pool represented the intestinal cells which absorbed folic acid and reduced and methylated it before passing it on to plasma (Whitehead, 1972) .

The plasma compartment distributed folate to urine and colon, for excretion, and to tissues for storage. Two compartments represented tissue storage, a fast-turnover tissue pool and a slow-turnover tissue pool. The red blood cell pool received the tracer through a marrow compartment which was added to represent folate incorporation into maturing leukocytes before their release into circulation (Bills, 1992).

Initial coefficients were assigned for each parameter based on a best guess. The differential equations were solved simultaneously using algorithms in the software package. The algorithm adjusted these coefficients with every iteration in order to minimize the sum squares of errors between predicted and experimental values in the four compartments where data was available. Transfer coefficients were finally derived that satisfactorily predicted experimentally determined values.

The earlier assumption that fluxes in the compartmental model were driven by first-order processes was not applicable to transfer of the tracer to the red blood cell and urine pools. For simplification, it was assumed that ^{14}C-folate was incorporated into the

red blood cell pool in a discrete pulse. This assumption was incorporated into the model by forcing the transfer coefficient from plasma to marrow, k(9,3) to 0 after 24 hours. This allowed ^{14}C-folate to enter the marrow pool by a first-order process for the first 24 hours. The 0.030 hr^{-1} transfer coefficient within that period permitted ^{14}C-folate uptake into the marrow pool that reflected the red blood cell pool's influx of ^{14}C-folate determined experimentally. The model was unable to predict the red blood cell ^{14}C-folate data when this provision was removed.

The red blood cell pool presented a special case in compartmental modeling since flux out of the red blood cell pool was governed by the lifespan of these cells in circulation. Once folate entered this pool, it became unavailable for removal due to polyglutamation, until the cells themselves were removed from circulation (Rothenberg, 1974; Ward, 1990; Brown, 1990). This was evident in the approximately 100-day presence of ^{14}C-folate in the red blood cell pool, closely matching the known lifespan these cells (Strumia, 1968). This process was incorporated into the model by adjusting the transfer coefficient of the flux out of the red blood cell pool. This transfer coefficient was changed from 4×10^{-5} hr^{-1} to 0.00072 hr^{-1} at 2300 hours.

Aged red blood cells were removed from circulation by a macrophage-mediated process that engulfed the cells and returned them to the spleen and liver for degradation (Rosse, 1966). The degradation pool, q10, represented this process. Although the ^{14}C-folate in these cells was capable of being recycled, their removal to a dead-end degradation pool did not affect the model since the total amount of ^{14}C-folate in the red blood cell pool represented just 0.014 % of the bolus.

Urine output of ^{14}C-folate was not governed by first-order processes. Experimental data showed that there was a constant output of the tracer into the urine over the 42-day period. Since plasma ^{14}C-folate was highly dynamic in the first 24 hours, flux to the urine pool could not depend on plasma concentration. Output of ^{14}C-folate in as metabolites or catabolites was driven by selective processes of renal glomerulii. These included active transport mechanisms which concentrated ^{14}C-folate against a gradient (Das, 1970; Henderson, 1988; Pristoupilova, 1986). It was therefore unjustifiable to use first-order flux equations to describe transfer of ^{14}C-folate from plasma to urine. Instead, the linear regression model that described the cumulative excretion of ^{14}C-folate in urine, shown in Figure 10, was used to mathematically model the flux of ^{14}C-folate to the urine pool.

Transfer coefficients, shown in Table 3, were derived that successfully predicted the amounts of ^{14}C-folate in the various pools. Figure 17 shows predicted and measured amounts of ^{14}C-folate in the plasma pool in the first 20 hours (top) and 200 days (bottom). The model was able to predict the measured plasma values for the entire study period.

Cumulative excretion of ^{14}C-folate predicted by the model is shown at the top of Figure 18. The feces pool received 9.39 nmol of unabsorbed ^{14}C-folate followed by endogenous losses to produce the predicted line. ^{14}C-Folate in the urine pool was predicted by the following equation: fmol ^{14}C-folate = 6525 * hours + 85500. This was the same linear regression model shown in Figure 10 in units of femtomoles and hours. The predicted losses of ^{14}C-folate in the urine pool closely matched the measured values.

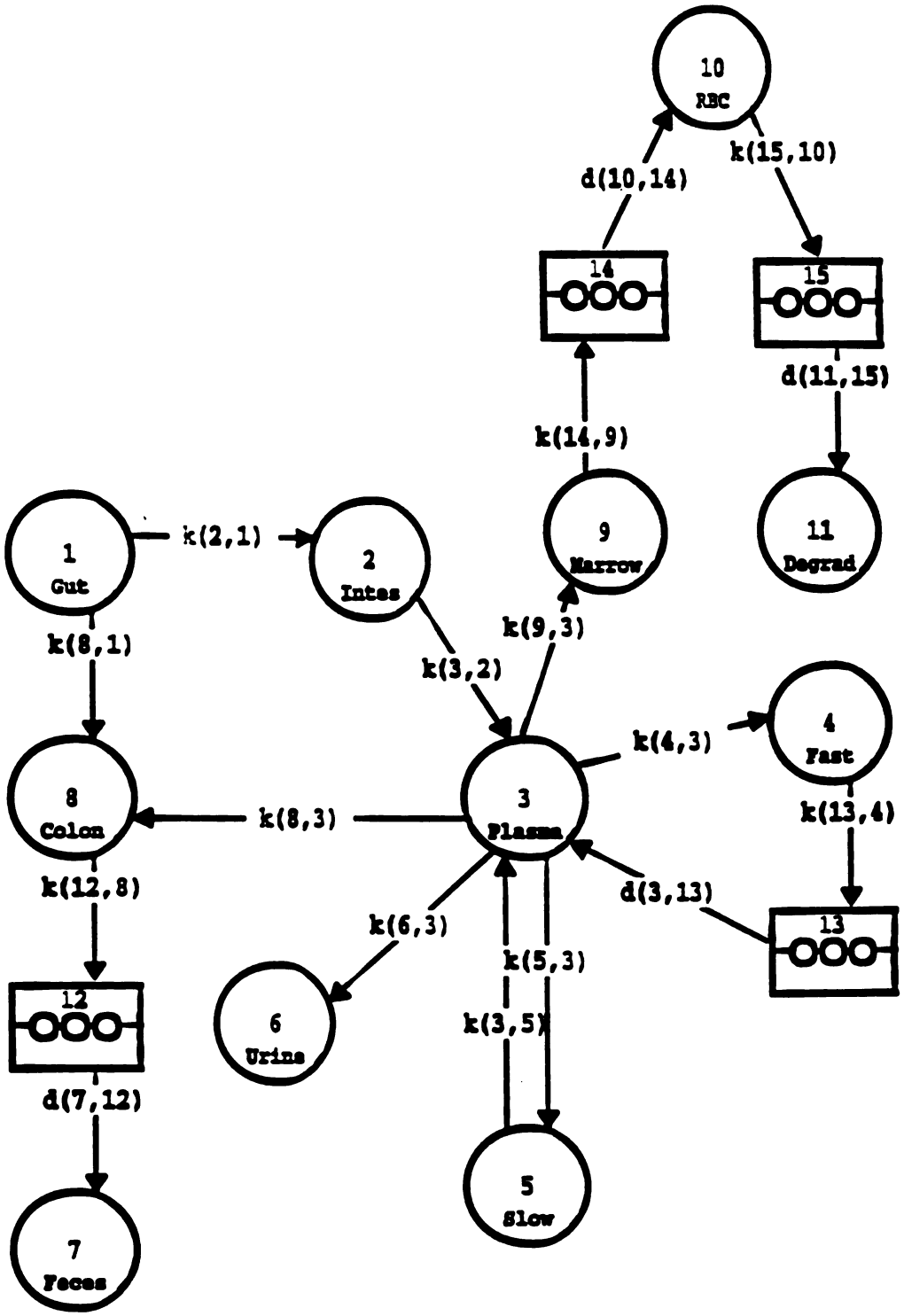

Figure 16. Comaprtmental model of folate kinetics in a human volunteeer. Compartments are numbered 1 through 11 and transfer coefficients shown as k(recipient,donor).

Table 4. Transfer coefficients from donor to recipient pools

Parameter	From	To	Transfer Coefficient, hr^{-1}
k(8,1)	Gut	Colon	0.000[2]
k(2,1)	Gut	Intestine	3.800
k(3,2)	Intestine	Plasma	0.094
k(4,3)	Plasma	Fast tissue	2.300
k(3,4)[1]	Fast tissue	Plasma	0.059
k(5,3)	Plasma	Slow tissue	1.900
k(3,5)	Slow tissue	Plasma	0.0022
k(9,3)	Plasma	Marrow	0.030[3]
k(10,9)[1]	Marrow	RBC	0.210[4]
k(11,10)[1]	RBC	Degrade	0.00004[5]
k(6,3)	Plasma	Urine	0.026[6]
k(8,3)	Plasma	Colon	0.020
k(7,8)[1]	Colon	Feces	1.300

[1] Transfer to recipient pool via a delay element
[2] Transfer determined by the bioavailability of the bolus
[3] Forced to 0 after 24 hours
[4] Forced from 0 to 0.21 after 58 hours
[5] Forced to 0.00072 after 2300 hours
[6] Forcing function used to describe transfer to the urine pool (see text)

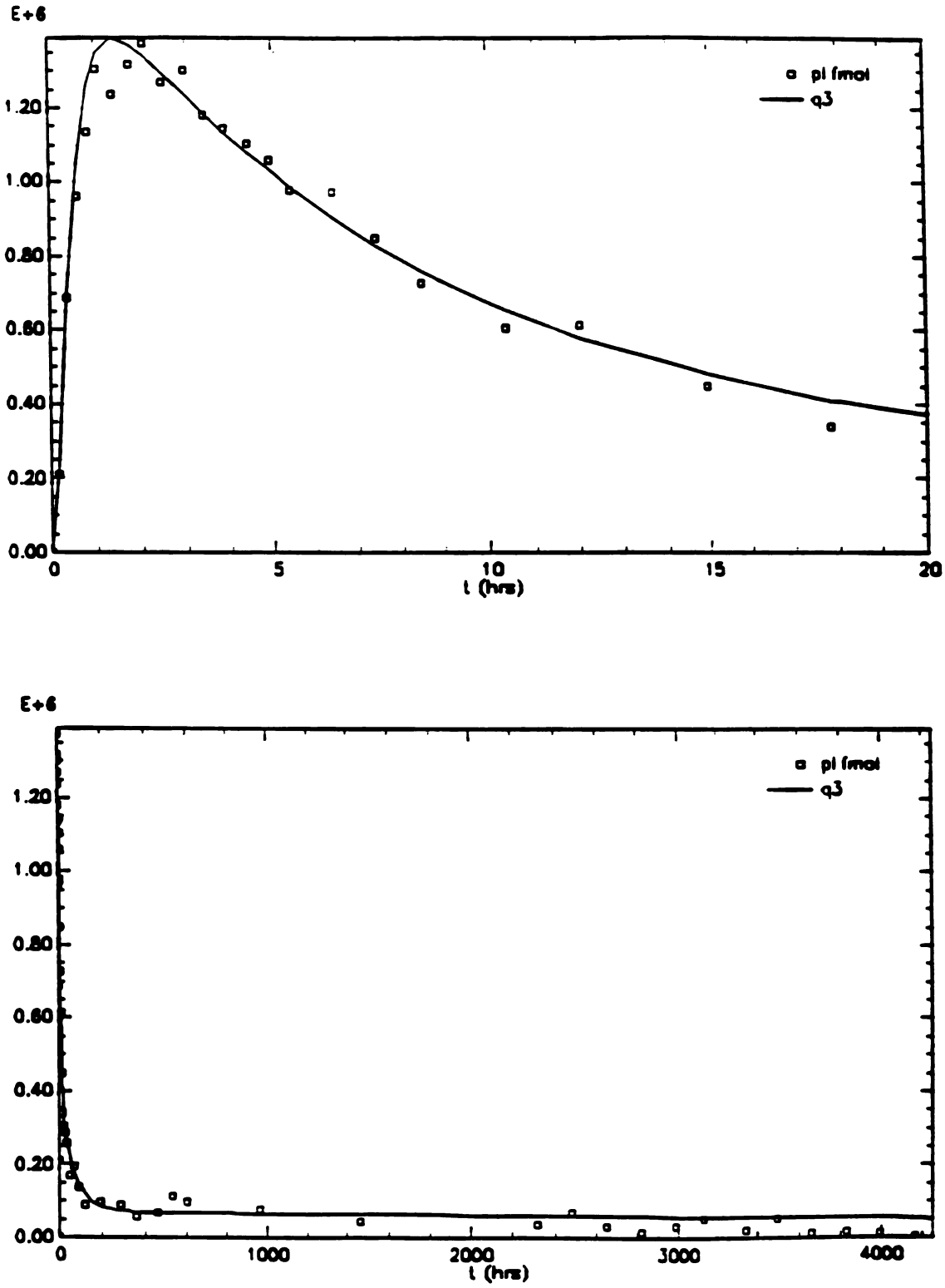

Figure 17. Model-predicted fmol ^{14}C-folate in the plasma pool for the first 20 hours (top) and 200 days (bottom) after the dose. Measured values are shown by the squares.

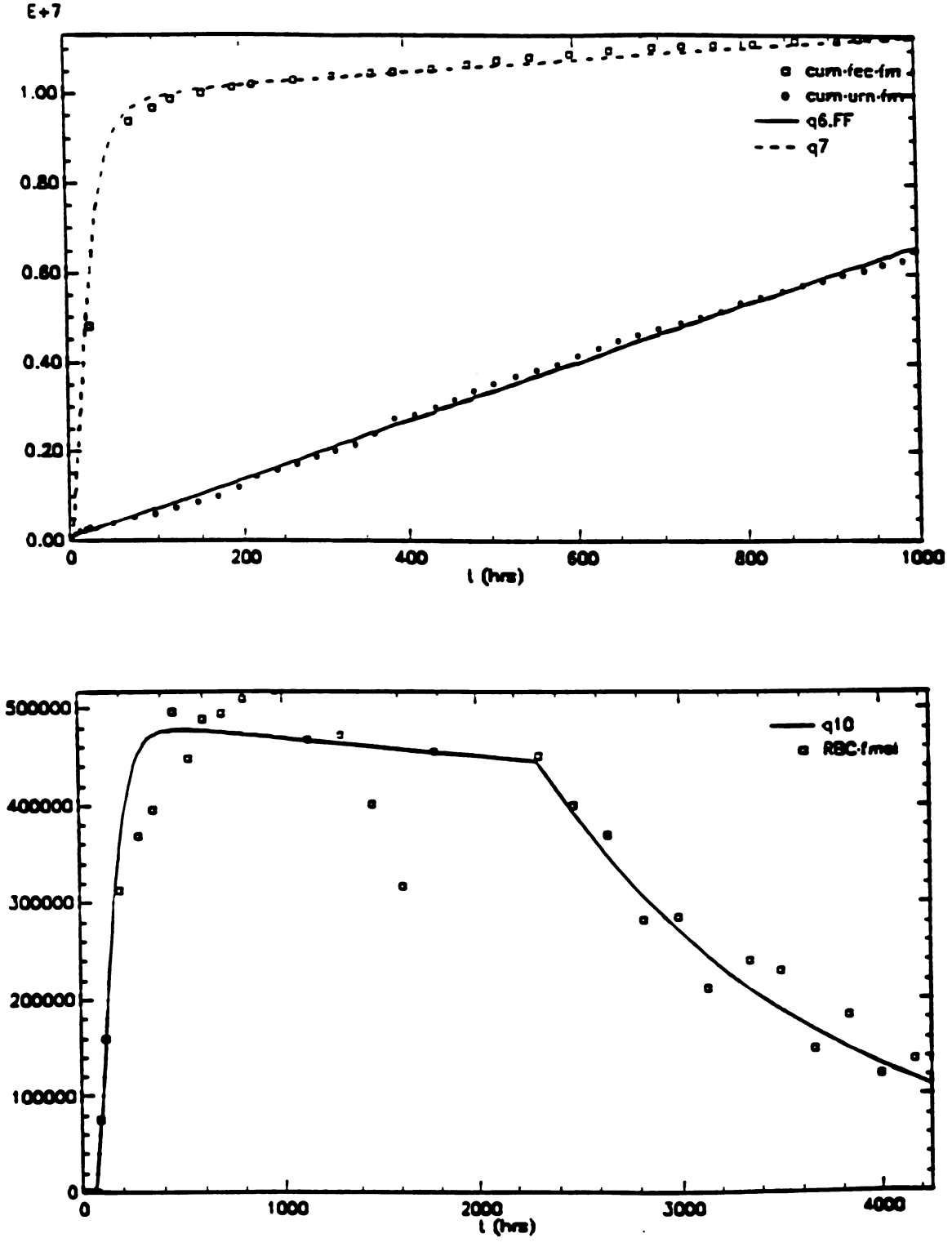

Figure 18. Model-predicted cumulative fmol ^{14}C-folate excreted in the urine and feces (top) and fmol ^{14}C-folate in the red blood cell pool (bottom). Measured values are shown by the squares. See text for description of modeling parameters.

Predicted ^{14}C-folate in the red blood cell pool is shown in the bottom of Figure 18. The model contained a 100-hour delay before allowing flux of tracer into the red blood cell pool. The marrow transferred its entire content of ^{14}C-folate to the cell compartment with a coefficient of 0.21 hr^{-1} resulting in a rapid rise of the tracer in this pool. The model then predicted a flux out of the red blood cell with a coefficient of 0.00004 hr^{-1} increasing to 0.00072 hr^{-1}at 2300 hours.

The plots shown in Figures 17 and 18 depict the model's success at predicting the amounts of ^{14}C-folate in the four compartments where experimental data was available. Modeling also allowed prediction of tracer transfer into and out of compartments not measured experimentally. These inaccessible compartments represented pools with biological correlates based on current understanding of folate metabolism. However, a compartment may not always represent a discretely identifiable pool, but rather a virtual pool representing tissues or organs that behave in the same manner. The fast and slow-turnover tissue pools were such an example where several organs such as liver, muscle and kidney may be involved. It would be impossible to measure tracer concentration in these organs experimentally; compartmental modeling overcame this limitation.

The predicted distribution of the tracer into the tissue pools not measured is shown in Figure 20. The top figure shows the ^{14}C-folate content of the fast (q4) and slow-turnover (q5) pools. As expected, the fast-turnover tissue ^{14}C-folate content rose and fell rapidly while the slow-turnover tissue rose to about three times the content of the slow pool and declined to 45 nmol ^{14}C-folate by day 200. Surprisingly, it was predicted the slow pool had retained approximately 57% of the bolus by day 200.

The amount of tracer in compartments that donated to and received ^{14}C-folate from the red blood cell compartment is shown in the bottom of Figure 20. These consisted of the marrow pool and a degradation pool which received and accumulated ^{14}C-folate from degrading red blood cells. This pool represented liver and spleen since these were the major organs involved in the macrophage-mediated removal and degradation of red blood cells from circulation (Magnani, 1991; Rosse, 1966). As mentioned earlier, transfer of ^{14}C-folate into the marrow occurred in the first 24 hours, while there was a 100-hour delay before subsequent transfer of the tracer to the red blood cell pool. The predicted marrow ^{14}C-folate content (q9) is shown at the bottom of Figure 20. Degraded ^{14}C-folate appeared slowly at first in the degradation pool (q11) and then rapidly after 2300 hours. The change in the transfer coefficient between the red blood cell pool to the degradation pool represented the approximate 100-day lifespan of red blood cells in circulation (Brouillard, 1974; Garby, 1971; Rodvien, 1974; Strumia, 1968).

Insight into the dynamics of the tracer during absorption was provided by predicting the amount of tracer in the gut and intestinal pools. Figure 19 shows the model-predicted behavior of ^{14}C-folate in the gut (q1) and intestine (q2). The gut compartment initially contained an amount equal to the portion of the bolus that was actually absorbed. There was then a rapid decline as ^{14}C-folate was taken up into cells of the intestine with a transfer coefficient of 3.8 hr^{-1}. The amount of tracer in the intestinal cells reached a maximum at one hour and declined slowly as the tracer was transferred to plasma with a coefficient of 0.094 hr^{-1}.

Cumulative excretion of the tracer in urine and feces were measured for the first 42 days. The model-predicted total excretion is shown at the top of Figure 18 (first 42

days is shown). The model predicted a total excretion of 15 nmol ^{14}C-folate in the feces and 27 nmol ^{14}C-folate in the urine by day 200. This resulted in a discrepancy since the sum of these losses, 42 nmoles ^{14}C-folate, and the predicted amount remaining in the body (mostly in the slow-turnover compartment, q5), 48 nmoles ^{14}C-folate, equaled 90 nmoles ^{14}C-folate. This value was greater than the 80 nmol ^{14}C-folate bolus. The model-predicted cumulative excretion in the urine was based on a linear regression model of data for the first 42 days of the study. This model was not validated for days beyond this range. This resulted in an overestimation of urinary excretion since a decline in the daily excretion rates was expected over the 200 days.

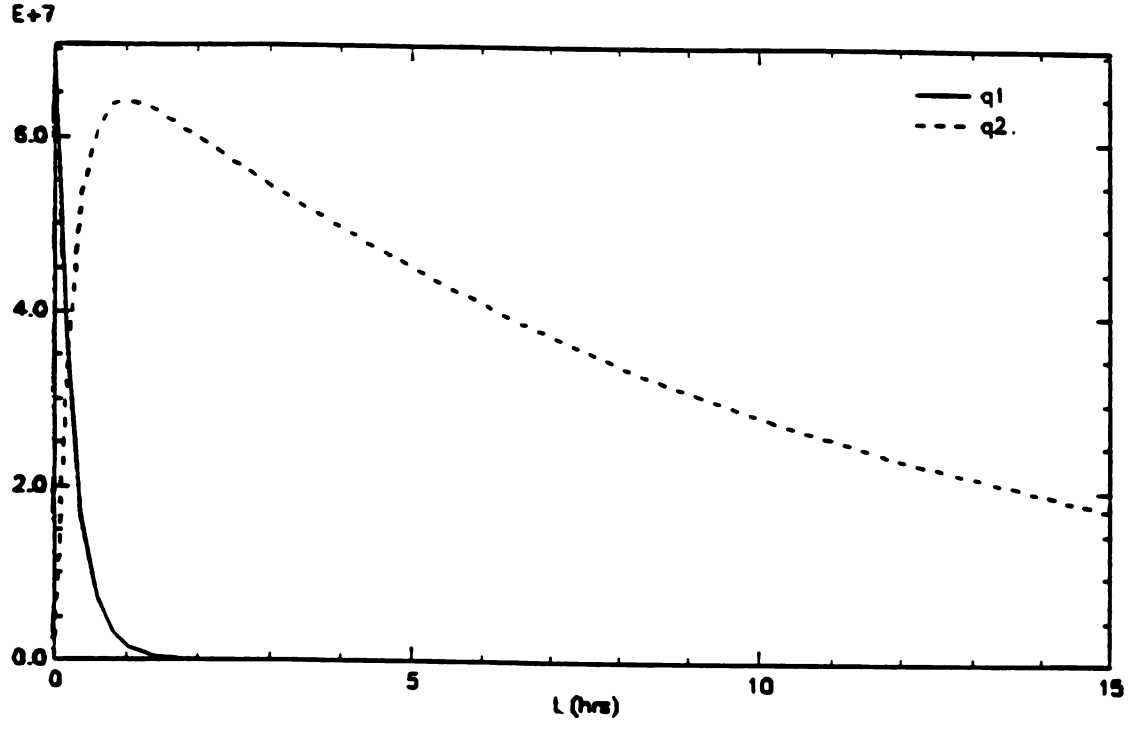

Figure 19. Model-predicted fmol ^{14}C-folate in inaccessible pools. The figure shows predicted amounts in the gut (q1) and intestine (q2) pools.

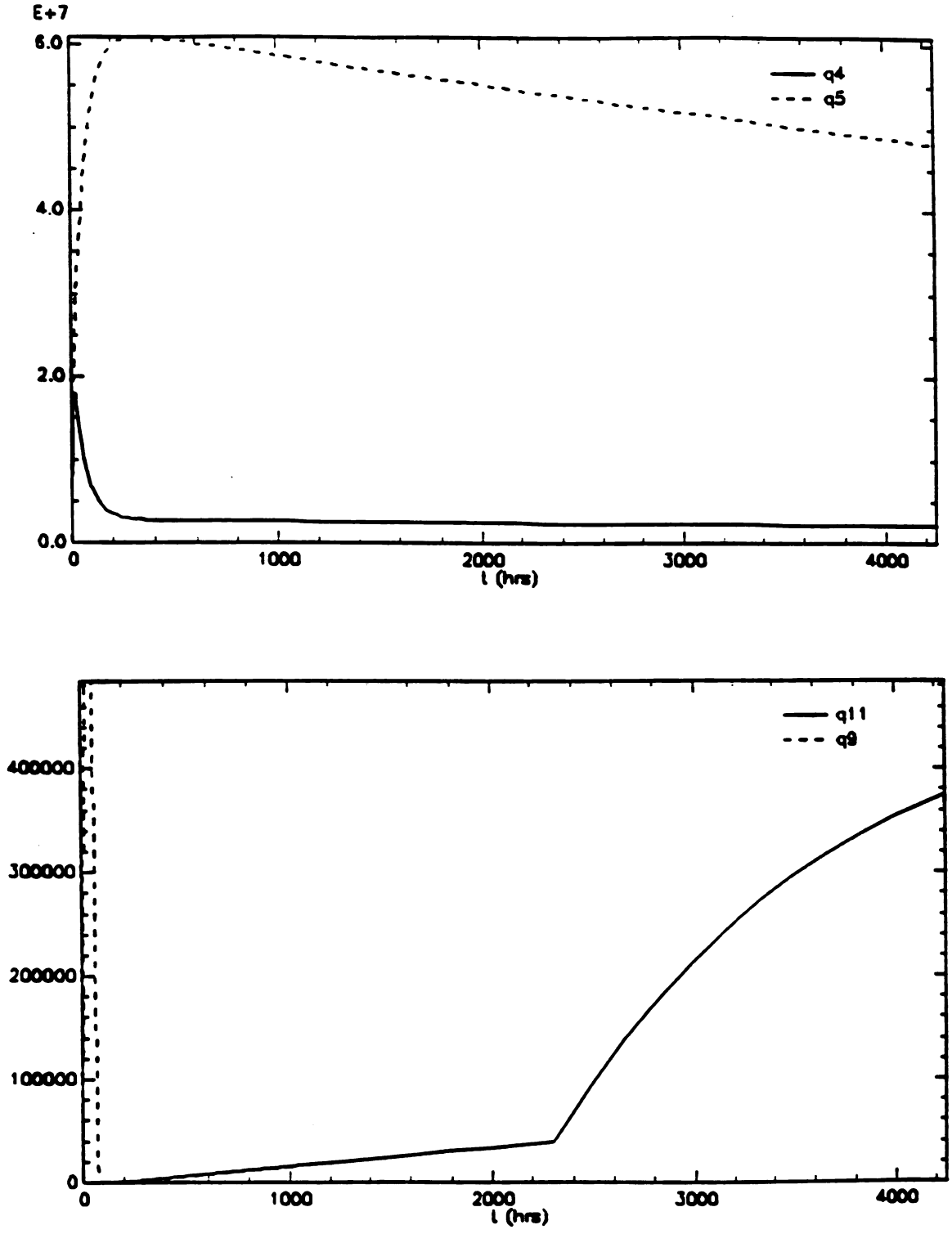

Figure 20. Model-predicted fmol ^{14}C-folate in inaccessible pools. The top figure shows predicted amounts in the fast (q4) and slow (q5) pools. The bottom figure shows predicted amounts in the marrow (q9) and degradation (q11) pools.

Discussion

This study represented the first major biomedical study in humans using AMS. A critical review of the analytical procedures must be made because the procedures used in this study may have far reaching implications to nutrition research. The validity of the AMS measurements has already been established (Creek, 1994; Vogel, 1992a; Vogel, 1992b; Vogel, 1995; Vogel, 1997). These measurements provide a ratio of $^{14}C/^{12}C$ and absolute concentration of ^{14}C can be calculated if the ^{12}C concentration is known.

In a recent study, total carbon was not measured and the radiocarbon data was presented as moles ^{14}C/g carbon (Stenstrom, 1996). In this study, the carbon concentration in every sample was measured using an improved protocol based on published methods (Pella, 1990). Urine samples had the lowest carbon concentration and the mean of three measurements was used for the calculations. Using the carbon concentration for each sample ensured calculation of the actual concentration of ^{14}C in each sample.

The carbon data, shown in Table 1, provided evidence that the subject was in carbon balance throughout the study. Since total carbon concentrations remained steady across samples, changes in the $^{14}C/^{12}C$ ratio measured by AMS were due to ^{14}C enrichment of the sample by ^{14}C-folate. In future studies, absolute concentrations of a ^{14}C-tracer may be calculated using reference values of ^{12}C concentration with minimal introduction of error since measured deviations in ^{12}C concentration were small relative to responses generated by the ^{14}C-tracer. This will significantly simplify the workload required to calculate ^{14}C concentration but must be applied on a case-by-case basis.

The folate concentration in every sample was measured by the standard microbiological assay. This assay, as in most biological assays, has good sensitivity but poor reproducibility. These problems were reviewed in Chapter 2 and include variability in sampling, assay conditions and specificity problems. Three determinations were made and the mean value used to evaluate the subject's overall folate balance.

The folate concentration in plasma and red blood cells over a 200-day period is shown in Figure 2. No significant trend was observed in the folate concentration supporting the notion that the subject's folate status was maintained throughout the study. The folate concentration in urine and feces is shown in Figure 3. Under normal conditions very little intact folate is lost in the urine (McNulty, 1987; McPartlin, 1992). Significant amounts of intact folate, however, were found in the urine when saturating amounts of folic acid, in the range of one milligram or more, were ingested (Kownacki-Brown, 1993). Urine samples collected on days 15, 16 and 30 contained significantly higher amounts of intact folate. Urine collected on days 15 and 16 also had elevated amounts of ^{14}C-folate (Figure 7). This reinforced the urine folate data and indicated that the increase in intact folates excretion on those days was real. The subject's diet record did not indicate any change in the foods consumed on those days. The possibility that large amounts of folate were ingested on those days was therefore ruled out. The subject's diary indicated that days 15, 16 and 30 were bad allergy days. This may indicate that aggravation of the subject's sensitivity to allergens may have resulted in folate excretion in the urine. It is known that febrile conditions increase the amount of retinol and retinol binding protein excreted in the urine (Stephensen, 1994). The urine data in this study provided the first evidence that an interaction may exist between the

acute phase response mechanism and increased urinary folate excretion. Further studies should be conducted in subjects susceptible to allergies using AMS to directly address this issue. If such an interaction exists, there could exist a population of individuals at risk for folate deficiency because of increased folate turnover because of allergies.

The bioavailability of the dose was determined by measuring ^{14}C in the feces. The first two stool samples collected one day and three days postdose contained a total of 8.8 nmol ^{14}C-folic acid. The transit time of material through the gastrointestinal tract was approximately 24 hours and it would be expected that the majority of unabsorbed folic acid would be lost in the first stool collection. However, about an equal amount appeared in the feces between one and three days postdose.

Animal studies have shown rapid cycling of absorbed folate through enterohepatic circulation (Shin, 1995). It was possible that a portion of ^{14}C-folic acid recovered in the feces after one day was absorbed tracer that was lost in the bile. Nevertheless, the sum of 8.8 nmol ^{14}C-folic acid was considered to be unabsorbed or unavailable folic acid and equated to an 89.5% bioavailability. This compared well with previous studies that showed nearly complete absorption of folic acid in healthy humans (Gregory, 1990; Bhandari, 1992; Gregory, 1997; Pfeiffer, 1997; Wei, 1996).

Folate compounds found in nature are typically reduced and polyglutamated. Folate polyglutamates must undergo enzymatic chain-length reduction that might affect their bioavailability. Food folate exists in a complex matrix of protein and carbohydrate. Incomplete extraction of this folate during digestion may also reduce its bioavailability. Future studies can be conducted to identify food folate bioavailability using AMS. These studies must use intrinsically labeled ^{14}C-folate, rather than simply adding ^{14}C-folate

polyglutamates to various food matrices. Intrinsically labeled ^{14}C-folate can be obtained by labeling plants or animal tissues with ^{14}C-precursors of folate.

The amount of ^{14}C-folate in red blood cells remained low for the first three days and rapidly increased until day 19. This clearly suggested that the red blood cells did not incorporate folate while in circulation. The slight increase in ^{14}C-folate concentration in the first 24 hours may have represented non-specific interactions between plasma ^{14}C-folate and red blood cell membranes, even after rigorous washing. This occurred during a period when plasma ^{14}C-folate concentrations were at their maximum. Once plasma ^{14}C-folate concentration dropped after 24 hours, red blood cell ^{14}C-folate also dropped. The four-day delay before appearance of any significant amount of ^{14}C-folate in red blood cells reflected the time required for folate incorporation into maturing reticulocytes in the marrow. These labeled cells were then released into circulation and retained the majority of their folate throughout their lifespan. They were then subjected to the normal macrophage-mediated removal from circulation. As these cells were removed from circulation, so was their labeled-folate, resulting in the observed decline in ^{14}C-folate after about 110 days.

The kinetic parameters describing folate dynamics were determined by a variety of mathematical modeling tools. As described earlier, the ^{14}C-folate concentration in plasma and red blood cells, and ^{14}C-folate output in urine and feces were used for the modeling. The models presented here described the absorption, distribution and elimination of ^{14}C-folic acid given as a single oral dose. Since there is no known biological discrimination between ^{14}C-folic acid and non-labeled folic acid, the models also described the behavior of ingested folic acid. The amount of ^{14}C-folic acid in the

dose, 35 μg or about 1/6th of the current RDA for folate, was equivalent to typical intakes of folate under physiologic conditions. The mechanisms for folate absorption, plasma transportation, tissue storage and renal clearance (i.e. intestinal brush border folate receptors, folate binding proteins, glutamate transferase and kidney folate receptors) were perturbed only to the same degree as a typical intake of folate. Therefore, models that described ^{14}C-folic acid dynamics also described folic acid dynamics under the same conditions.

The simplest approach for describing the data was linear regression modeling. Plasma and red blood cell rates of folate appearance and disappearance were described by the slopes of the linear regression fits. Folate appeared in plasma as early as ten minutes after ingestion of the dose. Folate has previously been shown to enter the portal vein in humans 10 minutes after a 1 mg oral dose of folic acid (Whitehead, 1967). Others have shown reduced folate was converted to 5-methyltetrahydrofolate during absorption (Perry, 1970). This was confirmed in this study by HPLC-AMS of plasma collected one hour after ingestion of ^{14}C-folic acid. There was no evidence of any significant amount of ^{14}C co-eluting with folic acid. This suggested that the reduction and methylation of folate at the intestinal level was very fast and efficient. The possibility that folic acid may be absorbed from the stomach should also be considered.

Plasma folate concentration increased rapidly at a rate of 434.8 fmol/mL/hr and decreased with fast and slow rates of 31.2 fmol/mL/hr and 0.153 fmol/mL/day, respectively. These rates suggested that folate was cleared from the plasma rapidly and by 10 hours postdose, a significant amount was transferred to other compartments. The slow elimination rate suggested that folate may be partitioned into two different pools in

plasma, perhaps a large proportion binding to plasma folate binding protein for fast tissue delivery, and a small proportion binding non-specifically to other plasma proteins such as albumin. This non-specifically bound folate might have a longer residence time in plasma with a slow elimination rate of about 0.153 fmol/mL/day.

The rates of ^{14}C-folate appearance and disappearance into and out of red blood cells were 94.4 and 13.3 fmol/gram hemoglobin/day, respectively. The four-day delay before significant incorporation of ^{14}C-folate represented the time for red blood cell synthesis and maturation in the marrow (Bills, 1992). During this period, folate taken up by the marrow was packaged into reticulocytes during colony-forming erythroid unit stage. It was presumed that marrow folate originated from the plasma, and as described above, received a pulse if ^{14}C-folate for the first day postdose. Plasma ^{14}C-folate had dropped significantly after 24 hours and there would not have been any substantial amount of ^{14}C-folate transferred to the marrow from plasma.

Mature red blood cells already in circulation did not take up plasma folate as evidenced by the ^{14}C-folate concentration in the first three days postdose. During this period, AMS measurements showed a slight rise in red blood cell ^{14}C-folate which dropped back to baseline by day 3. It is suggested that the small amounts of ^{14}C-folate detected in the red blood cell fraction during the first 2 days were the result of either small amounts of plasma ^{14}C-folate that remained in the cell pellet even after four wash cycles, or might represent non-specific ^{14}C-folate interactions with red blood cell membranes or membrane proteins. Nevertheless, these minor effects or interactions disappeared by day 3, after which long-term labeling of the red blood cells with ^{14}C-folate was observed.

The rate of this increase suggested that ^{14}C-folate was incorporated into cells over a short time-span after which the cells were released into circulation reaching a peak by day 19. This level was maintained for about 100 days followed by a slow decline. This pattern was similar to the pattern observed in the lifespan of red blood cells. In fact, ^{14}C-folate dynamics in red blood cells was dictated by the lifecycle of red blood cell synthesis, release into circulation and eventual removal and degradation. The sharp rise in the red blood cell labeling and the shallow decline suggests that cells entered circulation as a cohort, but were removed over a wide timeframe perhaps due to differences in the survival of some cells.

It is known that damage to red blood cells triggers a macrophage-mediated response resulting in their removal from circulation and degradation in the spleen and liver (Magnani, 1991; Rosse, 1966). The average lifespan of human red blood cells is estimated to be around 120 days (Brouillard, 1974; Garby, 1971; Rodvien, 1974; Strumia, 1968). This matches closely the observations made in this study. ^{14}C-Folic acid may be used in future studies for the purpose of studying red blood cell lifespan and survival. This would be an important contribution to the field of hematology since current methods of assessing cell lifespan have inherent limitations (Mock, 1997a; Mock, 1997b). The possibility existed that ^{14}C-folate from degraded cells was recycled back into newly formed cells to produce a tailing effect in the ^{14}C-folate concentration in circulation. It was thought that this would be minor effect since the total amount of ^{14}C-folate in the red blood cell pool was less than 0.014 % of the administered bolus.

Linear modeling was a useful tool for describing the rates of ^{14}C-folate appearance and disappearance from the various pools but should not be used to estimate

the flux of ^{14}C-folate between pools. If we assume plasma has a total volume of 3 L, the rates of absorption and fast elimination would be 1.3 nmol ^{14}C-folate/hr and 0.093 nmol ^{14}C-folate/hr, respectively. This is misleading since we know 71 nmol ^{14}C-folic acid was absorbed and the calculated absorption rate could not account for the amount of ^{14}C-folic acid absorbed.

The area under the plasma concentration curve should not be used to determine the total amount of absorbed ^{14}C-folic acid. The plasma concentration curve, in fact, represented multiple dynamic processes of absorption and distribution to various tissues. During the first hour, the rate of influx into the plasma pool exceeded the rate of removal from the pool and a positive slope was observed. After about one hour, the rate of efflux from the plasma pool exceeded the rate of influx and a decline in plasma ^{14}C-folate concentration was observed with a negative slope. The peak concentration represented the time when the rates of influx and efflux were equal and there was no net change in the concentration of plasma ^{14}C-folate. These flux rates should not be used directly to interpret bioavailability unless estimation of the relative differences between subjects or dosing regimens is desired.

^{14}C-Folate was eliminated from the body by excretion in the feces and urine. As described earlier, the first two feces samples represented loss of unabsorbed or unretained folate and were used to calculate the dose bioavailability. When feces ^{14}C-folate excretion was plotted as cumulative excretion, a linear pattern was observed after about day seven. This excretion corresponded to 0.033 nmol ^{14}C-folate/day. This represented less than 0.05% of the absorbed dose and demonstrated that feces was not a major route

of ^{14}C-folate excretion. The excretion probably represented losses of biliary ^{14}C-folate or perhaps sloughing of epithelial cells of the gastrointestinal tract containing ^{14}C-folate.

Urine exhibited excretion of about 600 pmol ^{14}C-folate in the first day corresponding to less than 0.9% of the absorbed dose. Urine output dropped to approximately 150 pmol ^{14}C-folate/day thereafter. The early loss of ^{14}C-folate may represent loss of degradation products of ^{14}C-folic acid which were not retained. The dose may have also contained impurities that were absorbed but not retained. The possibility that renal reabsorption of ^{14}C-folate may have been saturated also existed but was unlikely due to the small size of the administered dose.

Other studies have shown that human subjects must undergo a saturation regimen of daily intakes of greater than 1 mg folic acid before appearance of a 200 μg dose of folic acid can be detected in the urine. Even under these saturating conditions, less than 20% of the dose appeared in the urine after 48 hours (Rogers, 1997; von der Porten, 1992). It was, therefore, unlikely that the ^{14}C-folate was lost in the urine in the current study as a result of a saturation effect since the subject was not supplemented with folic acid and the administered dose contained only 35 μg folic acid. Overall, the urine represented the major route of ^{14}C-folate excretion with a rate of 0.16 nmol/day for the first 42 days.

Total excretion rate through urine and feces equaled approximately 0.2 nmol/day. At this rate, it would take one year to eliminate the 71 nmol ^{14}C-folate that was absorbed. This suggested that folate was highly retained in the body under these conditions. Liver represents the organ with the largest capacity to store folate with polyglutamate chains up to seven in length (Blair, 1976; Clifford, 1990; Connor, 1980; Connor, 1977; Hoppner,

1980; Houlihan, 1972). This suggests that polyglutamation of folate is an efficient mechanism for retention and storage of folate.

The three linear models described above provided a reasonable assessment of the dynamic parameters of ^{14}C-folate in plasma. However, a more elegant approach would be to describe the dynamics with a single model and a single equation. This was achieved by non-linear modeling. At first, a two-term polyexponential equation was derived as shown in Figure 10. The approach assumed that plasma was a single compartment with one input and one output. The two terms of the equation corresponded to the rate of ^{14}C-folate absorption and elimination from this compartment. The following two-term equation was derived: fmol ^{14}C-folate/mL = $546e^{-0.0917\ t} - 550.4e^{-1.6921\ t}$. This equation described ^{14}C-folate concentration in plasma for the first 20 hours postdose but failed to predict concentrations thereafter.

A three-term polyexponential equation was derived using curve-fitting software to describe ^{14}C-folate concentrations in plasma for the entire 200-days. This single equation predicted that the plasma compartment was more complex than a single compartment with a single input and output. This information was used to develop a compartmental model of folate dynamics.

The modeling techniques described so far were simple descriptive models that predicted ^{14}C-folate concentration in the sampled compartments. Compartmental modeling was able to describe folate dynamics into compartments that were inaccessible and to simulate folate dynamics in hypothetical experiments.

Most compartmental modeling in the past has used the specific activity and not the absolute concentration of the tracer (House, 1997; Johnson, 1996; Novotny, 1995;

Stites, 1997; Lowe, 1997; Scott, 1994a; Scott 1994b). However, measuring the specific activity by a ratio method, such as isotope ratio mass spectrometry, after isolating the nutrient can give misleading results. If the tracer concentration in a compartment does not change over a time period when there is an influx of nonlabeled nutrient, occurring as a result of dietary intake of the nutrient, for example, a decline in the specific activity will be observed. Without knowing the specific activity in all connecting pools, compartmental modeling will be unable to determine whether the observed decline in specific activity was due to an influx of non-labeled nutrient, or a loss of labeled nutrient from that pool. This dilemma can be rectified in the mind of the experimenter by measuring total nutrient concentration in all samples. However, if specific activity is used in the modeling process, the dilemma will persist.

Table 5. Comparison of stable isotope and AMS detection methods

	Deuterium	Radiocarbon
Method of detection	FAB-MS/MS	AMS
Limit of detection	picomole	attomole
Plasma sample needed	1 mL	20 μL
Sample preparation	complex	minimal
Dose	pharmacologic (mg)	physiologic (μg)
Dynamic range	narrow ($\sim 10^3$)	wide ($\sim 10^6$)
Isotope exchange	possible if in labile position	not possible
Biologic isotope effect	possible	not possible
Sample matrix	plasma	plasma, RBC urine, feces, tissues

The concentration of ^{14}C-folic acid in this study was used to mathematically describe folic acid dynamics in a human subject. The phenomenal sensitivity of accelerator mass spectrometry permitted the study to be conducted under physiological conditions with minimal exposure to radiation. Table 5 summarizes the advantages of using ^{14}C-labeled nutrients or drugs to study the dynamics of such compounds in humans. The extreme sensitivity permits administration of much smaller doses as well as collection of smaller samples. Blood collected by finger-stick is typically all that is required for most AMS measurements. This permits collection of multiple samples in a short time without affecting the subject or perturbing the system. Once the sample is collected, little or no sample preparation is required. The dynamic range of tracer enrichment can be tremendously broad in AMS studies. This has a great advantage over stable-isotope methods whose dynamic range is largely limited by higher levels of background isotope. The major disadvantages of AMS methodology is the great care that must be taken to prevent contamination with radiocarbon in the environment and the cost of the analysis. The advantages, however, surpass the drawbacks and make AMS ideally suited for study of nutrients and drugs in humans.

Conclusions

This study represented the first major application of accelerator mass spectrometry to human nutrition research. The phenomenol sensitivity of the instrument permitted the bioavailability and dynamics of a single oral dose of ^{14}C-folic acid to be safely studied in a human subject. The bioavailability of the dose was found to be 89%. The dynamics of the absorbed dose was described by linear, non-linear and compartmental modeling. The excretion data showed that 78% of the administered dose remained in the body by day 42 indicating that folic acid was highly retained. Red blood cell labeling by ^{14}C-folic acid permitted the analysis of red blood cell lifespan in circulation.

Advancements in elucidating the dynamics of vitamin metabolism in the past have been severely hampered due the lack of suitable methodologies. As a sensitive analytical tool, accelerator mass spectrometry will help to significantly advance our understanding of the fundamental interactions between nutrient kinetics in health and disease.

Literature cited

Bhandari, S. D. & Gregory, J. F. (1992). Folic acid, 5-methyl-tetrahydrofolate and 5-formyl-tetrahydrofolate exhibit equivalent intestinal absorption, metabolism and in vivo kinetics in rats. *Journal of Nutrition* **122,** 1847-54.

Bills, N. D., Koury, M. J., Clifford, A. J. & Dessypris, E. N. (1992). Ineffective hematopoiesis in folate-deficient mice. *Blood* **79,** 2273-80.

Blair, J. A., Staff, F. J. & Barford, P. A. (1976). The fate of 5-[^{14}C]methyl-tetrahydrofolate in the rat liver. *Biochemical Society Transactions* **4,** 910-2.

Bourne, D. W. A., Triggs, E. J. & Eadie, M. J. (1986). *Pharmacokinetics for the Non-Mathematical*. MTP Press.

Bourne, D. W. A. (1995). *Mathematical Modeling of Pharmacokinetic Data*. Technomic Publishing Company, Lancaster.

Brouillard, R. P. (1974). Measurement of red blood cell life-span. *Jama* **230,** 1304-5.

Brown, M. L. (1990). *Present knowledge in nutrition*, 6 edition. International Life Sciences Institute-Nutrition Foundation.

Clifford, A. J., Heid, M. K., Muller, H. G. & Bills, N. D. (1990). Tissue distribution and prediction of total body folate of rats. *J Nutr* **120,** 1633-9.

Clifford, A. J., Arjomand, A., Dueker, S. R., Schneider, P. D., Novotny, J. A., Buchholz, B. B. & Vogel, J. S. (1998). Compartmental Analysis of the Dynamics of Folic Acid Metabolism in an Adult Volunteer. In *Advances in Experimental Medicine and Biology*. Plenum *(in press)*.

Connor, M. J. & Blair, J. A. (1980). The identification of the folate conjugates found in rat liver 48 h after the administration of radioactively labelled folate tracers. *Biochem J* **186,** 235-42.

Connor, M. J., Blair, J. A. & Barford, P. A. (1977). Isolation, purification, characterization and metabolism of high-molecular-weight folate from rat liver. *Biochem Soc Trans* **5,** 1319-20.

Creek, M. R., Frantz, C. E., Fultz, E., Haack, K., Redwine, K., Shen, N., Turteltaub, K. W. & Vogel, J. S. (1994). C-14 Ams Quantification Of Biomolecular Interactions Using Microbore and Plate Separations. *Nuclear Instruments & Methods In Physics Research Section B-Beam Interactions With Materials and Atoms* **92,** 454-458.

Creek, M. R., Mani, C., Vogel, J. S. & Turteltaub, K. W. (1997). Tissue distribution and macromolecular binding of extremely low doses of [C-14]-benzene in B6C3F1 mice. *Carcinogenesis* **18,** 2421-2427.

Das, K. C. & Hoffbrand, A. V. (1970). Studies of folate uptake by phytohaemagglutinin-stimulated lymphocytes. *Br J Haematol* **19,** 203-21.

Garby, L. & Mollison, P. L. (1971). Deduction of mean red-cell life-span from 51Cr survival curves. *British Journal of Haematology* **20,** 527-36.

Gregory, J. F., Bailey, L. B., Toth, J. P. & Cerda, J. J. (1990). Stable-isotope methods for assessment of folate bioavailability. *Am J Clin Nutr* **51,** 212-5.

Gregory, J. F. (1997). Bioavailability of folate. *European Journal of Clinical Nutrition* **51 S1,** S54-9.

Henderson, G. B., Tsuji, J. M. & Kumar, H. P. (1988). Mediated uptake of folate by a high-affinity binding protein in sublines of L1210 cells adapted to nanomolar concentrations of folate. *J Membr Biol* **101,** 247-58.

Hoppner, K. & Lampi, B. (1980). Folate levels in human liver from autopsies in Canada. *Am J Clin Nutr* **33,** 862-4.

Houlihan, C. M. & Scott, J. M. (1972). The identification of pteroylpentaglutamate as the major folate derivative in rat liver and the demonstration of its biosynthesis from exogenous ^{3}H-pteroylglutamate. *Biochem Biophys Res Commun* **48,** 1675-81.

House, W. A. & Wastney, M. E. (1997). Compartmental analysis of zinc kinetics in mature male rats. *Am J Physiol* **273,** R1117-25.

Johnson, H. A., Baldwin, R. L. & Calvert, C. C. (1996). A theoretical model of protein synthesis and degradation to identify appropriate experimental designs. *FASEB Journal* **10,** A285.

Kautiainen, A., Vogel, J. S. & Turteltaub, K. W. (1997). Dose-dependent binding of trichloroethylene to hepatic DNA and protein at low doses in mice. *Chemico-Biological Interactions* **106,** 109-121.

Kownacki-Brown, P. A., Wang, C., Bailey, L. B., Toth, J. P. & Gregory, J. F.(1993). Urinary excretion of deuterium-labeled folate and the metabolite p-aminobenzoylglutamate in humans. *Journal of Nutrition* **123,** 1101-8.

Krumdieck, C. L., Fukushima, K., Fukushima, T., Shiota, T. & Butterworth, C. E., Jr. (1978). A long-term study of the excretion of folate and pterins in a human subject after ingestion of ^{14}C folic acid, with observations on the effect of diphenylhydantoin administration. *American Journal of Clinical Nutrition* **31,** 88-93.

Lowe, N. M., Shames, D. M., Woodhouse, L. R., Matel, J. S., Roehl, R., Saccomani, M. P., Toffolo, G., Cobelli, C. & King, J. C. (1997). A compartmental model of zinc metabolism in healthy women using oral and intravenous stable isotope tracers. *American Journal of Clinical Nutrition* **65,** 1810-1819.

Magnani, M. & De Flora, A. (1991). *Red blood cell aging*. Plenum Press, New York.

Martin, J. I., Landen, W. O., Jr., Soliman, A. G. & Eitenmiller, R. R. (1990). Application of a tri-enzyme extraction for total folate determination in foods. *J Assoc Off Anal Chem* **73,** 805-8.

McNulty, H., McPartlin, J. M., Weir, D. G. & Scott, J. M. (1987). Folate catabolism in normal subjects. *Hum Nutr Appl Nutr* **41,** 338-41.

McPartlin, J., Courtney, G., McNulty, H., Weir, D. & Scott, J. (1992). The quantitative analysis of endogenous folate catabolites in human urine. *Anal Biochem* **206,** 256-61.

Mock, D. M., Lankford, G. L., Burmeister, L. F. & Strauss, R. G. (1997a). Circulating red cell volume and red cell survival can be accurately determined in sheep using the [^{14}C]cyanate label. *Pediatric Research* **41,** 916-21.

Mock, D. M., Strauss, R. G. & Lankford, G. L. (1997b). [^{14}C]cyanate labeling of sheep red cells: covalent binding to hemoglobin continues in vivo for a day. *Pediatric Research* **41,** 424-9.

Novotny, J. A., Dueker, S. R., Zech, L. A. & Clifford, A. J. (1995). Compartmental analysis of the dynamics of beta-carotene metabolism in an adult volunteer. *Journal of Lipid Research* **36,** 1825-38.

Pella, E. (1990). Elemental organic analysis. *Am Lab* **22,** 116-25.

Perry, J. & Chanarin, I. (1970). Intestinal absorption of reduced folate compounds in man. *Br J Haematol* **18,** 329-39.

Pfeiffer, C. M., Rogers, L. M., Bailey, L. B. & Gregory, J. F. (1997). Absorption of folate from fortified cereal-grain products and of supplemental folate consumed with or without food determined by using a dual-label stable-isotope protocol. *American Journal of Clinical Nutrition* **66,** 1388-97.

Plante, L. T., Williamson, K. L. & Pastore, E. J. (1980). Preparation of folic acid specifically labeled with carbon-13 in the benzoyl carbonyl. *Methods in Enzymology* **66,** 533-5.

Pristoupilova, K., Hermanova, E., Slavikova, V., Holy, P., Elwood, P. C. & Kolhouse, J. F. (1986). The effect of folate binding protein on the colony-forming activity of GM-CFC cells in vitro. *Folia Haematol Int Mag Klin Morphol Blutforsch* **113,** 759-65.

Rodvien, R., Gillum, A. & Weintraub, L. R. (1974). Decreased glutathione peroxidase activity secondary to severe iron deficiency: a possible mechanism responsible for the shortened life span of the iron-deficient red cell. *Blood* **43,** 281-9.

Rogers, L. M., Pfeiffer, C. M., Bailey, L. B. & Gregory, J. F. (1997). A dual-label stable-isotopic protocol is suitable for determination of folate bioavailability in humans: evaluation of urinary excretion and plasma folate kinetics of intravenous and oral doses of [$^{13}C_5$] and [$^{2}H_2$]folic acid. *Journal of Nutrition* **127,** 2321-7.

Rosse, W. F. & Dacie, J. V. (1966). Immune lysis of normal human and paroxysmal nocturnal hemoglobinuria (PNH) red blood cells. II. The role of complement components in the increased sensitivity of PNH red cells to immune lysis. *Journal of Clinical Investigation* **45,** 749-57.

Rothenberg, S. P., Costa, M. d., Lawson, J. & Rosenberg, Z. (1974). The determination of erythrocyte folate concentration using a two-phase ligand-binding radioassay. *Blood* **43,** 437-43.

Rowland, M. & Tozer, T. N. (1995). *Clinical Pharmacokinetics*. Lea & Febiger, Philadelphia, PA.

Salter, D. N., Ford, J. E., Scott, K. J. & Andrews, P. (1972). Isolation of the Folate-Binding Protein from cow's milk by the use of Affinity Chromatography. *FEBS Letters* **20,** 302-6.

Scott, K. C. & Turnlund, J. R. (1994a). Compartmental model of copper metabolism in adult men. *Journal of Nutritional Biochemistry* **5,** 342-350.

Scott, K. C. & Turnlund, J. R. (1994b). A compartmental model of zinc metabolism in adult men used to study effects of three levels of dietary copper. *American Journal of Physiology* **267,** E165-E173.

Stites, T. E., Bailey, L. B., Scott, K. C., Toth, J. P., Fisher, W. P. & Gregory, J. F. (1997). Kinetic modeling of folate metabolism through use of chronic administration of deuterium-labeled folic acid in men. *Am J Clin Nutr* **65,** 53-60.

Stephensen, C. B., Alvarez, J. O., Kohatsu, J., Hardmeier, R., Kennedy, J. I. & Gammon, R. B. (1994). Vitamin A is excreted in the urine during acute infection. *Am J Clin Nutr* **60,** 388-92.

Strumia, M. M. & Strumia, P. V. (1968). The life span of red cells. *Medical Times* **96,** 1113-24.

Turteltaub, K. W., Mauthe, R. J., Dingley, K. H., Vogel, J. S., Frantz, C. E., Garner, R. C. & Shen, N. (1997). MeIQx-DNA adduct formation in rodent and human tissues at

low doses. *Mutation Research-Fundamental and Molecular Mechanisms Of Mutagenesis* **376,** 243-252.

Vogel, J. S. & Turteltaub, K. W. (1992a). Biomolecular Tracing Through Accelerator Mass Spectrometry. *Trac-Trends In Analytical Chemistry* **11,** 142-149.

Vogel, J. S. (1992b). Rapid Production Of Graphite Without Contamination For Biomedical Ams. *Radiocarbon* **34,** 344-350.

Vogel, J. S., McAninch, J. & Freeman, S. (1997). Elements in biological AMS. *Nuclear Instruments & Methods In Physics Research Section B-Beam Interactions With Materials and Atoms* **123,** 241-244.

Vogel, J. S., Turteltaub, K. W., Finkel, R. & Nelson, D. E. (1995). Accelerator Mass Spectrometry - Isotope Quantification At Attomole Sensitivity. *Analytical Chemistry* **67,** A353-A359.

von der Porten, A. E., Gregory, J. F. d., Toth, J. P., Cerda, J. J., Curry, S. H. & Bailey, L. B. (1992). In vivo folate kinetics during chronic supplementation of human subjects with deuterium-labeled folic acid. *Journal of Nutrition* **122**.

Wadsworth, L. A. (1997). Preventive nutrition: The comprehensive guide for health professionals, by A. Bendich, R.J. Deckelbaum. *Canadian Journal Of Public Health-Revue Canadienne De Sante Publique* **88,** 304-304.

Ward, G. J. & Nixon, P. F. (1990). Modulation of pteroylpolyglutamate concentration and length in response to altered folate nutrition in a comprehensive range of rat tissues. *J Nutr* **120,** 476-84.

Wei, M. M., Bailey, L. B., Toth, J. P. & Gregory, J. F. (1996). Bioavailability for humans of deuterium-labeled monoglutamyl and polyglutamyl folates is affected by selected foods. *Journal of Nutrition* **126,** 3100-8.

White, I. N. H., Martin, E. A., Mauthe, R. J., Vogel, J. S., Turteltaub, K. W. & Smith, L. L. (1997). Comparisons of the binding of [C-14]radiolabelled tamoxifen or toremifene to rat DNA using accelerator mass spectrometry. *Chemico-Biological Interactions* **106,** 149-160.

Whitehead, V. M. & Cooper, B. A. (1967). Absorption of unaltered folic acid from the gastro-intestinal tract in man. *British Journal of Haematology* **13,** 679-86.

Whitehead, V. M., Pratt, R., Viallet, A. & Cooper, B. A. (1972). Intestinal conversion of folinic acid to 5-methyltetrahydrofolate in man. *British Journal of Haematology* **22,** 63-72.

Appendices

APPENDIX I - Calculations

$$1\ \text{modern} = \frac{13.56\ \text{dpm}}{\text{g carbon}} = \frac{6.11\ \text{fCi}}{\text{mg carbon}} = \frac{97.9\ \text{amol radiocarbon}}{\text{mg carbon}}$$

$$1\ \text{mol}\ {}^{14}\text{C} = 14\ \text{g}\ {}^{14}\text{C}$$

$$1.24\ \text{fCi}\ {}^{14}\text{C-folic acid} = 1\ \text{fmol}\ {}^{14}\text{C-folic acid}$$

$$6.2741 \times 10^{-4}\ \text{g}\ {}^{14}\text{C} = 1\ \text{g}\ {}^{14}\text{C-folic acid}$$

Samples with carrier

$$\text{modern} = \frac{\text{radiocarbon}_{carrier} + \text{radiocarbon}_{sample}}{\text{carbon}_{carrier} + \text{carbon}_{sample}}$$

Carrier: Tributyrin (80 uL, 20 mg/mL)
Carbon composition: 59.6%
Carbon mass: 0.9536 mg
Moderns: ~ 0.1014 *(example)*

$$\text{radiocarbon}_{carrier} = 0.1014\ \text{modern} \times \frac{97.9\ \text{amol radiocarbon}}{\text{mg carbon}} \times 0.9536\ \text{mg carbon}$$
$$= 9.466\ \text{amol radiocarbon}$$

Sample:

$$\text{radiocarbon}_{sample} = \text{moderns} \times \frac{97.9\ \text{amol radiocarbon}}{\text{mg carbon}} \times (\text{carbon}_{carrier} + \text{carbon}_{sample}) - \text{radiocarbon}_{carrier}$$

Example:

$$\text{radiocarbon}_{sample}$$
$$= 1.2345\ \text{modern} \times \frac{97.9\ \text{amol radiocarbon}}{\text{mg carbon}} \times (0.9536\ \text{mg} + 0.0464\ \text{mg}) - 9.466\ \text{amol}$$
$$= 111.4\ \text{amol radiocarbon}$$

Samples without carrier

Example: Plasma (P1)

-either-

$$\text{radiocarbon}_{sample} = \text{moderns} \times \frac{97.9 \text{ amol radiocarbon}}{\text{mg carbon}} \times \text{carbon}_{sample}$$

(1.4180 moderns) – (1.0986 moderns) = 0.3194 moderns (adjusted)

(0.3194 moderns) x (97.9 amol ^{14}C/mg C) = 31.2692 amol ^{14}C/mg C

(31.2692 amol ^{14}C/mg C) x (44.38 mg C/mL plasma) = 1,387.7 amol ^{14}C/mL plasma

(387.7 amol ^{14}C/mLplasma) x (14 ag ^{14}C/amol ^{14}C) = 19,428.2 ag ^{14}C/mL plasma

(19,428.2 ag ^{14}C/mL) x (1 ag ^{14}C-folic acid/6.2741 x 10^{-4} ag ^{14}C)
= 3.0965 x 10^{7} ag ^{14}C-folic acid /mL

(3.0965 x 10^{7} ag ^{14}C-folic acid /mL) x (1 amol ^{14}C-folic acid/441.4 ag ^{14}C-folic acid)
= 70,151 amol ^{14}C-folic acid/mL plasma
= 70.1 fmol ^{14}C-folic acid/mL plasma

-or-

$$\text{radiocarbon}_{sample} = \text{moderns} \times \frac{6.11 \text{ fCi radiocarbon}}{\text{mg carbon}} \times \text{carbon}_{sample}$$

(1.4180 moderns) – (1.0986 moderns) = 0.3194 moderns (adjusted)

(0.3194 moderns) x (6.11 fCi/mg C) = 1.9515 fCi/mg C

(1.9515 fCi/mg C) x (44.38 mg C/mL plasma) = 86.61 fCi/mL plasma

(86.61 fCi/mL plasma) x (1 fmol ^{14}C-folic acid/1.24 fCi ^{14}C-folic acid)
= 69.9 fmol ^{14}C-folic acid/mL plasma

Example: Red blood cells (R1)

-either-

$$\text{radiocarbon}_{sample} = \text{moderns} \times \frac{97.9 \text{ amol radiocarbon}}{\text{mg carbon}} \times \text{carbon}_{sample}$$

(1.1525 moderns) – (1.1137 moderns) = 0.0388 moderns (adjusted)

(0. 0388 moderns) x (97.9 amol ^{14}C/mg C) = 3.7985 amol ^{14}C/mg C

(3.7985 amol ^{14}C/mg C) x (53.0 mg C/mL RBC) = 201.32 amol ^{14}C/mL RBC

(201.32 amol ^{14}C/mL RBC) x (14 ag ^{14}C/amol ^{14}C) = 2,818.5 ag ^{14}C/mL RBC

(2,818.5 ag ^{14}C/mL RBC) x (1 ag ^{14}C-folic acid/6.2741 x 10^{-4} ag ^{14}C)
= 4.49 x 10^{6} ag ^{14}C-folic acid /mL RBC

(4.49 x 10^{6} ag ^{14}C-folic acid /mL) x (1 amol ^{14}C-folic acid/441.4 ag ^{14}C-folic acid)
= 10,177.3 amol ^{14}C-folic acid/mL RBC

(10,177.3 amol ^{14}C-folic acid/mL RBC) x (1 mL RBC/0.090 g hemoglobin)
= 113,081 amol ^{14}C-folic acid/g hemoglobin
= <u>113.1 fmol ^{14}C-folic acid/g hemoglobin</u>

-or-

$$\text{radiocarbon}_{sample} = \text{moderns} \times \frac{6.11 \text{ fCi radiocarbon}}{\text{mg carbon}} \times \text{carbon}_{sample}$$

(1.1525 moderns) – (1.1137 moderns) = 0.0388 moderns (adjusted)

(0. 0388 moderns) x (6.11 fCi/mg C) = 0.23707 fCi/mg C

(0.23707 fCi/mg C) x (53.0 mg C/mL plasma) = 12.565 fCi/mL RBC

(12.565 fCi/mL plasma) x (1 fmol ^{14}C-folic acid/1.24 fCi ^{14}C-folic acid)
= 10.13 fmol ^{14}C-folic acid/mL RBC

(10.13 fmol ^{14}C-folic acid/mL RBC) x (1 mL RBC/0.090 g hemoglobin)
= <u>112.6 fmol ^{14}C-folic acid/g hemoglobin</u>

Example: Urine (U5)

-either-

$$\text{radiocarbon}_{sample} = \text{moderns} \times \frac{97.9 \text{ amol radiocarbon}}{\text{mg carbon}} \times \text{carbon}_{sample}$$

(5.8687 moderns) – (1.1657 moderns) = 4.7030 moderns (adjusted)

(4.7030 moderns) x (97.9 amol ^{14}C/mg C) = 460.4 amol ^{14}C/mg C

(460.4 amol ^{14}C/mg C) x (5.88 mg C/mL urine) = 2,707.3 amol ^{14}C/mL urine

(2,707.3 amol ^{14}C/mL urine) x (14 ag ^{14}C/amol ^{14}C) = 37,902.1 ag ^{14}C/mL urine

(37,902.1 ag ^{14}C/mL urine) x (1 ag ^{14}C-folic acid/6.2741 x 10^{-4} ag ^{14}C)
= 6.041 x 10^{7} ag ^{14}C-folic acid /mL urine

(6.041 x 10^{7} ag ^{14}C-folic acid /mL) x (1 amol ^{14}C-folic acid/441.4 ag ^{14}C-folic acid)
= 136,861 amol ^{14}C-folic acid/mL urine

(136,861 amol ^{14}C-folic acid/mL urine) x (1,368.6 mL urine/collection)
= 187,307,947 amol ^{14}C-folic acid/collection
= <u>187.3 pmol ^{14}C-folic acid/collection</u>

-or-

$$\text{radiocarbon}_{sample} = \text{moderns} \times \frac{6.11 \text{ fCi radiocarbon}}{\text{mg carbon}} \times \text{carbon}_{sample}$$

(5.8687 moderns) – (1.1657 moderns) = 4.7030 moderns (adjusted)

(4.7030 moderns) x (6.11 fCi/mg C) = 28.735 fCi/mg C

(28.735 fCi/mg C) x (5.88 mg C/mL urine) = 168.96 fCi/mL urine

(168.96 fCi/mL urine) x (1 fmol ^{14}C-folic acid/1.24 fCi ^{14}C-folic acid)
= 136.25 fmol ^{14}C-folic acid/mL urine

(136.25 fmol ^{14}C-folic acid/mL urine) x (1,368.6 mL urine/collection)
= 186,471.7 fmol ^{14}C-folic acid/collection
= <u>186.5 fmol ^{14}C-folic acid/collection</u>

Example: Feces (F5)

-either-

$$\text{radiocarbon}_{sample} = \text{moderns} \times \frac{97.9 \text{ amol radiocarbon}}{\text{mg carbon}} \times \text{carbon}_{sample}$$

(3.2027 moderns) – (1.1247 moderns) = 2.0780 moderns (adjusted)

(2.0780 moderns) x (97.9 amol ^{14}C/mg C) = 203.44 amol ^{14}C/mg C

(203.44 amol ^{14}C/mg C) x (9.38 mg C/mL urine) = 1,908.2 amol ^{14}C/mL feces

(1,908.2 amol ^{14}C/mL feces) x (14 ag ^{14}C/amol ^{14}C) = 26,715 ag ^{14}C/mL feces

(26,715 ag ^{14}C/mL feces) x (1 ag ^{14}C-folic acid/6.2741 x 10^{-4} ag ^{14}C)
= 4.260 x 10^{7} ag ^{14}C-folic acid /mL feces

(4.260 x 10^{7} ag ^{14}C-folic acid /mL) x (1 amol ^{14}C-folic acid/441.4 ag ^{14}C-folic acid)
= 96,513 amol ^{14}C-folic acid/mL feces

(96,513 amol ^{14}C-folic acid/mL feces) x (1,120.4 mL feces/collection)
= 108,133,223 amol ^{14}C-folic acid/collection
= <u>108.1 pmol ^{14}C-folic acid/collection</u>

-or-

$$\text{radiocarbon}_{sample} = \text{moderns} \times \frac{6.11 \text{ fCi radiocarbon}}{\text{mg carbon}} \times \text{carbon}_{sample}$$

(3.2027 moderns) – (1.1247 moderns) = 2.0780 moderns (adjusted)

(2.0780 moderns) x (6.11 fCi/mg C) = 12.697 fCi/mg C

(12.697 fCi/mg C) x (9.38 mg C/mL feces) = 119.09 fCi/mL feces

(119.09 fCi/mL feces) x (1 fmol ^{14}C-folic acid/1.24 fCi ^{14}C-folic acid)
= 96.04 fmol ^{14}C-folic acid/mL feces

(96.04 fmol ^{14}C-folic acid/mL feces) x (1,120.4 mL feces/collection)
= 107,607 fmol ^{14}C-folic acid/collection
= <u>107.6 pmol ^{14}C-folic acid/collection</u>

Appendix II-Radiocarbon Data (Moderns)

Sample	Replicate	Fraction Modern	S.D. of measurement	Mean	S.D. of mean	Date Measured
PLASMA						
P0	A	1.1049	0.0132	1.0986	0.0166	3/3/97
P0	B	1.1070	0.0132			3/3/97
P0	C	1.0720	0.0121			5/12/97
P0	D	1.0853	0.0172			5/12/97
P0	A	1.1210	0.0114			3/3/97
P0	B	broke				3/3/97
P0	C	1.1089	0.0094			3/24/97
P0	C	1.0913	0.0111			5/12/97
P1	A	1.4146	0.0146	1.4180	0.0204	3/3/97
P1	B	1.3995	0.0160			3/3/97
P1	C	1.4399	0.0164			5/12/97
P2	A	2.1318	0.0209	2.1278	0.0237	3/3/97
P2	B	2.1024	0.0230			3/3/97
P2	C	2.1493	0.0235			5/12/97
P3	A	2.6218	0.0282	2.6242	0.0188	3/3/97
P3	B	2.6441	0.0254			3/3/97
P3	C	2.6068	0.0282			5/12/97
P4	A	2.9639	0.0317	2.8869	0.0038	3/3/97
P4	B	2.9585	0.0317			3/3/97
P4	C	2.7385	0.0227			5/12/97
P5	A	3.0831	0.0474	3.0623	0.0228	3/3/97
P5	B	3.0379	0.0289			3/3/97
P5	C	3.0659	0.0329			5/12/97
P6	A	2.9631	0.0319	2.9019	0.1410	3/3/97
P6	B	3.0020	0.0321			3/3/97
P6	C	2.7407	0.0241			5/12/97
P7	A	3.1301	0.0350	3.1218	0.0666	3/3/97
P7	B	3.1839	0.0501			3/3/97
P7	C	3.0514	0.0533			5/12/97
P8	A	3.1301	0.0334	3.1381	0.0561	3/3/97
P8	B	3.1978	0.0342			3/3/97
P8	C	3.0864	0.0330			5/12/97
P9	A	2.9747	0.0318	2.8664	0.1700	3/3/97
P9	B	2.9540	0.0282			3/3/97
P9	C	2.6704	0.0288			5/12/97
P10	A	2.9519	0.0315	3.0426	0.1062	3/3/97
P10	B	3.0164	0.0323			3/3/97
P10	C	3.1594	0.0315			5/12/97
P11	A	2.9341	0.0411	2.9428	0.0296	3/3/97
P11	B	2.9757	0.0374			3/3/97
P11	C	2.9186	0.0313			5/12/97
P12	A	2.9422	0.0314	2.9002	0.0587	3/3/97
P12	B	2.9252	0.0315			3/3/97
P12	C	2.8331	0.0304			5/12/97
P13	A	2.8207	0.0304	2.7992	0.0616	3/3/97
P13	B	2.8472	0.0307			3/3/97
P13	C	2.7298	0.0294			5/12/97
P14	A	2.7202	0.0387	2.7446	0.0214	3/3/97
P14	B	2.7539	0.0227			3/3/97
P14	C	2.7598	0.0295			5/12/97

Appendix II-Radiocarbon Data (Moderns)

P15	A	2.6450	0.0234	2.6178	0.0251	3/3/97
P15	B	2.6130	0.0320			3/3/97
P15	C	2.5955	0.0280			5/12/97
P16	A	2.6194	0.0282	2.6030	0.0433	3/3/97
P16	B	2.6357	0.0237			3/3/97
P16	C	2.5538	0.0226			5/12/97
P17	A	2.4141	0.0214	2.4172	0.0084	3/3/97
P17	B	2.4108	0.0233			3/3/97
P17	C	2.4268	0.0452			5/12/97
P18	A	2.2133	0.0466	2.2015	0.0285	3/3/97
P18	B	2.1690	0.0237			3/3/97
P18	C	2.2223	0.0242			5/12/97
P19	A	2.0393	0.0201	2.0439	0.0312	3/3/97
P19	B	2.0152	0.0182			3/3/97
P19	C	2.0771	0.0371			5/12/97
P20	A	1.9949	0.0358	2.0449	0.1199	3/3/97
P20	B	1.9580	0.0182			3/3/97
P20	C	2.1817	0.0378			5/12/97
P21	A	broke		1.8132	0.0333	3/3/97
P21	B	broke				3/3/97
P21	C	1.8128	0.0234			3/24/97
P21	D	1.8468	0.0155			3/24/97
P21	C	1.7801	0.0223			5/12/97
P22	A	1.6521	0.0166	1.6402	0.0385	3/3/97
P22	B	1.6713	0.0147			3/3/97
P22	C	1.5971	0.0183			5/12/97
P23	A	1.5991	0.0179	1.6121	0.0116	3/3/97
P23	B	1.6215	0.0151			3/3/97
P23	C	1.6157	0.0223			5/12/97
P24	A	1.5865	0.0148	1.5534	0.0502	3/3/97
P24	B	1.5781	0.0133			3/3/97
P24	C	1.4956	0.0128			5/12/97
P25	A	1.5500	0.0157	1.5352	0.0232	3/3/97
P25	B	1.5472	0.0157			3/3/97
P25	C	1.5084	0.0143			5/12/97
P26	A	1.4389	0.0148	1.4758	0.0819	3/3/97
P26	B	1.4188	0.0155			3/3/97
P26	C	1.5696	0.0177			5/12/97
P27	A	1.3968	0.0127	1.3652	0.0394	3/3/97
P27	B	1.3777	0.0149			3/3/97
P27	C	1.3210	0.0153			5/12/97
P28	A	1.3562	0.0152	1.3752	0.0245	3/3/97
P28	B	1.3665	0.0141			3/3/97
P28	C	1.4028	0.0160			5/12/97
P29	A	1.3292	0.0153	1.3147	0.0137	3/3/97
P29	B	1.3020	0.0151			3/3/97
P29	C	1.3129	0.0137			5/12/97
P30	A	1.2522	0.0146	1.2417	0.0232	3/3/97
P30	B	1.2577	0.0123			3/3/97
P30	C	1.2150	0.0120			5/12/97
P31	A	*0.9411*	0.0095	1.2506	0.0212	3/24/97
P31	B	1.2656	0.0107			3/24/97
P31	C	1.2356	0.0144			5/12/97
P32	A	1.2176	0.0103	1.2350	0.0151	3/24/97
P32	B	1.2433	0.0108			3/24/97

Appendix II-Radiocarbon Data (Moderns)

P32	C	1.2441	0.0126			5/12/97
P33	A	1.1750	0.0111	1.1899	0.0146	3/24/97
P33	B	1.1906	0.0108			3/24/97
P33	C	1.2041	0.0109			3/24/97
P34	A	1.2084	0.0109	1.2016	0.0181	3/24/97
P34	B	1.2153	0.0110			3/24/97
P34	C	1.1811	0.0151			3/24/97
P35	A	1.2902	0.0213	1.2703	0.0197	4/28/97
P35	B	1.2699	0.0148			4/28/97
P35	C	1.2507	0.0180			4/28/97
P36	A	1.2640	0.0187	1.2391	0.0217	4/28/97
P36	B	1.2248	0.0123			4/28/97
P36	C	1.2284	0.0143			4/28/97
P39	A	1.1540	0.0126	1.2142	0.0791	7/7/97
P39	B	1.3038	0.0118			7/7/97
P39	C	1.1849	0.0107			7/7/97
P42	A	1.1662	0.0108	1.1680	0.0026	7/7/97
P42	B	1.1698	0.0138			7/7/97
P45	A	1.1451	0.0171	1.1545	0.0126	6/23/97
P45	B	1.1497	0.0104			6/23/97
P45	C	1.1688	0.0106			6/23/97
P46	A	1.3313	0.0191	1.2018	0.0878	6/23/97
P46	B	1.1740	0.0103			6/23/97
P46	C	1.2909	0.0159			6/23/97
P46	A	1.1593	0.0107			7/7/97
P46	B	1.1373	0.0105			7/7/97
P46	C	1.1177	0.0124			7/7/97
P47	A	1.1539	0.0128	1.1480	0.0084	7/7/97
P47	C	1.1420	0.0125			7/7/97
P48	A	1.1471	0.0106	1.1208	0.0473	7/7/97
P48	B	1.0662	0.0101			7/7/97
P48	C	1.1491	0.0106			7/7/97
P49	A	1.1582	0.0112	1.1478	0.0222	7/7/97
P49	B	1.1629	0.0132			7/7/97
P49	C	1.1223	0.0165			7/7/97
P50	A	1.1780	0.0108	1.1813	0.0098	7/28/97
P50	B	1.1923	0.0109			7/28/97
P50	C	1.1736	0.0107			7/28/97
P51	A	1.1315	0.0104	1.1310	0.0016	7/28/97
P51	B	1.1323	0.0120			7/28/97
P51	C	1.1293	0.0151			7/28/97
P52	A	1.2255	0.0109	1.1759	0.0508	7/28/97
P52	B	1.1240	0.0100			7/28/97
P52	C	1.1782	0.0105			7/28/97
P53	A	1.1107	0.0132	1.1196	0.0077	8/11/97
P53	B	1.1241	0.0154			8/11/97
P53	C	1.1240	0.0134			8/11/97
P54	A	1.0866	0.0130	1.1225	0.0406	8/11/97
P54	B	1.1665	0.0125			8/11/97
P54	C	1.1145	0.0150			8/11/97
P55	A	1.1264	0.0134	1.1200	0.0123	8/11/97
P55	B	1.1278	0.0165			8/11/97
P55	C	1.1057	0.0132			8/11/97
P56	A	1.1133	0.0124	1.1035	0.0139	9/29/97
P56	B	1.0936	0.0122			9/29/97

Appendix II-Radiocarbon Data (Moderns)

P57	A	1.0988	0.0122	1.1153	0.0233	9/29/97
P57	B	1.1317	0.0154			9/29/97
P58	A	1.0755	0.0170	1.0946	0.0244	10/12/97
P58	B	1.1220	0.0120			10/12/97
P58	C	1.0863	0.0116			10/12/97
RED BLOOD CELLS						
R0	A	1.0922	0.0131	1.1137	0.0267	3/10/97
R0	B	1.0929	0.0140			3/10/97
R0	C	1.1130	0.0133			3/10/97
R0	D	1.1134	0.0121			3/10/97
R0	A	1.1160	0.0133			3/10/97
R0	B	1.1698	0.0138			3/10/97
R0	C	1.0985	0.0131			3/10/97
R0	D	broke				3/10/97
R1	A	1.1235	0.0134	1.1525	0.0410	3/10/97
R1	B	1.1815	0.0238			3/10/97
R2	A	1.1665	0.0125	1.1585	0.0113	3/10/97
R2	B	1.1506	0.0110			3/10/97
R3	A	1.1392	0.0135	1.1459	0.0094	3/10/97
R3	B	1.1526	0.0136			3/10/97
R4	A	1.1321	0.0114	1.1480	0.0225	3/10/97
R4	B	1.1639	0.0117			3/10/97
R5	A	1.1564	0.0125	1.1535	0.0041	3/10/97
R5	B	1.1506	0.0106			3/10/97
R6	A	1.1539	0.0110	1.1624	0.0119	3/10/97
R6	B	1.1708	0.0112			3/10/97
R7	A	1.1631	0.0138	1.1631	0.0001	3/10/97
R7	B	1.1632	0.0182			3/10/97
R8	A	1.1714	0.0138	1.1714		3/10/97
R8	B	broke				3/10/97
R9	A	1.1324	0.0135	1.1418	0.0132	3/10/97
R9	B	1.1511	0.0228			3/10/97
R10	A	1.1548	0.0136	1.1657	0.0154	3/10/97
R10	B	1.1766	0.0138			3/10/97
R11	A	1.1449	0.0135	1.1505	0.0079	3/10/97
R11	B	1.1561	0.0136			3/10/97
R12	A	1.1794	0.0139	1.1588	0.0290	3/10/97
R12	B	1.1383	0.0156			3/10/97
R13	A	1.1355	0.0180	1.1395	0.0057	3/10/97
R13	B	1.1435	0.0176			3/10/97
R14	A	1.1651	0.0137	1.1807	0.0220	3/10/97
R14	B	1.1962	0.0140			3/10/97
R15	A	1.1306	0.0134	1.1465	0.0225	3/10/97
R15	B	1.1624	0.0125			3/10/97
R16	A	1.1578	0.0137	1.1456	0.0173	3/10/97
R16	B	1.1333	0.0148			3/10/97
R17	A	1.1397	0.0207	1.1460	0.0089	3/10/97
R17	B	1.1523	0.0124			3/10/97
R18	A	1.1295	0.0153	1.1347	0.0073	3/10/97
R18	B	1.1398	0.0135			3/10/97
R19	A	1.1318	0.0161	1.1244	0.0103	3/10/97
R19	B	1.1171	0.0142			3/10/97
R20	A	1.1815	0.0139	1.1560	0.0360	3/10/97
R20	B	1.1306	0.0134			3/10/97

Appendix II-Radiocarbon Data (Moderns)

R21	A	broke		1.1723		3/10/97
R21	B	1.1723	0.0138			3/10/97
R22	A	1.1329	0.0135	1.1338	0.0013	3/10/97
R22	B	1.1347	0.0135			3/10/97
R23	A	1.1544	0.0136	1.1507	0.0052	3/10/97
R23	B	1.1470	0.0136			3/10/97
R24	A	1.1218	0.0133	1.1259	0.0058	3/10/97
R24	B	1.1300	0.0104			3/10/97
R25	A	1.1418	0.0135	1.1526	0.0153	3/10/97
R25	B	1.1634	0.0144			3/10/97
R26	A	1.1353	0.0122	1.1278	0.0105	3/10/97
R26	B	1.1204	0.0133			3/10/97
R27	A	1.1464	0.0123	1.1229	0.0332	3/10/97
R27	B	1.0994	0.0131			3/10/97
R28	A	1.1239	0.0134	1.1210	0.0041	3/10/97
R28	B	1.1182	0.0122			3/10/97
R29	A	1.2139	0.0142	1.1993	0.0206	3/10/97
R29	B	1.1848	0.0126			3/10/97
R30	A	1.2673	0.0147	1.2933	0.0368	3/10/97
R30	B	1.3193	0.0152			3/10/97
R31	A	1.4269	0.0162	1.4246	0.0032	3/10/97
R31	B	1.4223	0.0207			3/10/97
R32	A	1.5437	0.0158	1.5313	0.0174	3/10/97
R32	B	1.5190	0.0169			3/10/97
R33	A	1.5393	0.0190	1.5608	0.0305	3/24/97
R33	B	1.5824	0.0142			3/24/97
R34	A	1.6040	0.0136	1.6726	0.0487	3/24/97
R34	B	1.7149	0.0224			3/24/97
R34	E	1.6864	0.0205			4/28/97
R34	F	1.7157	0.0209			4/28/97
R34	G	1.6418	0.0199			4/28/97
R35	A	1.6125	0.0245	1.6240	0.0162	4/28/97
R35	B	1.6355	0.0190			4/28/97
R36	A	1.6656	0.0179	1.6568	0.0124	4/28/97
R36	B	1.6481	0.0200			4/28/97
R37	A	1.7367	0.0173	1.6610	0.0790	5/12/97
R37	B	1.6671	0.0242			5/12/97
R37	C	1.5791	0.0253			5/12/97
R38	A	1.7113	0.0302	1.6883	0.0999	5/12/97
R38	B	1.7747	0.0197			5/12/97
R38	C	1.5789	0.0177			5/12/97
R39	A	1.7625	0.0162	1.6940	0.0599	5/12/97
R39	B	1.6515	0.0284			5/12/97
R39	C	1.6680	0.0167			5/12/97
R40	A	1.6498	0.0269	1.6462	0.0157	5/12/97
R40	B	1.6597	0.0208			5/12/97
R40	C	1.6290	0.0190			5/12/97
R41	A	1.5515	0.0194	1.5601	0.0215	5/12/97
R41	B	1.5846	0.0287			5/12/97
R41	C	1.5442	0.0145			5/12/97
R42	A	1.5859	0.0279	1.6028	0.0338	5/12/97
R42	B	1.6417	0.0184			5/12/97
R42	C	1.5808	0.0160			5/12/97
R43	A	1.5091	0.0154	1.5293	0.0272	5/12/97
R43	B	1.5186	0.0172			5/12/97

Appendix II-Radiocarbon Data (Moderns)

R43	C	1.5603	0.0147			5/12/97
R44	A	*2.4502*	0.0205	1.5700	0.0309	6/9/97
R44	B	*2.2118*	0.0161			6/9/97
R44	C	*1.5856*	0.0197			6/9/97
R44	A	1.5815	0.0137			7/28/97
R44	B	1.6133	0.0140			7/28/97
R44	C	1.6004	0.0138			7/28/97
R44	A	1.5318	0.0194			6/23/97
R44	B	1.5443	0.0139			6/23/97
R44	C	1.5485	0.014			6/23/97
R45	A	1.5593	0.0131	1.5414	0.0156	6/9/97
R45	B	1.5337	0.0152			6/9/97
R45	C	1.5311	0.0177			6/9/97
R46	A	1.5820	0.0138	1.6016	0.0490	6/9/97
R46	B	1.6581	0.0156			6/9/97
R46	C	1.5666	0.0136			6/9/97
R47	A	1.4941	0.0168	1.4933	0.0080	7/28/97
R47	B	1.5026	0.0130			7/28/97
R47	C	1.4935	0.0170			7/28/97
R47	D	1.4830	0.0132			7/28/97
R48	A	1.4472	0.0121	1.4553	0.0155	7/7/97
R48	B	1.4455	0.0132			7/7/97
R48	C	1.4732	0.0107			7/7/97
R49	A	1.4092	0.0206	1.4116	0.0053	7/7/97
R49	B	1.4176	0.0123			7/7/97
R49	C	1.4078	0.0118			7/7/97
R50	A	1.4165	0.0121	1.4133	0.0071	7/28/97
R50	B	1.4130	0.0227			7/28/97
R50	C	1.4036	0.0128			7/28/97
R50	D	1.4200	0.0130			7/28/97
R51	A	1.4245	0.0130	1.3742	0.0349	7/28/97
R51	B	1.3701	0.0129			7/28/97
R51	C	1.3547	0.0140			7/28/97
R51	D	1.3472	0.0132			7/28/97
R52	A	1.3406	0.0116	1.3397	0.0091	7/28/97
R52	B	1.3301	0.0117			7/28/97
R52	C	1.3483	0.0129			7/28/97
R53	A	1.3064	0.0198	1.2976	0.0082	8/11/97
R53	B	1.2962	0.0150			8/11/97
R53	C	1.2903	0.0149			8/11/97
R54	A	1.2890	0.0141	1.2880	0.0113	8/11/97
R54	B	1.2987	0.0150			8/11/97
R54	C	1.2762	0.0113			8/11/97
R55	A	1.2525	0.0137	1.2692	0.0366	8/11/97
R55	B	1.3112	0.0137			8/11/97
R55	C	1.2439	0.0148			8/11/97
R56	A	1.2428	0.0167	1.2505	0.0221	9/29/97
R56	B	1.2754	0.0175			9/29/97
R56	C	1.2333	0.0170			9/29/97
R57	A	1.1820	0.0227	1.2202	0.0366	9/29/97
R57	B	1.2236	0.0168			9/29/97
R57	C	1.2549	0.0173			9/29/97
R58	A	1.2237	0.0148	1.2229	0.0012	10/12/97
R58	B	no	current			10/12/97
R58	C	1.2220	0.0120			10/12/97

Appendix II-Radiocarbon Data (Moderns)

URINE						
U0	A	1.1820	0.0119	1.1657	0.0231	5/27/97
U0	B	1.1493	0.0098			5/27/97
U1	A	29.3337	0.5981	31.6966	0.1850	7/14/97
U1	B	29.5953	0.6014			7/14/97
U1	C	36.1609	0.2969			7/28/97
U2	A	9.8138	0.2024	10.2944	0.6641	7/14/97
U2	B	11.0522	0.2227			7/14/97
U2	C	10.0173	0.0841			7/28/97
U3	A	8.4895	0.1729	8.3004	0.2911	7/14/97
U3	B	8.4465	0.1705			7/14/97
U3	C	7.9652	0.0652			7/28/97
U4	A	8.1210	0.1659	7.6853	0.6161	7/14/97
U4	B	7.2497	0.1478			7/14/97
U5	A	6.1644	0.1261	5.8687	0.2907	7/14/97
U5	B	5.8584	0.1212			7/14/97
U5	C	5.5833	0.2472			7/28/97
U6	A	4.4588	0.0626	4.4984	0.0561	5/27/97
U6	B	4.5381	0.0537			5/27/97
U7	A	4.2766	0.0898	4.4061	0.1819	7/14/97
U7	B	4.6141	0.0950			7/14/97
U7	C	4.3276	0.0636			7/28/97
U8	A	3.7019	0.0760	3.9608	0.2400	7/14/97
U8	B	4.0044	0.0827			7/14/97
U8	C	4.1759	0.0412			7/28/97
U9	A	3.7913	0.3161	4.1438	0.3133	7/14/97
U9	B	4.2494	0.0874			7/14/97
U9	C	no	current			7/28/97
U9	D	4.3906	0.0438			10/12/97
U9	E	no	current			10/12/97
U10	A	4.0186	0.0825	4.1560	0.1351	7/14/97
U10	B	4.1607	0.0855			7/14/97
U10	C	4.2887	0.0550			7/28/97
U11	A	4.3752	0.1483	4.5597	0.4513	7/14/97
U11	B	4.2298	0.3685			7/14/97
U11	C	5.0740	0.0425			7/28/97
U12	A	5.8623	0.0541	6.2084	0.3459	5/27/97
U12	B	6.6206	0.0600			5/27/97
U12	A	6.3584	0.1239			9/29/97
U12	B	5.9923	0.1183			9/29/97
U13	A	3.8954	0.0806	3.9737	0.1696	7/14/97
U13	B	3.8575	0.0800			7/14/97
U13	C	4.1684	0.0350			7/28/97
U14	A	3.9407	0.0882	4.0764	0.1420	7/14/97
U14	B	4.1245	0.0849			7/14/97
U14	C	4.2542	0.0778			7/28/97
U14	D	3.9862	0.0499			7/28/97
U15	A	4.3041	0.0887	4.2110	0.0824	7/14/97
U15	B	4.1476	0.0853			7/14/97
U15	C	4.1811	0.0352			7/28/97
U16	A	poor	current	3.9737	0.0603	7/14/97
U16	B	3.9153	0.0807			7/14/97
U16	C	4.0357	0.0618			7/28/97
U16	D	3.9700	0.0576			7/28/97

Appendix II-Radiocarbon Data (Moderns)

U17	A	4.6465	0.2404	4.7551	0.1590	7/14/97
U17	B	4.6811	0.0964			7/14/97
U17	C	4.9376	0.0415			7/28/97
U18	A	6.0971	0.0646	6.5613	*0.6383*	5/27/97
U18	B	7.3974	0.0677			5/27/97
U18	A	6.1087	0.1210			9/29/97
U18	B	5.8832	0.1927			9/29/97
U18	D	6.6491	0.0802			10/12/97
U18	E	7.2322	0.0729			10/12/97
U19	A	7.0690	0.1445	7.0118	0.3618	7/14/97
U19	B	poor	current			7/14/97
U19	C	7.0088	0.1686			7/28/97
U19	D	7.3237	0.0610			7/28/97
U19	E	6.3444	0.1257			9/29/97
U19	F	6.7585	0.1340			9/29/97
U19	D	7.1856	0.0638			10/12/97
U19	E	7.3927	0.0786			10/12/97
U20	A	4.6032	0.0955	4.5922	0.1935	7/14/97
U20	B	4.6176	0.0949			7/14/97
U20	C	4.6112	0.0385			7/28/97
U20	D	4.2933	0.0541			7/28/97
U20	E	4.8357	0.0494			7/28/97
U21	A	4.3629	0.0891	4.4936	0.1174	7/14/97
U21	B	4.5901	0.0935			7/14/97
U21	C	4.5277	0.0397			7/28/97
U22	A	4.4184	0.0907	4.5284	0.2293	7/14/97
U22	B	4.2489	0.1093			7/14/97
U22	C	4.7271	0.0672			7/28/97
U22	D	4.4469	0.0786			10/12/97
U22	E	4.8006	0.0803			10/12/97
U23	A	4.0923	0.0843	4.5571	*0.4143*	7/14/97
U23	B	4.1182	0.0846			7/14/97
U23	C	4.8177	0.0419			7/28/97
U23	D	4.8400	0.0483			10/12/97
U23	E	4.9175	0.0596			10/12/97
U24	A	4.4656	0.0410	4.4209	0.0633	5/27/97
U24	B	4.3761	0.0407			5/27/97
U25	A	4.2185	0.0870	4.2073	0.0158	7/14/97
U25	B	4.1961	0.0860			7/14/97
U25	C	poor	current			7/28/97
U26	A	4.4512	0.0914	4.0257	0.4185	7/14/97
U26	B	4.0115	0.0827			7/14/97
U26	C	3.6145	0.0585			7/28/97
U27	A	4.0462	0.0830	3.9403	0.0943	7/14/97
U27	B	3.8652	0.0795			7/14/97
U27	C	3.9097	0.0478			7/28/97
U28	A	4.5737	0.0933	4.5924	0.1714	7/14/97
U28	B	4.4312	0.0909			7/14/97
U28	C	4.7725	0.0419			7/28/97
U29	A	4.4892	0.0449	4.3957	0.1322	5/27/97
U29	B	4.3023	0.0355			5/27/97
U30	A	4.2622	0.0484	4.2291	0.0468	6/18/97
U30	B	4.1960	0.0475			6/18/97
U31	A	3.8551	0.0483	3.8592	0.0059	6/18/97
U31	B	3.8634	0.0427			6/18/97

Appendix II-Radiocarbon Data (Moderns)

U32	A	3.9059	0.0457	3.8994	0.0091	6/18/97
U32	B	3.8930	0.0450			6/18/97
U33	A	3.7043	0.0445	3.7043		6/18/97
U33	B	no	current			6/18/97
U34	A	4.3466	0.0503	4.3986	0.0735	6/18/97
U34	B	4.4505	0.0515			6/18/97
U35	A	3.9128	0.0453	3.8963	0.0233	6/18/97
U35	B	3.8799	0.0917			6/18/97
U36	A	4.4804	0.0636	4.5799	0.1407	6/18/97
U36	B	4.6794	0.0572			6/18/97
U37	A	4.1448	0.0496	3.8027	0.4839	6/18/97
U37	B	3.4605	0.0514			6/18/97
U38	A	3.7668	0.0448	3.7164	0.0713	6/18/97
U38	B	3.6660	0.0436			6/18/97
U39	A	3.9174	0.0466	3.9222	0.0068	6/18/97
U39	B	3.9270	0.0492			6/18/97
U40	A	3.4747	0.0413	3.6252	0.2128	6/18/97
U40	B	3.7757	0.0448			6/18/97
U41	A	2.9556	0.0431	3.1148	0.2252	6/18/97
U41	B	3.2741	0.0433			6/18/97
U42	A	2.8033	0.0439	2.8955	0.1303	6/18/97
U42	B	2.9877	0.0416			6/18/97
U43	A	3.5267	0.0468	3.4908	0.0508	6/18/97
U43	B	3.4549	0.0459			6/18/97
U44	A	3.2653	0.0444	3.0848	0.2552	6/18/97
U44	B	2.9043	0.0421			6/18/97
U45	A	3.3328	0.0441	3.3575	0.0349	6/18/97
U45	B	3.3821	0.0450			6/18/97
U46	A	3.7018	0.0509	3.8719	0.2406	6/18/97
U46	B	4.0421	0.0507			6/18/97
U47	A	2.6139	0.0291	2.7443	0.1845	6/18/97
U47	B	2.8747	0.0256			6/18/97
U48	A	2.6712	0.0307	2.5551	0.1642	6/18/97
U48	B	2.4390	0.0411			6/18/97
U49	A	2.1549	0.1070	2.3471	0.2717	6/18/97
U49	B	2.5392	0.0291			6/18/97
U50	A	2.7656	0.0342	2.8860	0.1703	6/18/97
U50	B	3.0064	0.0292			6/18/97
U51	A	3.0719	0.0427	3.0684	0.0049	6/18/97
U51	B	3.0650	0.0332			6/18/97
U52	A	3.2501	0.0386	3.3579	0.1525	6/18/97
U52	B	3.4657	0.0411			6/18/97
U53	A	2.7157	0.0376	2.9125	0.2783	6/18/97
U53	B	3.1092	0.0369			6/18/97
U54	A	3.3290	0.0395	3.3845	0.0786	6/18/97
U54	B	3.4401	0.0409			6/18/97
U55	A	2.9171	0.0365	2.9417	0.0349	6/18/97
U55	B	2.9664	0.0394			6/18/97
U56	A	2.7549	0.0382	2.7819	0.0382	6/18/97
U56	B	2.8089	0.0437			6/18/97
U57	A	2.7027	0.0339	2.7384	0.0505	6/18/97
U57	B	2.7741	0.0347			6/18/97
U58	A	2.6980	0.0338	2.8243	0.1786	6/18/97
U58	B	2.9506	0.0405			6/18/97
U59	A	1.7589	0.0298	1.8244	0.0673	9/29/97

Appendix II-Radiocarbon Data (Moderns)

U59	B	1.8934	0.0321			9/29/97
U59	C	1.8209	0.0263			9/29/97
U60	A	1.8737	0.0247	1.8473	0.0387	9/29/97
U60	B	1.8029	0.0335			9/29/97
U60	C	1.8654	0.0213			9/29/97
U61	A	1.8302	0.0241	1.7977	0.0313	9/29/97
U61	B	1.7952	0.0241			9/29/97
U61	C	1.7678	0.0286			9/29/97
U62	A	1.7715	0.0234	1.7492	0.0541	9/29/97
U62	B	1.6875	0.0225			9/29/97
U62	C	1.7886	0.0253			9/29/97
FECES						
F0	A	1.1378	0.0204	1.1247	0.0319	3/3/97
F0	B	1.1601	0.0205			3/3/97
F0	C	1.1258	0.0285			3/10/97
F0	D	1.0734	0.0294			3/10/97
F0	E	1.1264	0.0200			3/10/97
F1	A	79.9755	0.8315	84.4337	3.5446	3/3/97
F1	B	85.1443	0.8792			3/3/97
F1	C	88.4429	1.2861			3/10/97
F1	D	81.6790	0.8551			3/10/97
F1	E	86.9265	0.6658			3/10/97
F2	A	56.8834	0.5916	63.0700	8.8154	3/3/97
F2	B	48.4194	0.7017			3/3/97
F2	C	68.3159	0.6962			3/10/97
F2	D	68.5271	0.5346			3/10/97
F2	F	64.4634	0.6805			3/24/97
F2	G	71.8105	0.5591			3/24/97
F2	E	*36.1668*	0.3800			3/10/97
F3	A	5.2040	0.0661	5.2519	0.4509	3/3/97
F3	B	5.0120	0.0789			3/3/97
F3	C	5.6727	0.0487			3/10/97
F3	D	4.6527	0.0695			3/10/97
F3	E	5.7179	0.0459			3/10/97
F4	A	5.0209	0.0616	5.3858	0.2857	3/10/97
F4	B	5.4325	0.0511			3/10/97
F4	C	broke				3/10/97
F4	D	5.3733	0.0573			3/24/97
F4	E	5.7165	0.0491			3/24/97
F5	A	3.2263	0.0444	3.2027	0.0222	3/10/97
F5	B	3.1996	0.0424			3/10/97
F5	C	3.1823	0.0247			3/10/97
F6	A	3.1707	0.0439	3.0809	0.1434	3/10/97
F6	B	2.9155	0.0314			3/10/97
F6	C	3.1565	0.0344			3/10/97
F7	A	2.3437	0.0297	2.3421	0.0363	3/10/97
F7	B	2.3051	0.0270			3/10/97
F7	C	2.3776	0.0267			3/10/97
F8	A	2.6571	0.0256	2.6449	0.0313	3/10/97
F8	B	2.6682	0.0289			3/10/97
F8	C	2.6093	0.0386			3/10/97
F9	A	2.3468	0.0374	2.2047	0.2718	3/24/97
F9	B	2.3761	0.0237			3/24/97
F9	C	1.8913	0.0247			3/24/97

Appendix II-Radiocarbon Data (Moderns)

F10	A	1.9832	0.0286	2.0478	0.0780	3/24/97
F10	B	2.0257	0.0323			3/24/97
F10	C	2.1345	0.0213			3/24/97
F11	A	1.8374	0.0184	1.8610	0.0333	3/24/97
F11	B	error	error			3/24/97
F11	C	1.8845	0.0295			3/24/97
F12	A	1.9027	0.1324	1.9702	0.0706	3/24/97
F12	B	1.9645	0.0185			3/24/97
F12	C	2.0435	0.0190			3/24/97
F13	A	2.2659	0.0237	2.3730	0.1394	4/28/97
F13	B	2.3224	0.0377			4/28/97
F13	C	2.5306	0.0369			4/28/97
F14	A	2.3400	0.0293	2.3495	0.1061	4/28/97
F14	B	2.4601	0.0310			4/28/97
F14	C	2.2485	0.0298			4/28/97
F15	A	2.4569	0.0321	2.1959	0.2374	4/28/97
F15	B	1.9929	0.0282			4/28/97
F15	C	2.1378	0.0336			4/28/97
F16	A	2.0430	0.0267	2.0292	0.0166	4/28/97
F16	B	2.0108	0.0462			4/28/97
F16	C	2.0338	0.0266			4/28/97
F17	A	1.7656	0.0278	1.8067	0.0644	5/12/97
F17	B	1.7736	0.0310			5/12/97
F17	C	1.8810	0.0206			5/12/97
F18	A	1.8870	0.0393	1.8554	0.0441	5/12/97
F18	B	1.8050	0.0183			5/12/97
F18	C	1.8743	0.0207			5/12/97
F19	A	1.8068	0.0209	1.6864	0.1104	5/12/97
F19	B	1.5900	0.0326			5/12/97
F19	C	1.6624	0.0299			5/12/97
F20	A	1.6245	0.0183	1.6342	0.0231	5/12/97
F20	B	1.6175	0.0163			5/12/97
F20	C	1.6606	0.0217			5/12/97
F21	A	1.6716	0.0171	1.6787	0.0068	5/12/97
F21	B	1.6851	0.0157			5/12/97
F21	C	1.6793	0.0217			5/12/97
F22	A	1.6311	0.0183	1.8190	0.3132	5/12/97
F22	B	2.1806	0.0298			5/12/97
F22	C	1.6454	0.0153			5/12/97
F23	A	1.5675	0.0178	1.5858	0.0356	5/12/97
F23	B	1.5631	0.0147			5/12/97
F23	C	1.6268	0.0223			5/12/97
F24	A	1.5978	0.0180	1.6805	0.0150	5/12/97
F24	B	1.5800	0.0179			5/12/97
F24	B	1.5680	0.0143			5/27/97
F24	D	1.9762	0.0193			6/9/97
F25	A	1.6422	0.0138	1.5389	0.1139	5/27/97
F25	B	1.4488	0.0258			5/27/97
F25	C	1.4321	0.0242			5/27/97
F25	D	1.6323	0.0160			6/9/97
F26	A	1.6667	0.0140	1.7626	0.0675	5/27/97
F26	C	1.5713	0.0216			5/27/97
F26	D	1.9926	0.0208			6/9/97
F26	E	1.8200	0.0284			6/9/97
F27	A	1.6814	0.0122	1.6674	0.0167	5/27/97

Appendix II-Radiocarbon Data (Moderns)

F27	B	1.6720	0.0140			5/27/97
F27	C	1.6489	0.0223			5/27/97
F28	A	1.5855	0.0212	1.6015	0.0926	6/9/97
F28	B	1.7010	0.0163			6/9/97
F28	C	1.5179	0.0305			6/9/97
F29	A	1.7278	0.0168	1.7224	0.0151	6/9/97
F29	B	1.7054	0.0268			6/9/97
F29	C	1.7341	0.0159			6/9/97
F30	A	1.6076	0.0148	1.6167	0.0568	6/9/97
F30	B	1.6774	0.0154			6/9/97
F30	C	1.5650	0.0144			6/9/97
F31	A	1.6166	0.0148	1.6530	0.0401	6/9/97
F31	B	1.6465	0.0151			6/9/97
F31	C	1.6959	0.0163			6/9/97
F32	A	1.6222	0.0161	1.6078	0.0139	6/9/97
F32	B	1.5945	0.0240			6/9/97
F32	C	1.6068	0.0158			6/9/97
F33	A	2.1613	0.0314	1.8942	0.3777	6/9/97
F33	C	1.6271	0.0260			6/9/97
F34	A	1.5697	0.0177	1.5848	0.0282	8/11/97
F34	B	1.5796	0.0270			8/11/97
F34	C	1.5468	0.0175			8/11/97
F34	A	1.5912	0.0173			6/23/97
F34	B	1.5898	0.0235			6/23/97
F34	C	1.6317	0.0137			6/23/97
F35	A	1.2370	0.0170	1.2231	0.0135	9/29/97
F35	B	1.2224	0.0168			9/29/97
F35	C	1.2100	0.0167			9/29/97
F36	B	*1.5500*	0.0251	1.2546	0.0337	9/29/97
F36	A	1.2337	0.0169			9/29/97
F36	C	1.2180	0.0207			9/29/97
F36	D	1.1515	0.0113			10/12/97
F36	E	1.2030	0.0117			10/12/97
F36	F	1.1712	0.0115			10/12/97
F37	A	1.2101	0.0206	1.1901	0.0195	9/29/97
F37	B	1.1891	0.0202			9/29/97
F37	C	1.1711	0.0199			9/29/97
F38	A	1.1811	0.0201	1.1714	0.0225	9/29/97
F38	B	1.1457	0.0195			9/29/97
F38	C	1.1875	0.0202			9/29/97

Appendix III-Total Folate Data - Plasma

ID	folate 1 (ng/mL)	folate 2 (ng/mL)	folate 3 (ng/mL)	mean (ng/mL)	mean (pmol/mL)	S.D.
P0	7.46	10.80	7.28	8.51	19.29	4.49
P1	9.32	14.47	11.86	11.88	26.92	5.83
P2	10.07	14.30	14.76	13.04	29.55	5.86
P3	8.8	14.95	10.53	11.43	25.89	7.19
P4	9.95	16.73	12.94	13.21	29.92	7.70
P5	9.47	14.18	12.33	11.99	27.17	5.38
P6	11.41	15.14	12.78	13.11	29.70	4.27
P7	11.93	11.34	13.77	12.35	27.97	2.87
P8	10.53	12.00	11.41	11.31	25.63	1.68
P9	11.62	15.74	14.76	14.04	31.81	4.88
P10	12.32	15.63	12.69	13.55	30.69	4.11
P11	12.79	16.32	15.12	14.74	33.40	4.07
P12	13.19	14.52	14.95	14.22	32.22	2.08
P13	10.05	17.03	10.03	12.37	28.02	9.14
P14	8.39	16.80	12.19	12.46	28.23	9.54
P15	7.96	14.97	11.47	11.47	25.98	7.94
P16	10.28	13.96	11.40	11.88	26.91	4.27
P17	8.87	14.01	14.21	12.36	28.01	6.86
P18	7.81	11.55	9.91	9.76	22.10	4.25
P19	6.32	9.52	9.25	8.36	18.95	4.02
P20	5.72	12.37	7.61	8.57	19.41	7.76
P21	6.79	11.87	7.56	8.74	19.80	6.20
P22	4.45	9.11	6.83	6.80	15.40	5.28
P23	5.21	8.32	6.53	6.69	15.15	3.54
P24	6.94	9.95	10.57	9.15	20.74	4.40
P25	8.48	13.96	10.63	11.02	24.97	6.26
P26	7.03	10.24	9.68	8.98	20.35	3.88
P27	7.16	5.54	9.00	7.23	16.39	3.92
P28	6.68	9.09	5.03	6.93	15.71	4.63
P29	5.99	9.46	2.92	6.12	13.87	7.41
P30	3.82	5.60	2.39	3.94	8.92	3.64
P31	10.70	7.27	9.62	9.20	20.84	3.97
P32	11.09	8.50	10.43	10.01	22.67	3.05
P33	12.55	7.45	6.03	8.68	19.66	7.77
P34	11.38	8.58	11.11	10.36	23.46	3.50
P35	10.12	10.31	8.69	9.71	21.99	2.01
P36	12.42	13.27	15.78	13.82	31.32	3.96
P37	9.51	10.48	16.08	12.02	27.24	8.03
P38	17.46	13.75	15.10	15.44	34.97	4.25
P39	8.10	9.54	8.24	8.63	19.54	1.80
P40	10.28	9.80	8.82	9.63	21.82	1.69
P41	12.10	10.40	9.60	10.70	24.24	2.89
P42	12.08	11.60	10.69	11.46	25.96	1.60
P43	14.90	15.90	10.93	13.91	31.51	5.96
P44	14.59	14.94	11.58	13.70	31.05	4.18
P45	13.36	10.69	6.82	10.29	23.31	7.45
P46	10.74	10.53	11.83	11.03	25.00	1.58
P47	15.84	9.84	20.05	15.24	34.53	11.62
P48	14.67	9.78	11.83	12.09	27.40	5.56
P49		11.38	10.23	10.81	24.48	1.84
P50		16.61	14.69	15.65	35.46	3.08
P51		18.31	14.69	16.50	37.38	5.80
P52		15.02	16.89	15.96	36.15	3.00
P53		10.37	10.19	10.28	23.29	0.29
P54		11.44	12.32	11.88	26.91	1.41
P55		11.25	9.79	10.52	23.83	2.34
P56		11.45	13.36	12.41	28.10	3.06
P57		11.39	11.87	11.63	26.35	0.77
P58		10.06	13.79	11.93	27.02	5.98

Appendix III-Total Folate Data - Red blood cells

ID	folate1 (ng/g Hb)	folate2 (ng/g Hb)	folate 3 (ng/g Hb)	mean (ng/g Hb)	mean (nmol/g Hb)	S.D.
R0	3.37	1.79	1.33	2.16	4.90	2.43
R1	2.81	2.22	1.90	2.31	5.24	1.05
R2	3.19	1.58	1.29	2.02	4.58	2.32
R3	2.31	2.18	1.83	2.11	4.77	0.55
R4	3.45	3.41	2.75	3.21	7.26	0.89
R5	1.96	2.35	1.78	2.03	4.60	0.67
R6	4.78	2.54	2.53	3.28	7.44	2.94
R7	4.24	2.65	2.06	2.98	6.76	2.55
R8	3.10	2.67	2.36	2.71	6.14	0.84
R9	2.18	2.76	2.21	2.38	5.40	0.75
R10	2.78	2.06	1.61	2.15	4.87	1.34
R11	2.73	2.36	1.92	2.34	5.29	0.92
R12	2.73	2.37	2.03	2.38	5.39	0.80
R13	2.38	2.09	2.15	2.21	5.01	0.35
R14	2.23	2.16	2.05	2.15	4.87	0.21
R15	2.11	2.98	2.17	2.42	5.48	1.10
R16	1.58	2.13	1.70	1.80	4.08	0.66
R17	2.91	3.10	2.52	2.84	6.44	0.67
R18	1.34	2.94	2.60	2.29	5.19	1.91
R19	1.21	2.92	2.63	2.26	5.11	2.07
R20	1.00	1.93	1.96	1.63	3.69	1.24
R21	1.02	2.19	2.31	1.84	4.17	1.62
R22	1.54	2.90	2.87	2.44	5.52	1.76
R23	2.12	2.31	2.11	2.18	4.94	0.25
R24	2.51	2.06	1.85	2.14	4.85	0.76
R25	1.17	3.15	1.64	1.99	4.50	2.35
R26	2.35	3.66	2.71	2.91	6.59	1.53
R27	2.29	1.69	1.09	1.69	3.83	1.35
R28	1.78	2.25	1.55	1.86	4.21	0.81
R29	2.53	3.80	2.86	3.06	6.94	1.49
R30	2.97	2.03		2.50	5.67	1.50
R31	2.36	2.25	2.11	2.24	5.08	0.29
R32		2.07	2.58	2.32	5.27	0.81
R33		2.00	2.71	2.36	5.34	1.13
R34		2.08	2.48	2.28	5.17	0.64
R35		1.90	1.66	1.78	4.04	0.39
R36		1.79	2.21	2.00	4.53	0.67
R37		2.00	1.49	1.74	3.95	0.83
R38		1.99	1.44	1.71	3.88	0.89
R39		2.76	2.56	2.66	6.03	0.33
R40		3.44	3.20	3.32	7.53	0.39
R41		2.46	2.71	2.58	5.85	0.40
R42		2.80	4.45	3.63	8.22	2.64
R43		2.36	4.01	3.19	7.22	2.64
R44		1.95	3.78	2.87	6.50	2.92
R45		3.11	3.98	3.55	8.04	1.40
R46		2.76	4.04	3.40	7.71	2.05
R47		2.93	3.69	3.31	7.51	1.22
R48		2.92	4.34	3.63	8.22	2.28
R49		2.89	4.02	3.46	7.83	1.81
R50		2.90	2.54	2.72	6.17	0.58
R51		2.62	2.35	2.48	5.63	0.43
R52		3.13	2.55	2.84	6.43	0.93
R53		2.97	4.29	3.63	8.22	2.11
R54		3.58	4.41	4.00	9.05	1.32
R55		2.56	3.99	3.28	7.42	2.30
R56		2.46	4.67	3.57	8.08	3.54
R57		3.51	4.59	4.05	9.18	1.74
R58		3.04	4.84	3.94	8.93	2.89

Appendix III-Total Folate Data - Urine

ID	folate 1 (ng/mL)	folate 2 (ng/mL)	folate 3 (ng/mL)	mean (ng/mL)	mean (pmol/mL)	S.D.
U0	39.54	38.16	41.99	39.90	90.39	6.17
U1	0.96	0	0	0.32	0.72	0.40
U2	1.91	0	0	0.64	1.44	0.40
U3	3.72	0	0	1.24	2.81	0.40
U4	1.34	0	0	0.45	1.01	0.40
U5	8.82	6.87	5.03	6.91	15.65	5.88
U6	8.1	6.38	4.72	6.40	14.50	5.68
U7	2.93	0.71	0.52	1.39	3.14	4.03
U8	7.74	2.12	1.96	3.94	8.93	8.24
U9	12.02	9.85	6.89	9.59	21.72	6.43
U10	12.03	9.95	6.7	9.56	21.66	10.82
U11	31.99	19.34	12.04	21.12	47.86	31.64
U12	56.67	29.15	23.38	36.40	82.46	44.54
U13	7.91	3.76	3.28	4.98	11.29	15.65
U14	9.92	2.09	1.79	4.60	10.42	10.72
U15	5.78	4.29	3.36	4.48	10.14	3.85
U16	7.32	3.18	2.54	4.35	9.85	9.82
U17	13.93	12.53	7.19	11.22	25.41	11.33
U18	43.38	76.15	89.62	69.72	157.94	97.37
U19	128.8	205.6	248.6	194.33	440.27	221.78
U20	9.95	15.48	11.49	12.31	27.88	12.32
U21	6.97	1.96	1.57	3.50	7.93	7.89
U22	1.64	4.16	4.75	3.52	7.97	3.60
U23	21.32	9.84	10.75	13.97	31.65	14.38
U24	4.6	5.77	4.7	5.02	11.38	3.03
U25	1.46	2.73	2.37	2.19	4.95	2.21
U26	7	11.42	8.76	9.06	20.53	7.22
U27	2.41	8.64	5.65	5.57	12.61	18.42
U28	5.6	9.2	10.32	8.37	18.97	11.67
U29	5.46	11.62	11.25	9.44	21.39	11.47
U30	5.59	4.15	3.63	4.46	10.10	2.10
U31	7.86	5.97	6.24	6.69	15.16	2.51
U32	6.84	13.1	9.53	9.82	22.25	12.66
U33	56.5	55.56	49.84	53.97	122.26	18.40
U34	6.35	14.91	13.45	11.57	26.21	14.82
U35	7.2	4.41	3.42	5.01	11.35	5.09
U36	51.3	20.62	17.4	29.77	67.45	42.43
U37	8.06	4.19	2.99	5.08	11.51	5.39
U38	8.33	12.52	9.14	10.00	22.65	7.79
U39	3.89	1.78	1.51	2.39	5.42	4.70
U40	1.03	2.33	2.06	1.81	4.09	2.23
U41	4.97	4.74	3.08	4.26	9.66	2.79
U42	3.73	5.5	2.27	3.83	8.68	5.63
U43	1.49	3.83	3.25	2.86	6.47	4.17
U44	3.71	4.37	4.35	4.14	9.39	1.30
U45	4.09	4.54	5.22	4.62	10.46	2.04
U46	13.64	16.77	11.78	14.06	31.86	7.21
U47	8.16	2.94	2.19	4.43	10.04	8.02
U48	10.28	5.47	2.96	6.24	14.13	9.20
U49	5.38	2.01	1.42	2.94	6.65	7.46
U50	3.68	1.47	1.31	2.15	4.88	5.76
U51	9.2	2.71	1.99	4.63	10.50	14.97
U52	38.32	31.4	20.03	29.92	67.78	28.49
U53	43.47	55.6	44.27	47.78	108.25	23.94
U54	67.09	118.1	91.41	92.20	208.88	110.62
U55	12.64	3.55	2.68	6.29	14.25	22.46
U56	9.35	11.93	5.89	9.06	20.52	15.48
U57	8.99	3.31	3.92	5.41	12.25	6.93
U58	11.07	4.12	3.31	6.17	13.97	9.44
U59		3.22	1.62	2.42	5.48	3.62
U60		4.72	2.49	3.61	8.17	4.46
U61		11.77	4.67	8.22	18.62	20.44
U62		21.99	12.03	17.01	38.54	25.93

Appendix III-Total Folate Data - Feces

ID	folate 1 (ng/mL)	folate 2 (ng/mL)	folate 3 (ng/mL)	mean (ng/mL)	mean (nmol/mL)	S.D.
F0	253.9	106.0	77.78	145.89	0.331	0.214
F1	187.3	104.9	100.2	130.80	0.296	0.111
F2	367.4	271.3	196.4	278.37	0.631	0.194
F3	344.3	146.6	96	195.63	0.443	0.297
F4	261.9	92.2	58.64	137.59	0.312	0.247
F5	152.7	120.1	106.90	126.57	0.287	0.053
F6	431	207.5	133.5	257.33	0.583	0.351
F7	301.9	191.0	100.3	197.73	0.448	0.229
F8	290.2	342.2	215.9	282.77	0.641	0.144
F9	329.2	277.6	175.3	260.70	0.591	0.177
F10	430.6	357.6	265.2	351.13	0.795	0.188
F11	222.6	191.4	109.2	174.40	0.395	0.133
F12	419.2	380.7	286.8	362.23	0.821	0.154
F13	342.2	222.9	115.4	226.83	0.514	0.257
F14	380.1	229.6	95.5	235.07	0.533	0.323
F15	402.8	287.2	222.5	304.17	0.689	0.207
F16	443.0	250.5	199.3	297.60	0.674	0.291
F17	280.9	100.5	31.4	137.60	0.312	0.292
F18	414.2	348.4	236.8	333.13	0.755	0.203
F19	254.8	263.2	234.2	250.73	0.568	0.034
F20	272.6	329.4	301.3	301.10	0.682	0.064
F21	262.9	150.3	86.8	166.67	0.378	0.202
F22	347.7	304.4	158.9	270.33	0.612	0.224
F23	293.4	229.7	183.1	235.40	0.533	0.125
F24	334.3	296.7	354.5	328.50	0.744	0.066
F25	213.8	228.1	247.7	229.87	0.521	0.039
F26	265.2	218.0	221.1	234.77	0.532	0.060
F27	235.3	174.7	155	188.33	0.427	0.095
F28	375.4	245.1	184.1	268.20	0.608	0.221
F29	394.6	323.5	184.4	300.83	0.682	0.242
F30	440.7	269.6	201.90	304.07	0.689	0.279
F31	435.7	371.8	217.90	341.80	0.774	0.254
F32	446.3	295.2	105.10	282.20	0.639	0.387
F33	417.3	308.7	242.50	322.83	0.731	0.200
F34	472.2	354.2	203.90	343.43	0.778	0.305
F35		438.7	415.40	427.05	0.967	0.037
F36		216.2	178.40	197.30	0.447	0.061
F37		428.9	415.70	422.30	0.957	0.021
F38		312.7	274.80	293.75	0.665	0.061

Appendix IV-Calculations for Plasma

Sample	Day	Modern	% Carbon	14C-FA per mL plasma (fmol)	S.D. (fmol/mL)
P0	0.000	1.0986	4.29	0.00	0.00
P1	0.007	1.4180	4.44	69.84	1.00
P2	0.016	2.1278	4.49	227.63	2.53
P3	0.025	2.6242	4.24	318.99	2.28
P4	0.035	2.8869	4.28	377.25	0.50
P5	0.043	3.0623	4.47	432.50	3.22
P6	0.058	2.9019	4.61	409.82	19.91
P7	0.074	3.1218	4.38	436.42	9.32
P8	0.085	3.1381	4.53	455.18	8.14
P9	0.102	2.8664	4.83	420.47	24.94
P10	0.123	3.0426	4.51	432.00	15.08
P11	0.142	2.9428	4.31	392.02	3.94
P12	0.162	2.9002	4.27	379.24	7.68
P13	0.183	2.7992	4.37	366.29	8.06
P14	0.204	2.7446	4.34	351.85	2.74
P15	0.225	2.6178	4.33	324.35	3.11
P16	0.267	2.6030	4.36	323.41	5.39
P17	0.308	2.4172	4.33	281.64	0.98
P18	0.352	2.2015	4.43	240.70	3.12
P19	0.432	2.0439	4.31	200.89	3.06
P20	0.500	2.0449	4.36	203.40	11.93
P21	0.622	1.8132	4.24	149.14	2.74
P22	0.742	1.6402	4.23	112.87	2.65
P23	0.867	1.6121	3.97	100.47	0.72
P24	0.992	1.5534	4.31	96.62	3.12
P25	1.193	1.5352	4.41	94.84	1.44
P26	1.50	1.4758	4.60	85.50	4.74
P27	2	1.3652	4.32	56.69	1.64
P28	3	1.3752	4.74	64.57	1.15
P29	4	1.3147	4.26	45.32	0.47
P30	5	1.2417	4.15	29.23	0.55
P31	8	1.2506	4.33	32.42	0.55
P32	12	1.2350	4.37	29.37	0.36
P33	15	1.1899	4.29	19.30	0.24
P34	19	1.2016	4.39	22.28	0.34
P35	22	1.2703	4.42	37.42	0.58
P36	25	1.2391	4.63	32.02	0.56
P37	29		4.39		
P38	33		4.50		
P39	40	1.2142	4.52	25.77	1.68
P40	47		4.49		
P41	54		4.65		
P42	61	1.1680	4.40	15.03	0.03
P43	67		4.59		
P44	74		4.40		
P45	96	1.1545	4.47	12.31	0.13
P46	103	1.2018	4.45	22.61	1.65
P47	110	1.1480	4.56	11.09	0.08
P48	117	1.1208	4.50	4.93	0.21
P49	124	1.1478	4.44	10.77	0.21
P50	130	1.1813	4.38	17.86	0.15
P51	139	1.1310	4.56	7.28	0.01
P52	145	1.1759	4.53	17.25	0.74
P53	152	1.1196	4.52	4.68	0.03
P54	159	1.1225	4.55	5.36	0.19
P55	166	1.1200	4.38	4.61	0.05
P56	173	1.1035	4.46	1.07	0.01
P57	187	1.1153	4.38	3.60	0.08
P58	201	1.0946	4.55	-0.89	-0.02

Appendix V-Calculations for Red blood cells

Sample	Day	Modern	% C	Hb g / mL RBC	14C-folate fmol / g Hb	S.D.
R0	0.00	1.1137	7.07	0.137	0.0	69.7
R1	0.01	1.1525	5.23	0.090	113.6	120.0
R2	0.02	1.1585	5.07	0.086	132.8	33.4
R3	0.03	1.1459	5.75	0.098	95.5	28.0
R4	0.03	1.1480	4.89	0.084	102.0	66.9
R5	0.04	1.1535	5.99	0.104	114.2	11.8
R6	0.06	1.1624	5.41	0.093	139.7	34.3
R7	0.07	1.1631	5.01	0.086	145.0	0.2
R8	0.09	1.1714	4.93	0.085	166.1	0.0
R9	0.10	1.1418	4.99	0.086	81.4	38.4
R10	0.12	1.1657	5.63	0.096	150.6	44.7
R11	0.14	1.1505	4.67	0.084	102.5	21.9
R12	0.16	1.1588	5.74	0.096	130.4	83.8
R13	0.18	1.1395	4.96	0.087	76.7	16.8
R14	0.20	1.1807	4.46	0.076	199.4	65.4
R15	0.23	1.1465	5.01	0.087	93.3	63.9
R16	0.27	1.1456	5.34	0.091	90.5	49.2
R17	0.31	1.1460	4.58	0.077	94.7	26.1
R18	0.35	1.1347	5.28	0.091	61.9	21.4
R19	0.43	1.1244	5.56	0.094	30.9	29.8
R20	0.50	1.1560	5.80	0.103	119.6	101.8
R21	0.62	1.1723	5.27	0.088	173.7	0.0
R22	0.74	1.1338	4.40	0.076	58.3	3.7
R23	0.87	1.1507	5.17	0.079	119.9	16.8
R24	0.99	1.1259	5.97	0.101	35.1	16.8
R25	1.19	1.1526	5.55	0.093	113.6	44.6
R26	1.50	1.1278	4.72	0.078	41.2	30.7
R27	1.99	1.1229	6.95	0.119	26.9	97.1
R28	2.99	1.1210	6.63	0.113	21.4	11.9
R29	3.98	1.1993	5.41	0.093	252.6	60.7
R30	4.96	1.2933	5.69	0.098	529.7	108.4
R31	7.98	1.4246	6.01	0.088	1040.5	10.9
R32	11.98	1.5313	7.89	0.137	1228.8	51.2
R33	14.97	1.5608	6.41	0.110	1316.8	89.8
R34	19.00	1.6726	7.97	0.136	1650.9	143.9
R35	21.99	1.6240	7.52	0.130	1492.7	47.5
R36	25.19	1.6568	10.01	0.169	1627.6	37.0
R37	28.98	1.6610	12.61	0.210	1650.1	238.1
R38	33.24	1.6883	8.97	0.152	1699.0	295.4
R39	40.19	1.6940	8.68	0.149	1723.4	177.9
R40	47.20	1.6462	9.27	0.151	1558.0	45.8
R41	54.20	1.5601	7.80	0.133	1575.2	76.0
R42	61.19	1.6028	8.30	0.143	1339.2	92.5
R43	67.37	1.5293	9.75	0.165	1057.0	69.3
R44	74.23	1.6004	9.39	0.159	1519.3	96.4
R45	96.23	1.5414	7.83	0.132	1505.2	54.9
R46	103.23	1.6016	8.36	0.142	1333.1	133.9
R47	110.23	1.4933	7.53	0.127	1234.1	26.1
R48	117.35	1.4553	7.79	0.135	942.5	42.9
R49	124.36	1.4116	7.29	0.120	953.3	17.0
R50	130.35	1.4133	8.75	0.153	708.9	16.7
R51	139.35	1.3742	10.62	0.141	802.5	107.5
R52	145.36	1.3397	8.64	0.155	765.2	30.9
R53	152.35	1.2976	8.97	0.159	493.8	21.9
R54	159.37	1.2880	7.63	0.127	609.9	39.6
R55	166.35	1.2692	8.71	0.144	408.0	96.1
R56	173.36	1.2505	8.95	0.130	454.2	73.4
R57	187.37	1.2202	7.87	0.110	427.8	146.9
R58	201.36	1.2229	9.83	0.123	346.1	3.8

Appendix VI-Calculations for Urine

Sample	Day	Modern	Mass (g)	% C	14C-FA pmol	S.D.	Cumulative 14C-FA	Cumulative S.D.
U0	0	1.1657	1403.0	0.471	0.00	0.0	0.0	0.0
U1	0.25	31.6966	756.1	0.333	379.97	10.5	380.0	10.5
U2	0.50	10.2944	281.5	0.916	116.46	7.2	496.4	17.7
U3	0.75	8.3004	234.4	0.885	73.26	6.5	569.7	24.2
U4	1	7.6853	772.1	0.265	65.96	4.6	635.7	28.8
U5	2	5.8687	1368.6	0.588	187.18	6.3	822.8	35.1
U6	3	4.4984	1484.4	0.439	107.52	1.9	930.4	37.0
U7	4	4.4061	1327.5	0.702	149.34	3.8	1079.7	40.8
U8	5	3.9608	1104.3	0.899	137.39	11.2	1217.1	52.1
U9	6	4.1438	1101.9	0.953	154.69	16.4	1371.8	68.5
U10	7	4.1560	1777.4	0.490	128.77	6.0	1500.6	74.4
U11	8	4.5597	1383.6	0.742	172.43	22.5	1673.0	97.0
U12	9	6.2084	1105.2	0.957	263.94	18.0	1936.9	114.9
U13	10	3.9737	2713.3	0.366	137.89	8.6	2074.8	123.5
U14	11	4.0764	1026.6	0.982	145.27	6.9	2220.1	130.4
U15	12	4.2110	1392.1	0.682	143.08	3.9	2363.2	134.3
U16	13	3.9737	1670.2	0.586	136.00	2.8	2499.2	137.1
U17	14	4.7551	1405.8	0.596	148.78	6.1	2647.9	143.2
U18	15	6.5613	1807.2	0.570	275.18	32.2	2923.1	175.4
U19	16	7.0118	1613.0	0.647	302.10	19.4	3225.2	194.8
U20	17	4.5922	1905.7	0.486	157.17	5.8	3382.4	200.6
U21	18	4.4936	1156.6	0.863	164.46	5.7	3546.8	206.3
U22	19	4.5284	963.3	1.019	163.39	11.5	3710.2	217.9
U23	20	4.5571	994.4	1.095	182.72	22.5	3892.9	240.4
U24	21	4.4209	2059.0	0.491	163.01	3.3	4056.0	243.6
U25	22	4.2073	1490.0	0.684	153.50	0.8	4209.5	244.5
U26	23	4.0257	1432.8	0.634	128.64	19.3	4338.1	263.8
U27	24	3.9403	2609.0	0.409	146.57	5.3	4484.7	269.1
U28	25	4.5924	2088.1	0.496	175.69	9.4	4660.4	278.5
U29	26	4.3957	1466.0	0.673	157.78	6.4	4818.1	284.8
U30	27	4.2291	914.0	1.183	163.92	2.5	4982.1	287.3
U31	28	3.8592	1082.5	0.881	127.20	0.3	5109.3	287.6
U32	29	3.8994	1779.6	0.532	128.04	0.5	5237.3	288.0
U33	30	3.7043	2253.2	0.423	119.65	0.0	5357.0	288.0
U34	31	4.3986	1428.5	0.631	144.21	3.2	5501.2	291.2
U35	32	3.8963	1147.2	0.959	148.61	1.2	5649.8	292.5
U36	33	4.5799	1000.9	1.017	171.93	7.3	5821.7	299.8
U37	34	3.8027	897.2	1.093	127.94	23.1	5949.6	322.9
U38	35	3.7164	1548.1	0.688	134.55	3.8	6084.2	326.7
U39	36	3.9222	1592.2	0.586	127.19	0.3	6211.4	327.0
U40	37	3.6252	1431.8	0.711	123.83	10.5	6335.2	337.5
U41	38	3.1148	1192.6	0.983	113.14	12.8	6448.4	350.4
U42	39	2.8955	1536.0	0.801	105.26	7.9	6553.6	358.3
U43	40	3.4908	1509.0	0.773	134.27	2.9	6687.9	361.2
U44	41	3.0848	1532.7	0.777	113.11	14.6	6801.0	375.9
U45	42	3.3575	1579.7	0.778	133.35	2.1	6934.3	377.9
U46	63	3.8719	1261.8	0.687	116.10	10.3		
U47	64	2.7443	1088.9	1.003	85.30	9.7		
U48	65	2.5551	1091.6	1.016	76.27	9.0		
U49	66	2.3471	1540.9	0.735	66.24	15.3		
U50	67	2.8860	1919.7	0.516	84.32	8.0		
U51	68	3.0684	1663.8	0.609	95.42	0.2		
U52	69	3.3579	1361.6	0.671	99.18	7.0		
U53	70	2.9125	1557.4	0.655	88.17	13.9		
U54	71	3.3845	1913.8	0.521	109.54	3.8		
U55	72	2.9417	1796.9	0.489	77.16	1.7		
U56	73	2.7819	2254.0	0.375	67.68	1.8		
U57	74	2.7384	981.6	1.099	83.95	2.7		
U58	75	2.8243	976.9	1.110	89.03	9.7		
U59	174	1.8244	1414.0	0.737	33.97	3.5		
U60	175	1.8473	1248.0	0.742	31.24	1.8		
U61	176	1.7977	1797.0	0.293	16.47	0.8		
U62	177	1.7492	1625.0	0.716	33.60	3.1		

Appendix VII-Calculations for Feces

Sample	Days	Modern	Mass of collection (g)	KOH added (mL)	Total sample mass (g)	% Carbon	14C-folate in collection (nmol)	S.D.	cumulative 14C-folate losses (nmol)	cumulative S.D.
F0	0.00	1.1247	154.4	1400	1554.4	0.965	0.000	0.002	0.000	0.002
F1	1.04	84.4337	144.5	1000	1144.5	1.003	4.714	0.201	4.714	0.203
F2	3.05	63.0700	222.6	1000	1222.6	1.132	4.223	0.601	8.937	0.804
F3	4.10	5.2519	180.3	1000	1180.3	1.125	0.270	0.030	9.207	0.030
F4	5.01	5.3858	144.2	1000	1144.2	0.873	0.210	0.014	9.417	0.044
F5	6.45	3.2027	120.4	1000	1120.4	0.938	0.108	0.001	9.524	0.045
F6	7.97	3.0809	189.8	1000	1189.8	1.088	0.125	0.009	9.649	0.054
F7	8.99	2.3421	259.9	1000	1259.9	1.023	0.077	0.002	9.726	0.056
F8	11.11	2.6449	233.3	1000	1233.3	1.202	0.111	0.002	9.838	0.058
F9	13.04	2.2047	241.6	1000	1241.6	1.189	0.079	0.020	9.916	0.078
F10	15.08	2.0478	220.0	1000	1220.0	1.135	0.063	0.005	9.979	0.084
F11	16.24	1.8610	172.8	1000	1172.8	1.054	0.045	0.002	10.024	0.086
F12	18.08	1.9702	289.9	1000	1289.9	1.238	0.067	0.006	10.090	0.091
F13	19.95	2.3730	254.4	1000	1254.4	1.147	0.089	0.010	10.179	0.101
F14	21.40	2.3495	180.5	1000	1180.5	1.299	0.093	0.008	10.272	0.109
F15	22.92	2.1959	232.0	1000	1232.0	1.119	0.073	0.016	10.344	0.125
F16	24.81	2.0292	322.5	1000	1322.5	1.186	0.070	0.001	10.414	0.126
F17	26.79	1.8067	203.8	1000	1203.8	1.157	0.047	0.004	10.461	0.131
F18	28.90	1.8554	299.3	1000	1299.3	1.196	0.056	0.003	10.517	0.134
F19	30.32	1.6864	177.1	1000	1177.1	0.984	0.032	0.006	10.549	0.141
F20	31.95	1.6342	224.5	1000	1224.5	1.262	0.039	0.002	10.588	0.142
F21	33.91	1.6787	199.2	1000	1199.2	1.147	0.038	0.000	10.625	0.143
F22	35.90	1.8190	306.5	1000	1306.5	1.195	0.053	0.024	10.679	0.167
F23	37.94	1.5858	182.4	1000	1182.4	1.021	0.027	0.002	10.706	0.169
F24	39.00	1.6805	239.3	1000	1239.3	1.035	0.035	0.001	10.741	0.170
F25	40.35	1.5389	219.1	1000	1219.1	1.457	0.036	0.010	10.778	0.180
F26	41.39	1.7626	205.0	1000	1205.0	1.073	0.041	0.004	10.818	0.184
F27	43.26	1.6674	203.9	1000	1203.9	0.928	0.030	0.001	10.848	0.185
F28	65.03	1.6015	230.4	1000	1230.4	1.365	0.039	0.008		
F29	67.02	1.7224	197.6	1000	1197.6	1.400	0.049	0.001		
F30	68.40	1.6167	167.4	1000	1167.4	1.115	0.032	0.004		
F31	70.08	1.6530	207.9	1000	1207.9	1.130	0.036	0.003		
F32	72.03	1.6078	222.6	1000	1222.6	1.397	0.041	0.001		
F33	73.36	1.8942	141.9	1000	1141.9	0.965	0.042	0.021		
F34	75.08	1.5848	303.7	1000	1303.7	1.255	0.037	0.002		
F35	174.4	1.2231	226.0	1000	1226.0	3.252	0.019	0.001		
F36	176.1	1.1955	184.0	1000	1184.0	1.736	0.007	0.003		
F37	177.1	1.1901	243.0	1000	1243.0	1.532	0.006	0.002		

APPENDIX VIII – Radiation Exposure

Common Radiation Exposure (Natural & Human Made)

One Coast-to-Coast Airline Flight	3 mrem
Natural Background Radiation in the U.S.	150-300 mrem / yr
Chest Radiograph A/P View	15-25 mrem / view
Chest Radiograph Lateral View	50-65 mrem / view
Computerized Tomography	2,000-6,000 mrem

Radiation Exposure Limits and Guidelines

Target Tissue	Regulatory Limit (mrem / yr)	UC Davis Guidelines (mrem / yr)	**^{14}C-folic acid study (mrem)**
Whole Body	5,000	2,500	**1**
Extremities	50,000	25,000	n/a
Fetus	500	50	n/a

Biologically Significant Radiation Exposures

Risk of Contracting Cancer Increases by 0.09 %	1,000 mrem
Temporary Blood Count Change	25,000 mrem
Permanent Sterilization in Women	250,000 mrem
Permanent Sterilization in Men	100,000 mrem
Cataract Formation	600,000 mrem
Skin Erythema	300,000 mrem

Source: UC Davis Environmental Health and Safety